

**HYDROSTATIC YAW BEARING DESIGN FOR 500 KW HORIZONTAL AXIS  
WIND TURBINE**

**by**

**Selma YILMAZ**

**Submitted to the Graduate School of Engineering and Natural Sciences  
in partial fulfillment of the requirements for the degree of  
Master of Science**

**Sabanci University**

**August, 2013**

**© Selma Yılmaz, 2013**

**All Rights Reserved**

**Approved By**

**Assc. Prof. Mahmut F. Akşit (Thesis Advisor).....**

**Assc. Prof. Kemalettin Erbatur.....**

**Assc. Prof. Kemal Kılıç.....**

**Date of Approval**

**13.08.2013**

# **HYDROSTATIC YAW BEARING DESIGN FOR A 500 KW HORIZONTAL AXIS WIND TURBINE**

**Selma YILMAZ**

**Industrial Engineering, MSc. Thesis, 2013**

**Thesis Supervisor: Ascc. Prof. Mahmut F. Akşit**

*Keywords:* Hydrostatic bearing, yaw bearing, slewing bearing, wind turbine, film thickness, capillary, stiffness

## **Abstract**

As wind turbines get larger, nacelle structure that is carried by yaw bearings becomes heavier. In order to bear these increasing loads, yaw bearing needs to have more than one row of rolling elements which cause increase in weight and consequently the cost of the yaw bearing in classical design [1]. As the industry trends demand larger and larger wind turbines, the slew bearing costs keep increasing. In addition to cost, slew bearings suffer other reliability problems in very large turbines. As the turbine size keeps increasing both overall nacelle weight and wind loads acting on the yaw system (radial, axial and moment loads) get very large. During operation these heavy loads act on a single/local point on the bearing for extended periods during which heavy loads oscillate with varying wind speeds/loads. Large cyclic loads acting on a specific point on bearing race cause indentation marks which is also called Brinelling failure. As turbine capacities keep growing well beyond 10 MW with offshore units, the need for a robust low cost alternative grows.

Hydrostatic bearings are well known systems that are used in large and heavy load machinery. This thesis aims to investigate applicability and feasibility of alternative hydrostatic yaw bearing design for a sample horizontal axis wind turbine. Motivation of the thesis is to develop a hydrostatic bearing design for yaw system for a 500 KW wind turbine, and demonstrate advantages and disadvantages of the hydrostatic bearing yaw system in comparison to classical rolling element bearings by evaluating load capacity, rigidity, stiffness, cost and life.

# **500 KW'LIK YATAY EKSENLİ RÜZGAR TÜRBİNİ İÇİN HİDROSTATİK YATAK TASARIMI**

**Selma YILMAZ**

**Endüstri Mühendisliği, Yüksek lisans tezi, 2013**

**Tez Danışmanı: Doç. Dr. Mahmut F. Akşit**

## **Özet**

Rüzgar türbinleri büyüdükçe döner türbin yataklarının taşıdığı yük gittikçe artmaktadır. Yüklerin artmasıyla birlikte döner türbin yatağı birden fazla sütuna ihtiyaç duyar bu da ağırlığı arttırdığı gibi fiyatı da arttıracaktır. Günümüzdeki rüzgar türbinleri trendi türbinlerin gittikçe büyümesi yönünde olduğu gibi yatak takımlarının fiyatlarının da artması yönündedir. Fiyatla birlikte, yatak takımları büyük rüzgar türbinlerinde güvenilirlik problemlerine de neden olmaktadır. Türbin boyutu ile birlikte toplam ağırlık arttığı gibi yatak sistemine etki eden rüzgar yükleri de artmaktadır. Rüzgar türbinlerinin çalışması sırasında bu yüksek yükler rüzgar hızı ile yataktaki salınım periyodunun uzamasına neden olur ve tek lokal bir noktaya etki eder. Yataktaki belirli noktaya etki eden periyodik yükler Brinelling hatası denilen girinti izi oluşturur. Açık denizlerde türbin kapasitesi 10MW güçlerde büyümeye devam ederken, düşük fiyatlı alternatif çözüme gerek vardır.

Hidrostatik yataklar geniş ve ağır yük mekaniğinde kullanımı iyi bilinen bir sistemdir. Bu tezin amacı hidrostatik yatakların örnek olarak 500 KW'lık yatay eksenli rüzgar türbinlerinde uygulanabilirliğinin ve kullanımının araştırılmasıdır. Tezin motivasyonu, 500 KW'lık rüzgar türbini döner yatak sistemi için hidrostatik yatak geliştirilmesi ve klasik döner elemanlı rulman karşısında yük kapasitesi, rijitlik, fiyat, ömür ve dayanım açısından avantaj ve dezavantajlarının karşılaştırılmasıdır.

## TABLE OF CONTENT

1	Introduction .....	1
1.1	Basic history .....	1
1.2	Wind turbine types.....	2
1.2.1	Vertical Axis Wind Turbines .....	2
1.2.2	Horizontal Axis Turbines (HAWTs) .....	3
1.3	Main Components and Issues of HAWT .....	4
1.3.1	Yaw System .....	5
1.3.2	Types of Yaw Bearings for Horizontal Axis Wind Turbines .....	7
2	Problem Definition and Motivation.....	10
3	Design Requirements for the Yaw Bearing of 500 kW HAWT.....	12
3.1	Calculation of Vertical Loads on the Yaw Bearing of 500 kW HAWT.....	14
3.2	Calculation of Moments caused by Gravitational Forces on the Yaw Bearing of 500 kW HAWT.....	16
3.3	Calculation of the Bearing Moments caused by the Wind Load Offset on the Yaw Bearing of 500 kW HAWT .....	19
3.4	Calculation of the Generator Induced Moment on the Yaw Bearing of 500 kW HAWT.....	22
3.5	Calculation of the Brake Torque on the Yaw Bearing for 500 kW HAWT ...	26
3.6	Resultant Forces and Moments on the Yaw Bearing of 500 kW HAWT.....	29
4	Design & Analysis of the Yaw Bearing for a 500 kW HAWT .....	32
4.1	Slewing Bearing Mechanism and Slewing Bearing Types.....	32
4.2	Selection of Slewing Bearing for 500 kW HAWT .....	35
4.3	Fatigue Life Calculations.....	40
4.4	Material Selection of a Slewing Bearing and Production Method .....	42
5	Design and Analysis of the Hydrostatic Yaw Bearing.....	45
5.1	Hydrostatic Bearings.....	46
5.1.1	Lubrication theory and Reynolds Equation .....	46

5.1.2	Working Principles of Hydrostatic Bearings .....	47
5.1.3	Type of Hydrostatic Bearings .....	50
5.1.4	Hydrostatic Bearing Design Considerations and Control Parameters .....	51
5.2	Designing a Hydrostatic Yaw Bearing for 500 kW HAWT .....	53
5.2.1	Load Determination .....	53
5.2.2	Selection of Bearing Type and Pad Geometry.....	56
5.2.3	Determination of Hydrostatic Bearing Parameters .....	60
5.2.4	Design of Flow Control Device .....	65
5.2.5	Design and Performance Determination of the Hydrostatic Yaw Bearing of 500 kW HAWT .....	78
6	Design Iterations.....	91
6.1	General Procedure.....	91
6.1.1	Design Iteration-1 .....	91
6.1.2	Design Iteration-2 .....	94
6.2	Comparison.....	102
6.2.1	First case .....	102
6.2.2	Second case.....	103
7	Conclusion & future work	

## LIST OF FIGURES

Figure 1.1 Eole C, a 4200 kW vertical axis Darrieus wind turbine with 100 m rotor diameter at Cap Chat, Quebec, Canada. The machine, which is the world's largest wind turbine, is no longer operational [3].....	3
Figure 1.2 Three bladed upwind turbines being tests at Riso, August 1986 [3].....	4
Figure 1.3 Major components of a HAWT [4] .....	5
Figure 1.4 Schematic representation of the main components of HAWT [5] .....	6
Figure 1.5 Typical yaw drive with brake (Van Bibber and Kelly, 1985)[3] .....	7
Figure 1.6 Schematic diagram of a slide bearing [3] .....	8
Figure 1.7 Typical active yaw system involving a slewing bearing [3] .....	9
Figure 2.1 Side view of the designed part of the 500 kW HAWT .....	11
Figure 3.1 Schematic representation of the loads of a horizontal axis wind turbine-1 [7] .....	12
Figure 3.2 Schematic representation of the loads of a horizontal axis wind turbine-2 [7] .....	13
Figure 3.3 a) General view of coordinate system of the blades b) General view of coordinate system of system of hub [7] .....	13
Figure 3.4 General view of loads and coordinate system of yaw system [7] .....	14
Figure 3.5 Axial loads on a yaw bearing .....	14
Figure 3.6 Vertical loads on the yaw bearing of 500 kW horizontal axis wind turbine .	15
Figure 3.7 Moments due to gravitational forces on the yaw bearing of 500 kW horizontal axis wind turbine. ....	16
Figure 3.8 Center of graviy of the yaw bearing.....	18
Figure 3.9 Center of gravity of blades and hub with position vector .....	18
Figure 3.10 Moments induced by wind forces on a horizontal axis wind turbine [4]....	19
Figure 3.11 Wind forces on the rotor of a horizontal axis wind turbine [3].....	20
Figure 3.12 Distance between the center of the mass of the blades and face of the yaw bearing [3].....	21
Figure 3.13 Wind force vector and position vector of the wind force according to the yaw bearing center of gravity .....	22
Figure 3.14 Power transmission from rotor to the generator [8] .....	23
Figure 3.15 Up and down forces due to geneator working [8] .....	25
Figure 3.16 Schematic view of generator force couple .....	25



Figure 3.17 Position vectors and force couples on the wind turbine .....	25
Figure 3.18 Mechanical brake on the high speed shaft.....	27
Figure 3.19 Angular speed vs time .....	28
Figure 3.20 Forces on the brake disc due to braking .....	29
Figure 3.21 Forces and moments effect the yaw bearing .....	30
Figure 4.1 a) Transmission of an axial loads in a slewing bearing b) Transmission of radial loads in a slewing bearing [20] .....	32
Figure 4.2 Transmission of moments in a slewing bearing [20] .....	32
Figure 4.3 An illustration of a slewing bearing [20].....	33
Figure 4.4 a) Single row cylindrical roller slewing bearing with an external gear b) Single row cylindrical roller slewing bearing with an internal gear [6] .....	34
Figure 4.5 Static force limiting diagram [6] .....	36
Figure 4.6 Typical example of loads and moments on a slewing bearing [6] .....	36
Figure 4.7 Static loading diagram of selected triple rowed slewing bearing [11] .....	38
Figure 4.8 Technical drawing of triple rowed roller bearing from the catalogue [11] ...	39
Figure 4.9 Static loading diagram of selected triple rowed slewing bearing [11] .....	40
Figure 4.10 Static and dynamic loading diagram of a similar triple rowed slewing bearing [13].....	41
Figure 4.11 Standard manufacturing process of slewing bearings [14] .....	44
Figure 5.1 Flat circular pad with a central recess [18].....	47
Figure 5.2 Schematic illustration of hydrostatic bearing operation [20] .....	48
Figure 5.3 Schematic illustration of hydrostatic bearing under decreasing and increasing loads [20] .....	49
Figure 5.4 Hydrostatic bearing schematics a) before and b) after lift-off [21].....	50
Figure 5.5 Hierarchy of Externally Pressurized Bearings. [22].....	50
Figure 5.6 Design table of a hydrostatic bearing. [22] .....	51
Figure 5.7 Flow chart of design .....	53
Figure 5.8 Moments and forces @ nominal working condition .....	54
Figure 5.9 Moments and forces @ emergency condition .....	55
Figure 5.10 Resultant forces on the yaw bearing for 500 kW HAWT .....	56
Figure 5.11 Combination of journal and thrust bearings[23] .....	57
Figure 5.12 The designed lift pad configuration.....	57
Figure 5.13 Eccentric loads on hydrostatic bearings [17] .....	57
Figure 5.14 Hydrostatic slideway [17] .....	58

Figure 5.15 Designed hydrostatic yaw bearing .....	58
Figure 5.16 Hydrostatic opposed pads: a) equal pads b) unequal pads [17] .....	59
Figure 5.17 Hydrostatic opposed axial bearing: pressure diagrams [17] .....	59
Figure 5.18 Circular hydrostatic pads.[17] .....	60
Figure 5.19 Bolting places on the inner ring .....	60
Figure 5.20 Inner ring of the hydrostatic yaw bearing .....	61
Figure 5.21 Opposed pad bearings, load determination of the pads [23] .....	62
Figure 5.22 Circular pad bearing with restrictor [22] .....	65
Figure 5.23 Effect of a restrictor on pad pressures [22] .....	66
Figure 5.24 Constant flow control system a) A constant flow pump b) A constant flow valve for each recess [22] .....	68
Figure 5.25 Constant flow control system: one pump for each bearing [22] .....	68
Figure 5.26 Orifice-compensated hydrostatic bearing [26] .....	69
Figure 5.27 Capillary compensated hydrostatic bearing [26] .....	71
Figure 5.28 Flat circular pad bearing with orifice flow control [18] .....	73
Figure 5.29 Flat circular pad bearing with capillary controlled flow [18] .....	74
Figure 5.30 Flow and pressure characteristics of various flow control devices [22] .....	75
Figure 5.31 A glass capillary tubing restrictor [24] .....	76
Figure 5.32 Capillary tubing size chart [29] .....	77
Figure 5.33 Working principle of hydrostatic bearing [24] .....	78
Figure 5.34 Mechanism of designed hydrostatic yaw bearing [24] .....	79
Figure 5.35 a) Upward forces on upper pads. b) Downward forces on the lower pads .....	81
Figure 5.36 a) Electrical analogy of 1 pad of hydrostatic bearing b) Schematic view of oil circulation of 1 pad of hydrostatic bearing [31] .....	86
Figure 5.37 Fluid flow into the bearing by regulating by resistance [32] .....	87
Figure 5.38 Hydrostatic yaw bearing: a) Schematic view b) Circuit design .....	87
Figure 5.39 Schematic view of oil circulation of combinational hydrostatic pad. ....	87
Figure 5.40 Schematic view of oil circulation and pipe design .....	88
Figure 5.41 a) Inner ring with pads b) Outer ring .....	88
Figure 5.42 Inner and outer rings before mounting .....	89
Figure 5.43 Hydrostatic yaw bearing after inner and outer rings assembled .....	89
Figure 6.1 General load characteristics [16] .....	92
Figure 6.2 Loads vs film thickness @ $10^7$ Pa .....	92

Figure 6.3 Comparison to load vs film thickness graphs.....	93
Figure 6.4 Loads vs film thickness for 5 cases .....	93
Figure 6.5 Pad geometry of first design.....	95
Figure 6.6 New pad geometry.....	95
Figure 6.7 Rectangular pad with rounded corner rectangular pad [18] .....	95
Figure 6.8 Rectangular pad parameters [17].....	96
Figure 6.9 Height of the bearing .....	96
Figure 6.10 Pad coefficients [17].....	97
Figure 6.11 Pad coefficients [17].....	100
Figure 6.12 Pad design according to the case two .....	104
Figure 6.13 Annular pad hydrostatic bearing [23].....	104
Figure 6.14 Annular pad hydrostatic bearing [33].....	105

## LIST OF TABLES

Table 1.1 Material properties for materials used in slide bearings [3] .....	8
Table 3.1 Vertical Loads.....	15
Table 3.2 Gravitational forces and moments on the yaw bearing for 500 kW horizontal axis wind turbine.....	17
Table 3.3 Moment vectors due to gravitational forces .....	19
Table 3.4 Wind forces and resulting moment generated on the yaw bearing for 500 kW horizontal axis wind turbine .....	21
Table 3.5 Wind force and moment vector .....	22
Table 3.6 Torque generated at generator .....	24
Table 3.7 Torque generated at generator (Gear box and friction torques included).....	24
Table 3.8 Calculation of deceleration from rotational speed.....	28
Table 3.9 Brake torque for a 500 kW horizontal axis wind turbine .....	28
Table 3.10 Forces and moments occurs on the yaw bearing .....	29
Table 3.11 Resultant moments.....	31
Table 4.1 Slewing bearing selection guide [6] .....	34
Table 4.2 Rated forces and moments.....	37
Table 4.3 Bearing Dimensions [11] .....	38
Table 4.4 Chemical composition and mechanical properties of slewing bearing materials [13].....	42
Table 5.1 Bearing selection for special performance requirements [16].....	45
Table 5.2 Determined forces and moments on the yaw bearing for a 500 kW HAWT .	53
Table 5.3 Loads on the yaw bearing for 500 kW HAWT.....	56
Table 5.4 Bearing dimensions .....	60
Table 5.5 Typical minimum viscosity values for hydraulic components [25] .....	64
Table 5.6 Ranking of compensating elements [26] .....	75
Table 5.7 Inputs for a 500 kW hydrostatic yaw bearing calculations.....	80
Table 5.8 Calculated area, area factor and flow factor for upper and lower pads .....	81
Table 5.9 Load check for upper pads by trial and error.....	82
Table 5.10 Load check for lower pads by trial and error.....	83
Table 5.11 Calculated capillary diameter and capillary lengths for upper and lower pads .....	84
Table 5.12 Load check for lateral pads by trial and error .....	85

Table 5.13 Calculated capillary diameter and capillary lengths for lateral pads .....	85
Table 6.1 Differences in parameters with regard to changing supply pressures .....	94
Table 6.2 Pad geometries .....	96
Table 6.3 Calculated area, area factor and flow factor for lower pads .....	97
Table 6.4 Calculated number of pads for each geometry .....	98
Table 6.5 Calculated parameters for rectangular pads bearing with $10^7$ Pa supply..... pressure .....	98
Table 6.6 Capillary length to diameter ratios .....	99
Table 6.7 Capillary lengths and diameters.....	99
Table 6.8 Calculated area, area factor and flow factor for lower pads .....	100
Table 6.9 Calculated number of pads for each geometry .....	101
Table 6.10 Calculated parameters for rectangular pads bearing with $2,5 \times 10^7$ Pa supply pressure .....	101
Table 6.11 Capillary length to diameter ratios .....	102
Table 6.12 Capillary length and diameter.....	102
Table 6.13 Stiffness comparison of the trials .....	103
Table 6.14 Stiffness comparison of the trials .....	103

## NOMENCLATURE

$F_a$  : Axial force

$F_z$  : Vertical Load

$g$  : Gravitational acceleration of mass

$m$ : Mass

$M_y$ : Moment around y axis

$\vec{r}$  : Position vector

$\rho$  : Air density

$F_x$  : Force along x direction

$A$ : Area that blades swept

$M_x$ : Moment around x axis

$P$  : Power

$T$  : Torque

$\omega$  : Angular speed

$V_R$  : Rotational speed

$\alpha$  : Angular deceleration

$F_r$  : Radial force

$L_f$  : Fatigue life

$f_n$  : Dynamic load factor

$\phi$  : Direction x

$u$  : Velocity in the direction x

$\xi$  : Viscosity

$h$ : Film thickness

$R_o$ : Radius of the bearing

$R_i$  : Radius of the recess

$Q$  : Flow rate

$q_f$  : Flow factor

$P_a$  : Atmospheric pressure

$P_r$  : Recess pressure

$P_{\text{pump}}$  : Pump pressure

$P_s$  : Supply pressure

$W$  : Load

$d$  : Diameter

$Re$  : Reynolds number

$Q_c$  : Capillary flow

$a_f$  : Area factor

## **Acknowledgement**

I would like to give my sincere and deep gratitude to my thesis advisor Assoc. Prof. Mahmut F. Akşit for his continuous support and practical guideline during the timeline of the thesis. I feel very lucky to find a chance to study with him and thanks to his fatherly behaviours during whole my study. I am also grateful to my committee members Assoc. Prof. Kemal Kılıç and Assoc. Prof. Kemalettin Erbatur for their interpretation on the dissertation. I am also thankful to my fiance H. Kemal Külcü for his continuous supports and means for my life. I would like to thank to my closest friends Gülen Uncu, Elif Duygu Güney, Birgül Salihoğlu for their friendships and also I would like to thank Gülnur Kocapınar and Ceren Çelebi for accepting me as a third room mate for the whole year and their support. Finally, I would like to express my best gratitude to my family members especially my mother for her never ending love and continuous support from the beginning of my life.

Lastly, I owe Assoc. Dr. Mahmut F. Akşit a debt of gratitude due to his help to go to erasmus and finish my master study.



## **Objective of the Project**

This work investigates applicability of hydrodynamic bearing mechanism on yaw system of a horizontal axis wind turbine. A sample 500 kW wind turbine has been selected as case study. At first, typical rolling element yaw bearing has been selected for the problem. A hydrostatic yaw bearing has been designed and compared with the prior standard bearings for performance such as life, cost, stiffness, wear to evaluate feasibility of usage such a hydrostatic bearing for medium and large size wind turbines.

## **1 Introduction**

Wind turbines usage is now increasing day by day together with the increase in need of energy. In order to satisfy this demand and raising requirements in energy sector, wind turbines have been changing so quickly in size and design. The history of the wind turbines, types of wind turbines and components of horizontal axis wind turbines will be given in detail in this chapter.

### **1.1 Basic history**

Windmills were an essential example of using of wind energy in the history before industrial revolution has taken place. Wind energy could be transformed to electrical energy that was demonstrated by Danish scientist Paul La Cour in the 19th century but it was not chosen because of its being expensive [2].

First oil price crisis was seen in 1973 which was triggered to studies deeply on modern wind turbines though they have started in 1930s. During this period, huge prototypes of wind turbine had been constructed with many technical and economic troubles. Small turbine as several tens of kilowatts was preferred to use instead of bigger one. Small turbines had economical advantages than bigger ones in term of low energy production cost, and owing to that reason they were bought by some people [2]

Denmark was pioneer of the wind turbine and most of turbine was built in there. Name of the control method of these turbines was ‘‘Danish concept’’. Danish concept can be defined as turbine has fixed three rotor blades rotating constant speed and needed power is provided by the stall effect. Asynchronous generator is used in the turbines [2].

Large turbines were started to be produced due to technical progression of wind technology. Next larger turbine improved thanks to technical development of wind turbine. Name of the process is ‘‘upscaling’’. Researches of the eighties were created Today’s commercial wind turbines with devoloping of mechanical components, electrical system and turbine control. Mechanics of rotor blades were changed by some manufacturers and it was gained more freedom to limit power during storm but also to maximize the power output at lower wind speed. Others used another technic to make rotational speed of the all rotor variant. Another group used synhcronous generetor instead of asynchronous one and could exclude the gearbox. Thus, many type of control consepts can be found in the market [2].

## **1.2 Wind turbine types**

Wind turbines can be classified into two main groups according to the blade axis: Vertical axis wind turbines and horiztontal axis wind turbines.

### **1.2.1 Vertical Axis Wind Turbines**

Verical axis wind turbines (VAWTs) with C-shape blades seen in the Figure 1.1 had used in the past century.



**Figure 1.1 Eole C, a 4200 kW vertical axis Darrieus wind turbine with 100 m rotor diameter at Cap Chat, Quebec, Canada. The machine, which is the world's largest wind turbine, is no longer operational [3].**

Generator and gear-box is reachable due to the position in the VAWTs turbines and because of this reason, yaw mechanism is not necessary. These types of turbines have many disadvantages like low efficiency, so system requires essential changes especially main bearing that rotor is settled nearly on ground with limited wind [3].

### **1.2.2 Horizontal Axis Turbines (HAWTs)**

Horizontal axis turbines seen in the Figure 1.2 are mainly operated all over the world. Today, all commercial wind turbines are built as type of HAWTs where propeller type rotors are used in turbines by horizontally. The direction of the wind is a basic design parameter and HAWTs should be installed parallel to it [3].



**Figure 1.2 Three bladed upwind turbines being tests at Riso, August 1986 [3]**

Upwind rotors mounted in front of the vertical tower are used in the HAWTs type turbines where wind is met in there. Yaw mechanism is required for upwind rotors to hold rotors parallel with the direction of wind. Downwind rotors do not meet with wind due to position. Main drawback of downwind rotors is swing which caused much more fatigue loads [3].

### **1.3 Main Components and Issues of HAWT**

Major elements of a horizontal axis wind turbine can be listed as; the rotor which comprises of blades and hub; the drive train consists of the rotating elements of the wind turbine such as shafts, gearbox, coupling, a mechanical brake; and the generator; nacelle and main frame includes wind turbine housing, bedplate and the yaw system; tower, foundation, machine controls and lastly the electrical system which includes cables, switchgear, transformers and electronic power converters in it [4].

A representative illustration of a horizontal axis wind turbine is given below in Figure 1.3.

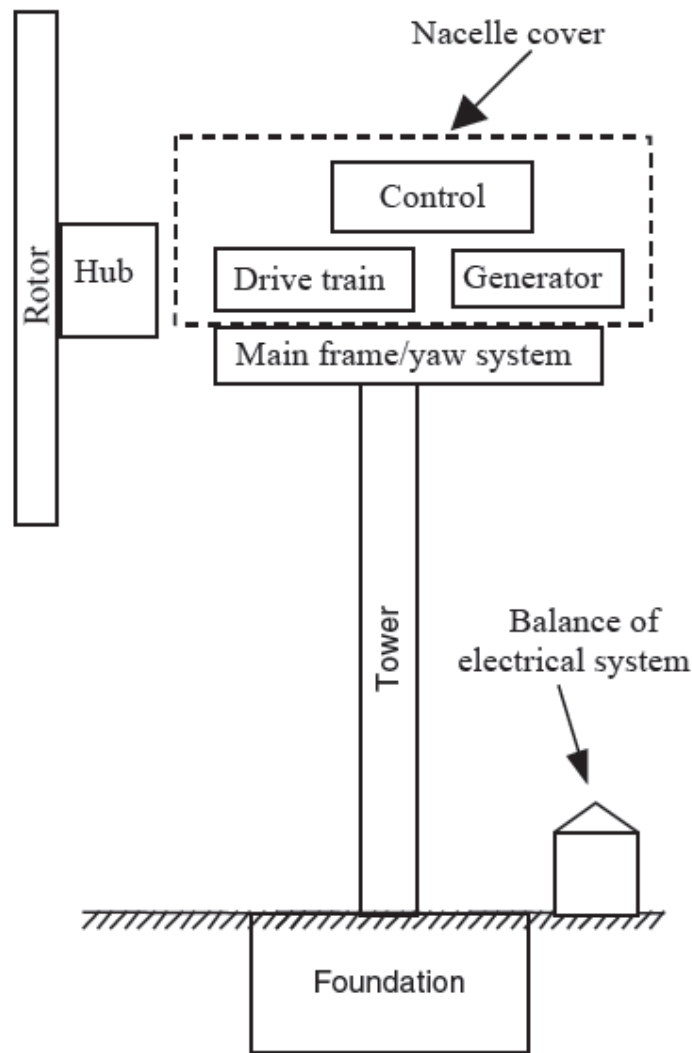


**Figure 1.3 Major components of a HAWT [4]**

There are many alternatives while designing a horizontal axis wind turbine. Selections are made through these alternatives to determine how many blades wind turbine should have, to decide whether the wind turbine should be downwind or upwind, to choose the type of material that blades are produced, to choose the way of production type of the blades and shape of the blades, to decide type of hub, to determine the type of yaw system and which type of bearing should be adapted to the yaw system [4].

### **1.3.1 Yaw System**

Yaw system provides nacelle to be in a right position with respect to wind direction during operation. By the help of the yaw mechanism, the rotor's direction is changed according to the direction of the wind to make the rotor axis aligned with the wind direction for maximum energy output. If there is a difference between the rotor axis and the horizontal projections of the wind direction yaw errors are formed. Yaw error which

is also called yaw angle, originates because of the misalignment between the rotor shaft and the wind direction, and it can be explained as the angle between the rotor axis and the wind direction horizontal projection [3].

A schematic representation of the yaw system with the other major components of a horizontal axis wind turbine is given Figure 1.4. Yaw system is placed between the nacelle and the tower, which is illustrated with a red circle.

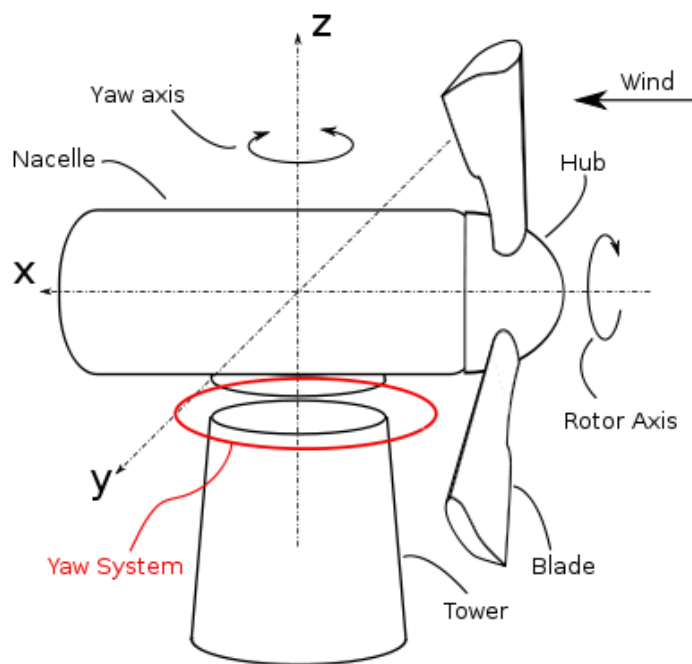


**Figure 1.4 Schematic representation of the main components of HAWT [5]**

There are two types of yaw systems that can be used in the wind turbines: passive yaw system and active yaw system. Wind turbines which have passive yaw system use power of wind to orient the rotor. To operate properly, passive wind turbines generally need to use tail vanes if these are upwind type or coning of the blades if these are downwind type. Passive yaw systems are used only in small wind turbines; they are not suitable for large wind turbines. In addition, passive yaw system may cause other problems in operation such as cable twisting during the repeated rotation of the nacelle due to winds moving in one way during a long period. Passive yaw system also called free yaw system which makes the turbine line up according to the wind. It is preferred for downwind, small horizontal wind turbines. The active yaw system is preferred for upwind, large and medium sized horizontal axis wind turbines. As turbines keep getting

larger, active yaw system is also being used for the downwind type horizontal axis wind turbines [3]. Active yaw systems generally compose of a yaw bearing which is a link between the nacelle and tower, that provides nacelle rotation in accordance with the wind direction; one or more yaw motors, yaw brakes and a yaw control system which orients the bearing according to the signs obtained from the wind direction sensors which is generally placed on the nacelle [4].

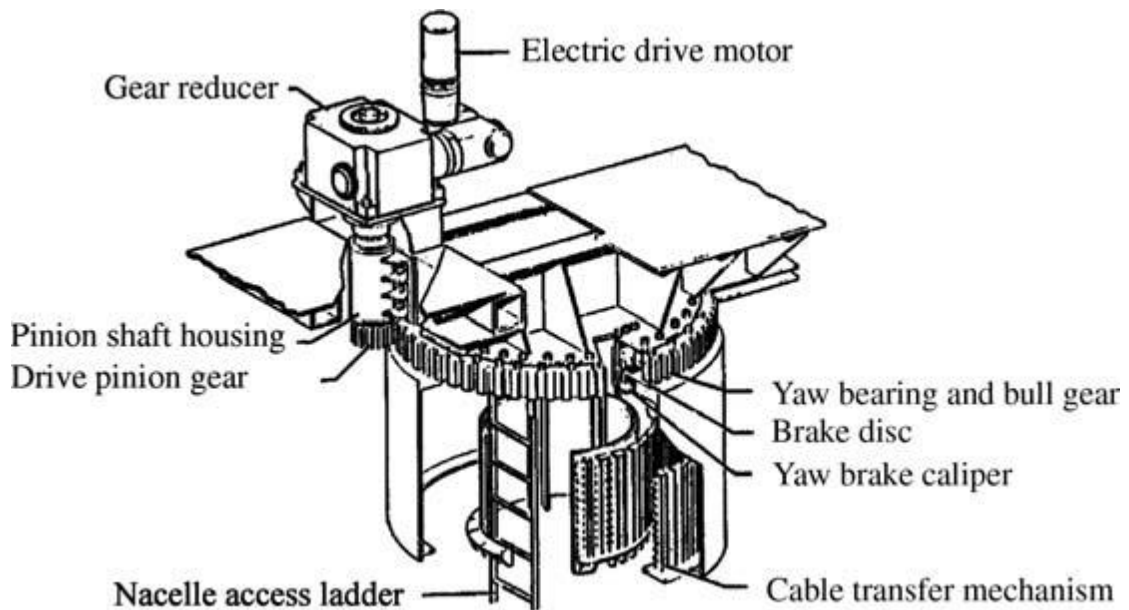


**Figure 1.5 Typical yaw drive with brake (Van Bibber and Kelly, 1985)[3]**

Yaw brakes are typically used to prevent excessive wear or fracture of yaw drive in a short period which is faced because of the yaw motion of the system. A typical yaw drive with a brake is given above in Figure 1.5. In the course of changing winds, a torque around the tower axis happens. In order to make the nacelle stationary, yaw brakes are used [3].

The most important part of the yaw mechanism is the yaw bearing which supports the nacelle, and conveys the thrust loads to the tower [4].

### **1.3.2 Types of Yaw Bearings for Horizontal Axis Wind Turbines**

There are two different types of yaw bearings which are used for horizontal axis wind turbines: sliding bearings and rolling element bearings.

### 1.3.2.1 Sliding Bearings

Schematic representation of a sliding bearing is given in Figure 1.6. Sliding bearing is composed of sliding plates and claws which is a connection between the nacelle and the tower [3].

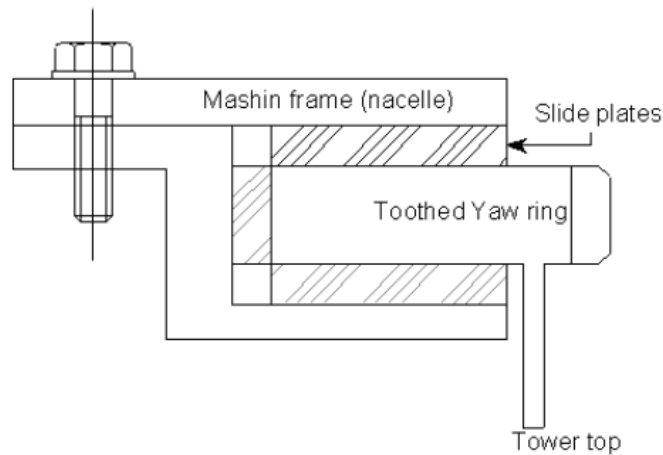


**Figure 1.6 Schematic diagram of a slide bearing [3]**

Sliding bearings are required to be durable and slide smoothly. That is why these types of bearings are made of materials which have high strength and good wear properties in sliding. Sliding plates are seen in Figure 1.6. These plates are generally made by cast polyamide or similar type of materials like polyurethane in order to provide smooth sliding. These sliding plates are greased during operation to reduce friction as well as to prevent corrosion of steel parts that are in contact with the bearing [3]. Different material options typically used in sliding bearings are listed in the Table 1.1 below;

**Table 1.1 Material properties for materials used in slide bearings [3]**

Properties	Materials	PA 66	PUR	PET	POM
Tensile Strength		52 MPa	83 MPa	46 MPa	61 MPa
Compressive Strength		60 MPa	N/A	97 MPa	31 MPa
Flexural Module		1379 MPa	3447 MPa	2758 MPa	2620 MPa
Hardness Rockwell R		100	119	120	127
Temperature					
Maximum		129 ° C	110 ° C	100 ° C	N/A
Minimum		-79 ° C	-40 ° C	- 15 ° C	-N/A



### 1.3.2.2 Slewing Bearings

Rolling element bearings have been used like slewing bearings for the wind turbine yaw systems. Rolling element bearings can bear both axial and radial loads in addition to the moment loads. A typical rolling element bearing as a slewing bearing is shown in the Figure 1.7 below;

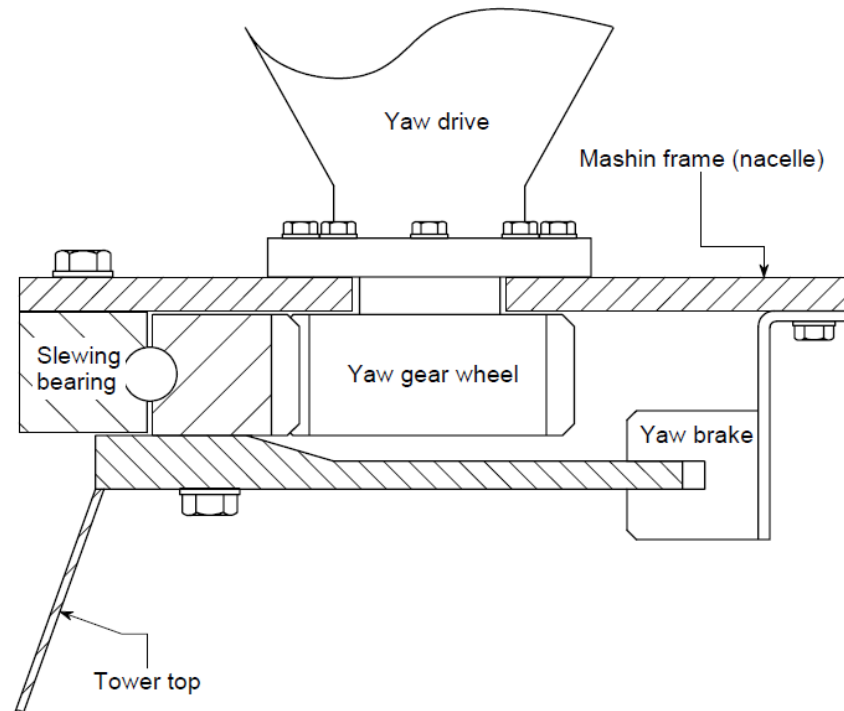


**Figure 1.7 Typical active yaw system involving a slewing bearing [3]**

Slewing bearing is more developed type of bearing for wind turbine yaw systems compared to the sliding bearings. In general, it can be said that slewing bearings are also large rolling element bearings [6]. Both slewing bearings and sliding bearings can be categorized as contact bearings. The most important parameter of a slewing bearing is having less frictional resistance than a sliding bearing. This enables yaw system operation without large yaw motors, and provides better brake control than a sliding bearing [3].

Slewing bearings are preferred for operation in horizontal axis wind turbines for many years due to the advantages mentioned above as well as the fact that they have high load capacity and high reliability in comparison to sliding bearings.

## **2 Problem Definition and Motivation**

Wind turbines need to align the direction of the blade rotation axis according to the direction of the wind. To facilitate nacelle direction change, yaw mechanism has been using in wind turbines. Yaw mechanism has a yaw bearing which works for transmitting loads and moments to the tower. Yaw bearing supplies flexibility to rotate hub and nacelle towards the correct direction of wind [1].

In this work, typical slew bearing yaw system design will be referred as “classical design”.

As wind turbines get larger, nacelle structure that yaw bearings carry becomes heavier. In order to bear these increasing loads, yaw bearing needs to have more than one row which cause increase in weight and consequently the cost of the yaw bearing in classical design [1]. As the industry trends demand larger and large wind turbines, the slew bearing costs keep increasing. In addition to cost, slew bearings suffer other reliability problems in very large turbines. As the turbine size keeps increasing both overall nacelle weight and wind loads acting on the yaw system (radial, axial and moment loads) get very large. During operation these heavy loads act on a single/local point on the bearing for extended periods during which heavy loads oscillate with varying wind speeds/loads. Cyclic large loads acting on a specific point on bearing race can cause indentation marks which are also called Brinelling failure. As turbine capacities keep growing well beyond 10 MW with offshore units, the need for a robust low cost alternative grows.

Hydrostatic bearings are well known systems that are used in large and heavy load machinery. This thesis aims to investigate applicability and feasibility of a hydrostatic yaw bearing design for a sample 500 KW horizontal axis wind turbine. Motivation of the thesis is to develop a hydrostatic bearing design for yaw system of a 500 KW wind turbine, and demonstrate advantages and disadvantages of the hydrostatic bearing yaw system in comparison to classical rolling element bearings by evaluating load capacity, stiffness, cost, life, noise, corrosion life and wear.

Before designing a hydrostatic yaw bearing, this work also includes design and selection of a slew bearing for the same 500 kW unit as a classical bench mark. Then, the same yaw system has been designed using hydrostatic bearings. The results indicate

that the hydrostatic system is more cost effective and capable of carrying greater loads more robustly than the classical design.

As the subject of this work a classical 500 kW horizontal axis wind turbine has been selected. The turbine is designed as Class II turbine with blade diameter of 45 meters. The full load wind speed is 11.5 m/s. The rotor speed is 30 rpm while generator rotates at 850 rpm. Turbine is controlled by an active yaw system by using a slewing bearing.

An assembly view of designed 500 kW horizontal axis wind turbine is given below in Figure 2.1;

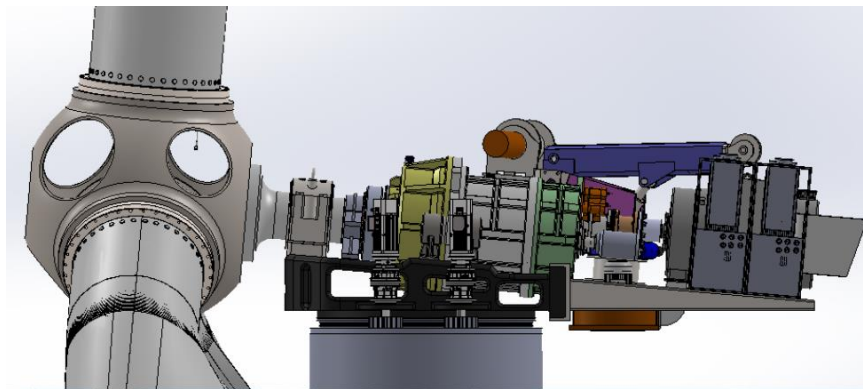


**Figure 2.1 Side view of the designed part of the 500 kW HAWT**

In the third section, yaw bearing types and design requirements while selecting the bearing type will be given; in the fourth section, the yaw system in a wind turbine, which types of bearings have been used for yaw system and designing of slewing bearing will be mentioned; in the fifth section, designing of a hydrostatic yaw bearing for 500 kW horizontal axis wind turbine will be mentioned step by step, in the sixth section, optimization study for the design hydrostatic yaw bearing will be given in details and this work will end up with the conclusion, comparison and future work.

### 3 Design Requirements for the Yaw Bearing of 500 kW HAWT

After some literature survey and by investigating other applications in the past, a suitable rolling element bearing for the yaw mechanism of the 500 kW HAWT has been selected within the scope of this work. The suitable bearing for yaw mechanism is determined based on the forces and moments that the yaw bearing is subjected to. Then, appropriate bearing is selected from manufacturer catalogues to meet these load conditions. Therefore, loads and moments have been calculated first and a proper bearing has been selected later.

A yaw bearing of a horizontal axis wind turbine is exposed to some loads and moments due to the weight of the nacelle and its components' weights, wind loads, torques generated from brake and generator.

A schematic representation of loads in general is given below in Figure 3.1 and Figure 3.2;

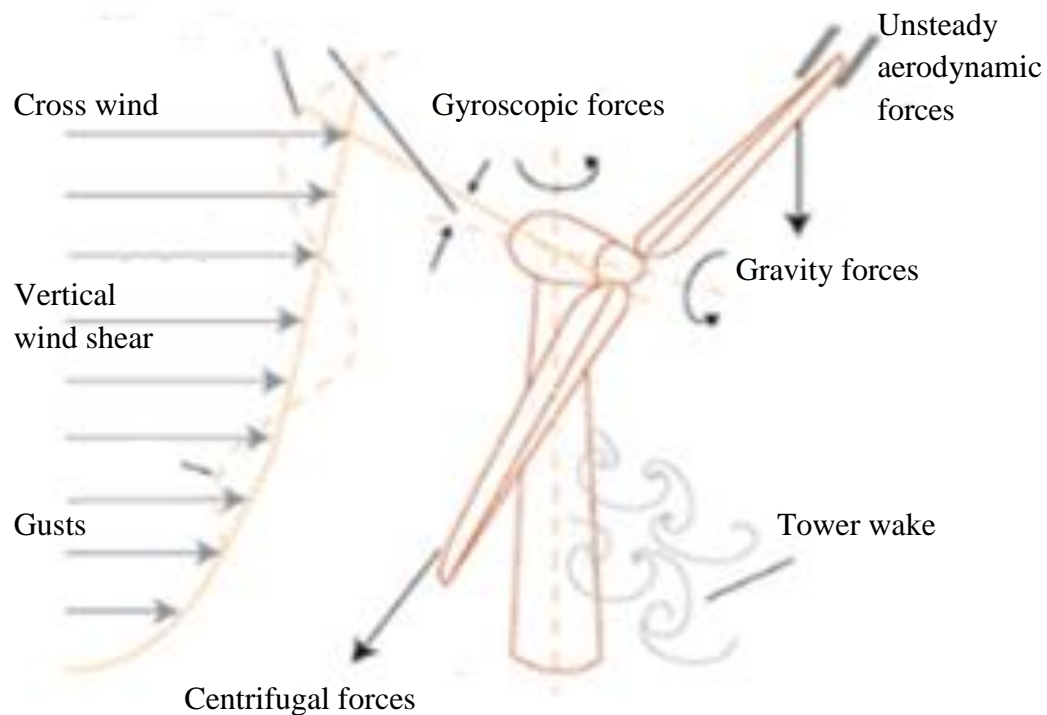


**Figure 3.1 Schematic representation of the loads of a horizontal axis wind turbine-1 [7]**

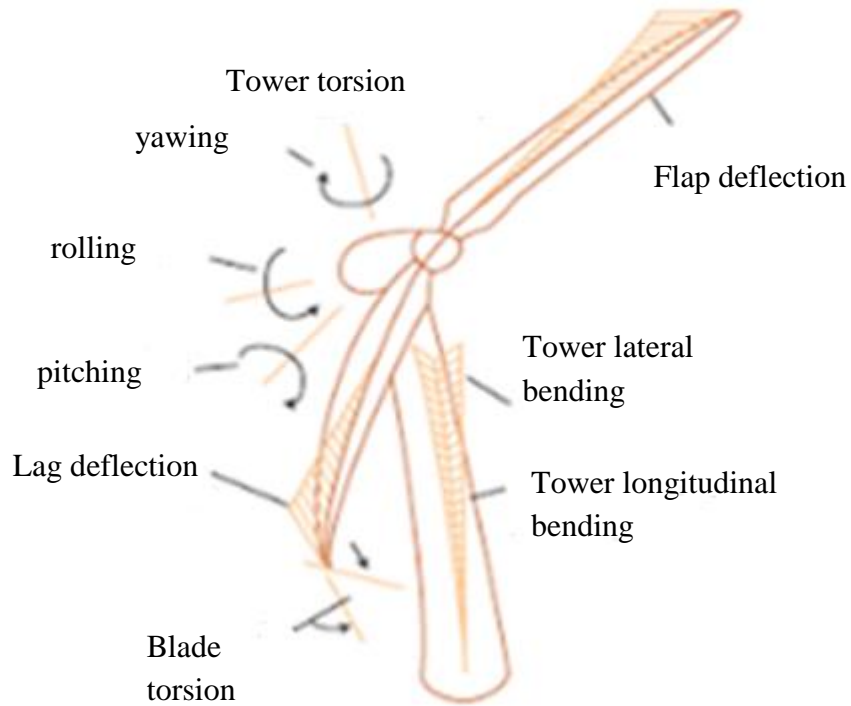


**Figure 3.2 Schematic representation of the loads of a horizontal axis wind turbine-2 [7]**

For the purpose of determining the loads and moments on the yaw bearing for a horizontal axis wind turbine, various coordinate systems according to the blades, hub and yaw bearing are shown in

Figure 3.3 and Figure 3.4.

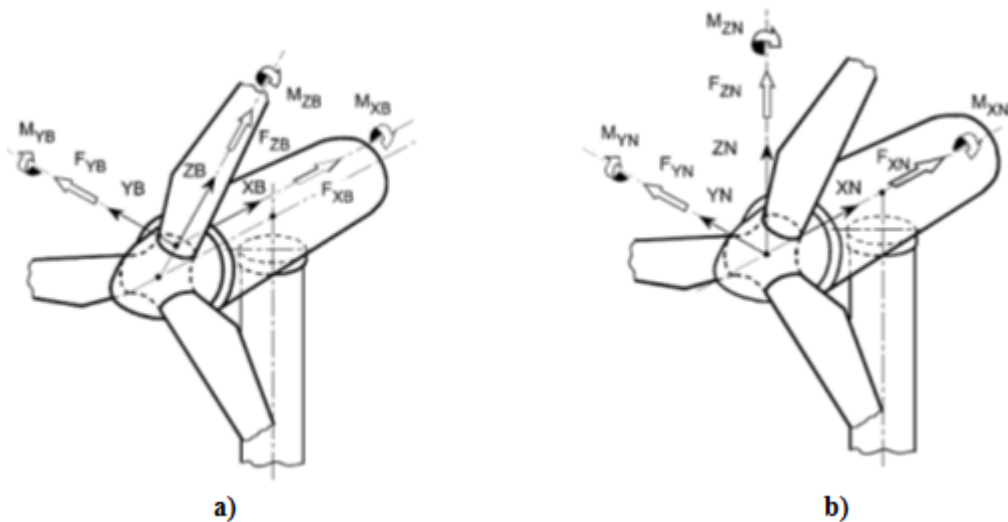


**Figure 3.3 a) General view of coordinate system of the blades b) General view of coordinate system of system of hub [7]**

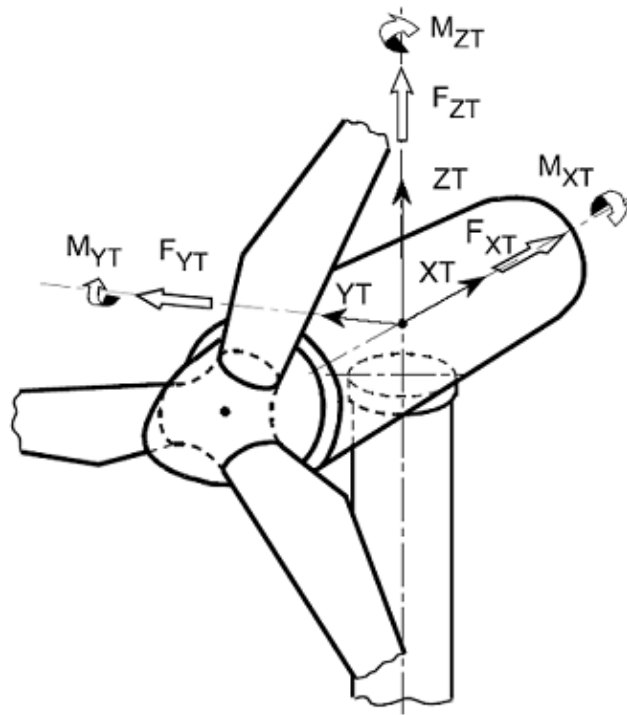


**Figure 3.4 General view of loads and coordinate system of yaw system [7]**

Loads and moments on a yaw bearing can be classified as follows: Vertical loads, gravitational loads, wind loads, generator torque, and brake torque.

### **3.1 Calculation of Vertical Loads on the Yaw Bearing of 500 kW HAWT**

Vertical loads can be described as loads along z axis which are called axial loads (as they act axially on the yaw bearing). The direction of an axial force is parallel to the axis of the rotation of the yaw bearing. An illustration of axial loads on a yaw bearing is shown in Figure 3.5.

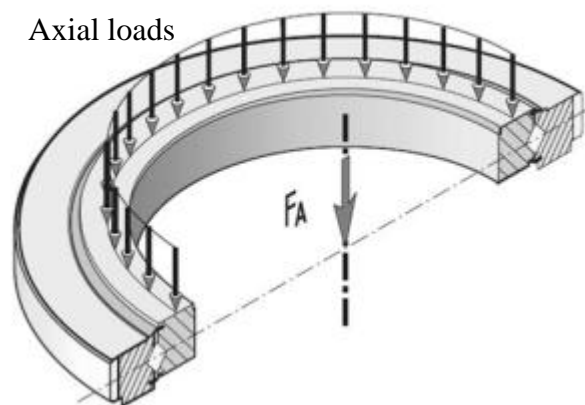


**Figure 3.5 Axial loads on a yaw bearing**

The static loads consist of the weight of the nacelle, rotor and the other components of the wind turbine, acting vertically down as an axial force on the bearing. Sum of the downward forces generate an axial force on the yaw bearing. Vertical loads acting as axial forces on the yaw bearing are given below in Figure 3.6.

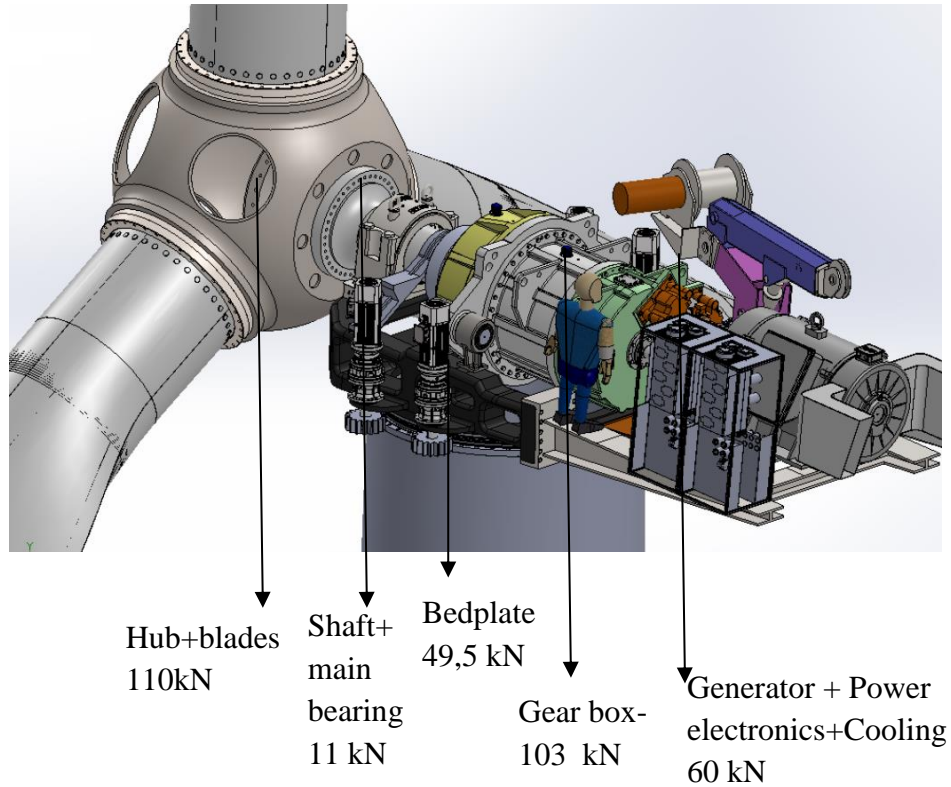


**Figure 3.6 Vertical loads on the yaw bearing of 500 kW horizontal axis wind turbine**

**Table 3.1 Vertical Loads**

Components	g (m/s <sup>2</sup> )	Fz (N)	Fz (kN)
Hub	10	50.000	50
Blades	10	60.000	60
Bedplate	10	49.500	49,5
Yaw motors	10	15.000	15
Nacelle	10	15.000	15
Generator	10	60.000	60
Shaft+ Main bearing	10	10.617	10,617
Gear box	10	102.860	102,86
Crane	10	13.000	13
<b>Total F<sub>z</sub></b>		-380980	-380,98

Sum of the vertical loads is equal to 380,98 kN which gives the axial load on the yaw bearing. Axial load is represented by 'F<sub>a</sub>'. Thus, F<sub>a</sub> = - 380,98 kN.

### 3.2 Calculation of Moments caused by Gravitational Forces on the Yaw Bearing of 500 kW HAWT

Gravitational forces on the yaw bearing depend on the masses of the components on the bearing and acceleration of the gravity [3].

The gravitational force is calculated according to the formula given below;

$$F_g = \sum_{i=1}^n m g \quad (1)$$

‘g’ represents the gravitational acceleration of mass and  $g = 10 \text{ m/s}^2$  and ‘m’ represents the mass of the component of the wind turbine.

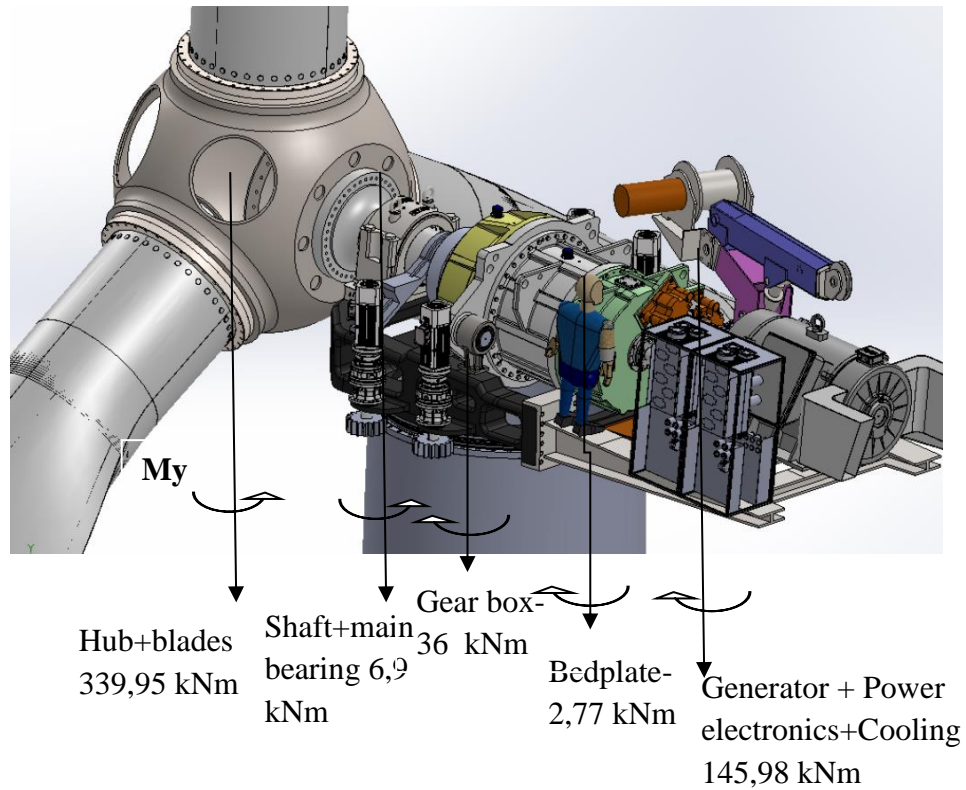


**Figure 3.7 Moments due to gravitational forces on the yaw bearing of 500 kW horizontal axis wind turbine.**

The components that generate gravitational forces on the yaw bearing are: Hub, blades, nacelle, generator and power electronics, bedplate, main bearing and shaft, gear box. Weights of these components are multiplied by the distances between their center of gravity and the center of yaw bearing to generate moments along the y axis. Forces and moments generated from these forces are indicated in Table 3.2.



**Table 3.2 Gravitational forces and moments on the yaw bearing for 500 kW horizontal axis wind turbine**

<b>Components</b>	<b>Fz (kN)</b>	<b>Distance between the component's center of mass and yaw bearing center of mass (m)</b>	<b>My (kNm)</b>
<b>Hub</b>	50	3,085	-154,25
<b>Blades</b>	60	3,085	-185,1
<b>Bedplate</b>	49,5	0,056	2,772
<b>Nacelle</b>	15	1,5	-22,5
<b>Generator +Cooling system + Power electronics</b>	60	2,433	145,98
<b>Shaft + Main bearing</b>	10,617	0,653	-6,9329
<b>Gear box</b>	102,86	0,35	36,001
<b>Crane</b>	13	1,15	14,95
<b>Total My</b>			-169,08

Center of gravity of the blades is assumed coincident with the hub's center of the gravity for the designed wind turbine. Moments caused by the weights of the yaw motors are ignored because 4 yaw motors are used for the designed wind turbine and these yaw motors are placed symmetrically around the yaw bearing. Due to symmetric allocation of yaw motors, their moment effects are canceled out.

The resultant moment is around y axis is equal to the total amount of moments in the direction of y axis. Sum of the moments give the resultant moment around y axis as -169,08 kNm. Moment around the y axis is shown by ' $M_y$ '.

Moment due to gravitational forces along direction z can also be calculated by using cross product of vectors. Firstly, position vectors are determined and then, by multiplying the position vectors with force vectors, moments can be calculated.

As a reference point, center of mass of the yaw bearing is taken 0,0,0. Center of gravity of the bearing is shown in Figure 3.8 below.



**Figure 3.8 Center of graviy of the yaw bearing**

Weights, center of gravity of the blades and hub and position vector are given in Figure 3.9 below.

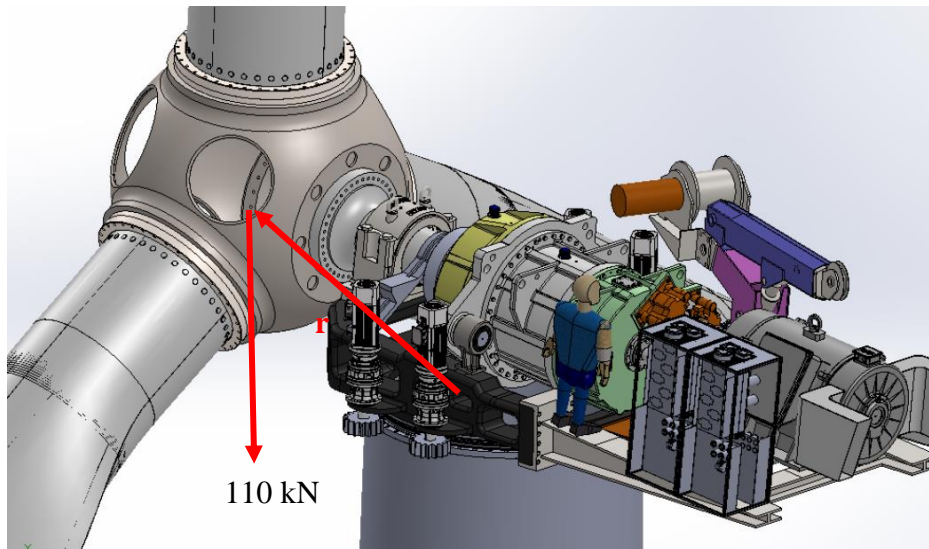


**Figure 3.9 Center of gravity of blades and hub with position vector**

Position vector is taken from the center of yaw bearing to center of hub for the parts hub and blades. This figure is an example of a position vector and  $r$  symbolizes the position vector of hub and blades in that figure. Bedplate coordinate is almost same with the yaw bearing. That's why, mass effect of the bedplate is canceled out.

Force vectors and position vectors according to the center of the gravity of yaw bearing for the whole parts of wind turbine are given in

**Table 3.3 Moment vectors due to gravitational forces**

Components		$\vec{F}_z$	$\vec{r}$	$\vec{M}_y$
1	Hub + Blades	-110k	-3,4i + 1,4k	-374j
2	Nacelle	-15k	-1,15i + 0,2j + 0,4k	-3i-17,25j
3	Generator +Cooling system + Power electronics	-60k	2,5i + 0,1j	-6i+150j
4	Shaft + Main bearing	-11k	-1,65i - 10,5j	-1,65i-10,5j
5	Gear box	-102k	0,43i + 0,085j + 0,8k	-8,8i+45j
6	Crane	-13k	1,15i + 0,034j + 0,75k	-0,45i+15j
Total $\vec{M}_y$				-20i-169,75j

### 3.3 Calculation of the Bearing Moments caused by the Wind Load Offset on the Yaw Bearing of 500 kW HAWT

Wind loads act as exterior forces on the wind turbine. Due to the wind forces on the rotor, the main moment is induced on the turbine rotor as working torque about x axis. This torque is countered by the generator. However, as wind force acts with a vertical offset distance from yaw bearing, another moment occurs on the yaw bearing about y axis. An illustration which shows moments generated by generator, wind and brake forces is given in Figure 3.10.

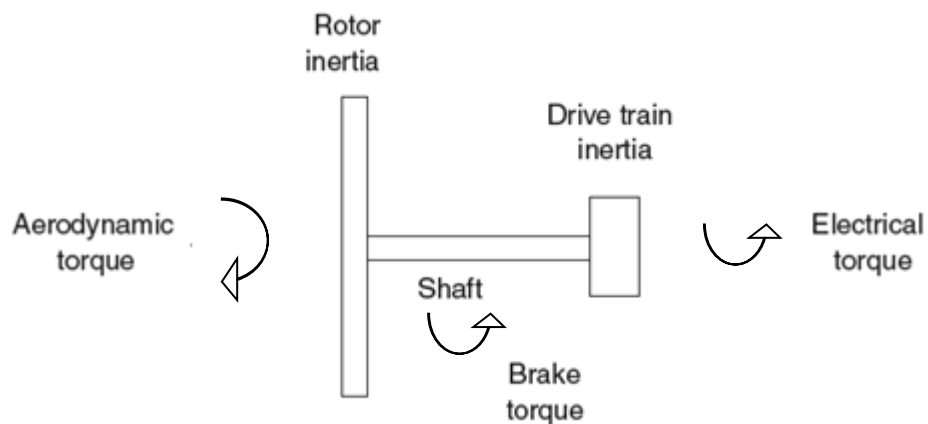


**Figure 3.10 Moments induced by wind forces on a horizontal axis wind turbine [4]**

Wind forces cause moment on the yaw bearing as indicated in Figure 3.10. Wind force can be calculated with the formula given below;

$$P_{ideal} = Fv_0 = F \sqrt{\frac{F}{2\rho A}} \quad (2)$$

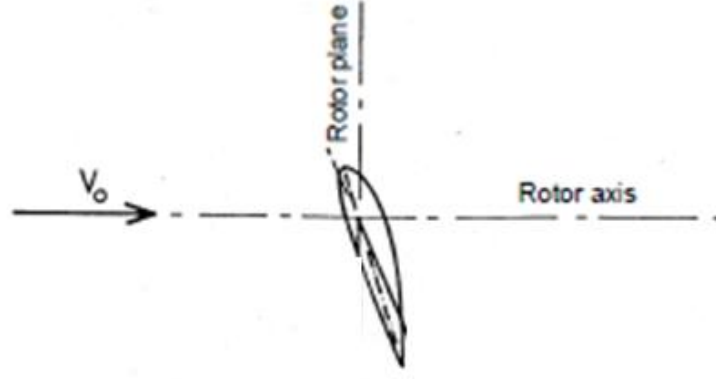


**Figure 3.11 Wind forces on the rotor of a horizontal axis wind turbine [3]**

Wind forces act mainly in the x direction, which is parallel to the rotor axis and 'V<sub>0</sub>' indicates the velocity of the wind. 'F' represents the axial force that the rotor shaft is exposed to, ' $\rho$ ' represents the air density, which is equal to 1,225 kg/m<sup>3</sup>, and 'A' represents the area that the blades swept in the formula. The radius of the rotor is 22.5 m and nominal mechanical power at blades is assumed to be 660 kW to produce 500 kW power at grid. In the view of such information, the axial force on the rotor is equivalent to 121.047 N. Wind force which is equal to axial force is shown by F<sub>x</sub>. This force generates a moment about y axis due to the fact that it acts at some offset distance to the yaw bearing. This moment due to axial wind forces is shown by M<sub>y</sub>, and M<sub>y</sub> is calculated by multiplying the wind forces with the distance between the center of mass of the blades and the face of the yaw bearing.

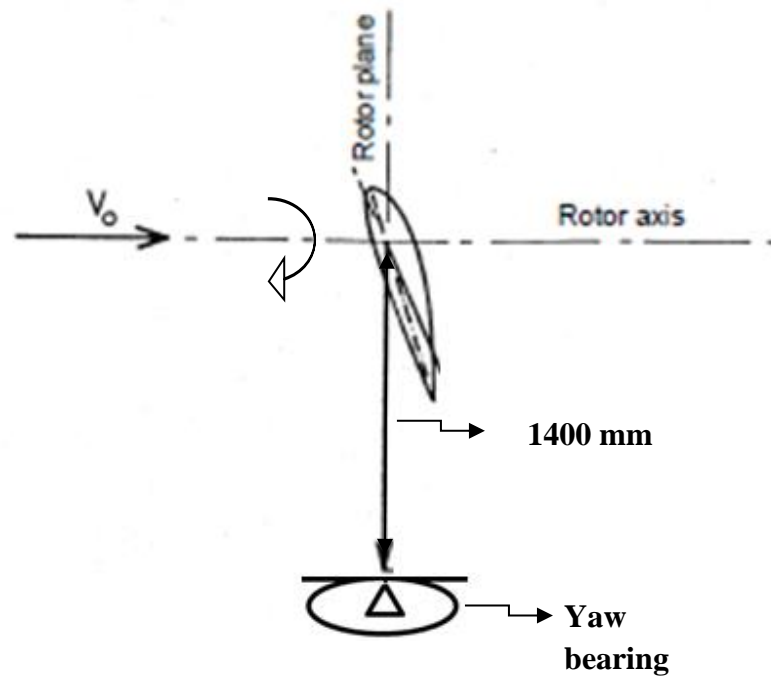


**Figure 3.12 Distance between the center of the mass of the blades and face of the yaw bearing [3]**

The resulting moment is  $M_y = 169,5 \text{ kNm}$ .

**Table 3.4 Wind forces and resulting moment generated on the yaw bearing for 500 kW horizontal axis wind turbine**

Power (kW)	Air density (kg/m <sup>3</sup> )	Radius of the blade (m)	$F_x$ (kN)	Distance between cog of the rotor and face of the yaw system (mm)	$M_y$ (kNm)
660	1,225	23	121	1400	169,5

Moment due to wind forces can also be calculated by using the cross product of force vector and position vector. Position vector and force vector is shown in Figure 3.13.

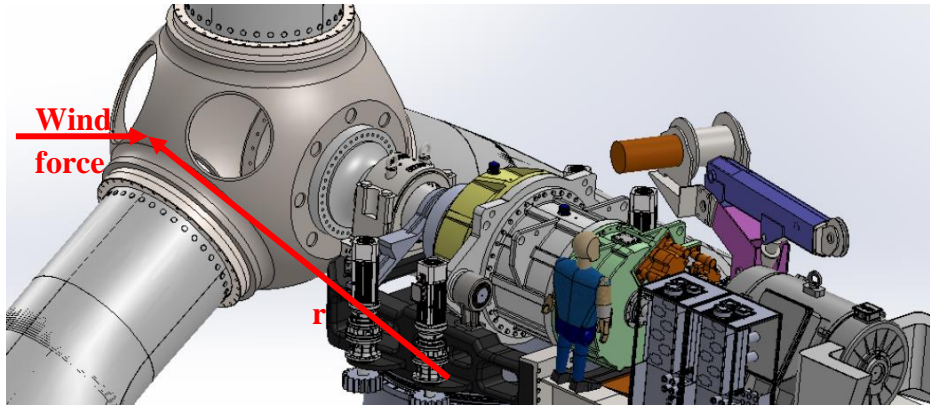


**Figure 3.13 Wind force vector and position vector of the wind force according to the yaw bearing center of gravity**

**Table 3.5 Wind force and moment vector**

$\vec{F}_x$	$\vec{r}$	$\vec{M}_y$
- 121i	-3,4i + 1,4k	169,5j

### 3.4 Calculation of the Generator Induced Moment on the Yaw Bearing of 500 kW HAWT

The generator converts the mechanical energy into electrical energy in a wind turbine. During blades rotary motion, kinetic power of the wind is transformed in to mechanical energy on the rotor, and through rotor and gear train this mechanical energy is conveyed to the generator. Lastly, electrical energy is obtained from the generator [3]. The generator is one of the sources of the moment loads in a wind turbine system. This moment also affects the yaw bearing in a horizontal axis wind turbine. Assuming the wind turbine is working at a constant rated speed, driving torque from the high speed shaft is equal to the torque that the generator counters. Generator torque can be calculated by using the formula (3) as follows;

$$P = T\omega \quad (3)$$

‘T’ symbolizes the torque that the generator undergoes, ‘ $\omega$ ’ symbolizes the angular speed of the high speed shaft and ‘P’ symbolizes the power. While calculating the moment that the generator induces, losses during transmission of power from rotor to

generator should be taken account. In the course of energy transmission from rotor to generator, losses due to the low speed shaft bearings, gear box, and high speed shaft can be considered. The power flow through the drive train with assumed power losses is shown in Figure 3.14 the below;

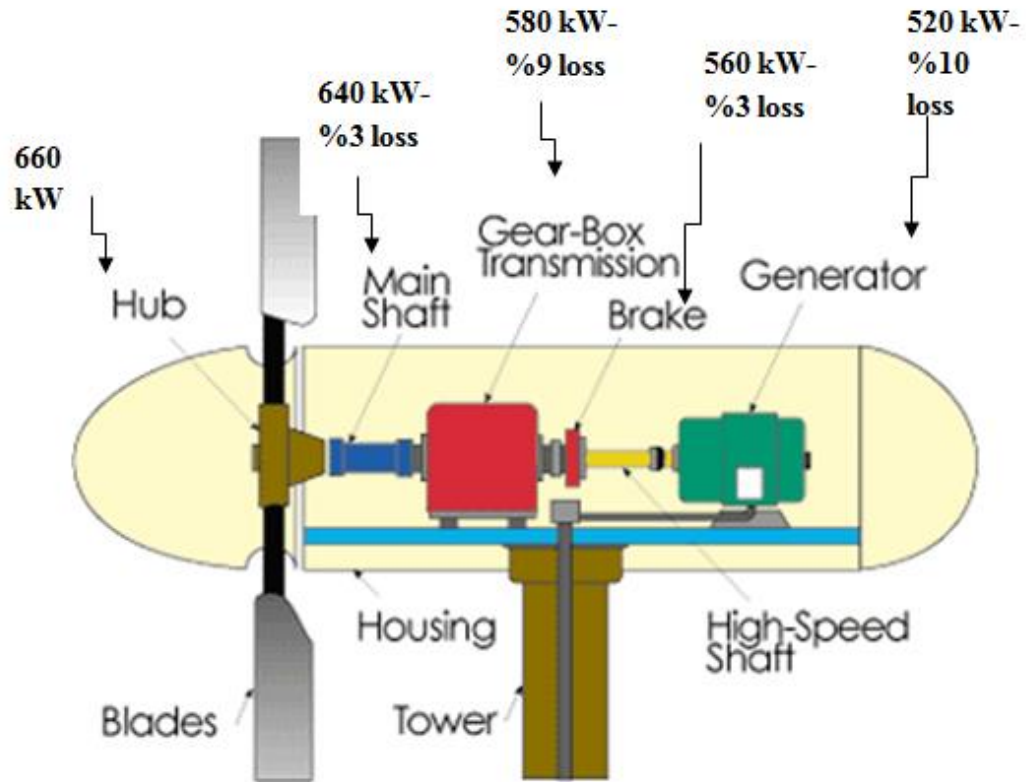


**Figure 3.14 Power transmission from rotor to the generator [8]**

As shown in Figure 3.14 the input mechanical power from rotor is estimated at 660 kW due to wind forces. 660 kW power is transmitted to main shaft and output power from the main shaft is 640 kW because of assumed %3 miscellaneous losses including bearings. This power is conveyed to gear box and output power from gearbox is 580 kW as a result of assumed % 9 loss. Therefore, 580 kW power transmitted through the coupling. The output power after mechanical coupling is assumed at 560 kW. Finally, it is assumed that produced power at generator outlet is 520 kW due to %10 loss. It is also assumed 20 kW power loss margin for power electronics and transformers before grid connection. The power loss numbers are specially selected high, i.e. with lower efficiency values than actual, to obtain a conservative analysis.

By the help of the input power to the generator and angular velocity which is calculated by using the speed of revolution of the rotor, generator torque is determined.

Angular speed of high speed shaft is taken at 800 rpm (worst case); it was converted into rad/sec;

$$800 \text{ rpm} = 800 * 2 * \pi / 60 \text{ rad/sec} \quad (4)$$

Then, power was divided by angular speed and torque was calculated.

**Table 3.6 Torque generated at generator**

<b>Power (kW)</b>	<b>Revolution (rev/min)</b>	<b>Speed</b>	<b>Angular speed (rad/sec)</b>	<b>Torque (Nm)-M<sub>x</sub></b>
560	800		83,7758	- 6684,5

Generator torque is - 6684,5 Nm and symbolized by M<sub>x</sub>. Normally, aeromechanical torques generated at blades are countered not only by generator itself but also by torque losses in gearbox and friction forces at main bearing and couplings. In order to make a conservative analysis and simplify the solution procedure, the minor torque losses between the blades and the generator have been neglected, and all the of the 660 kW blade torque has been assumed to be countered by the generator torque itself. Although the nominal working generator speed is 850 rpm, generator speed has been assumed at the lower end of speed tolerance at 800 rpm for even more conservative approach to give the maximum generator counter torque.

**Table 3.7 Torque generated at generator (Gear box and friction torques included)**

<b>Power (kW)</b>	<b>Revolution (rev/min)</b>	<b>Speed</b>	<b>Angular speed (rad/sec)</b>	<b>Torque (Nm)-M<sub>x</sub></b>
660	800		83,7758	- 7878,17

Due to generator torque during operation, there is a force couple exists which try to rotate the bearing around x-axis. This force couple occurs on the points where the generator touches the surface of the bedplate.



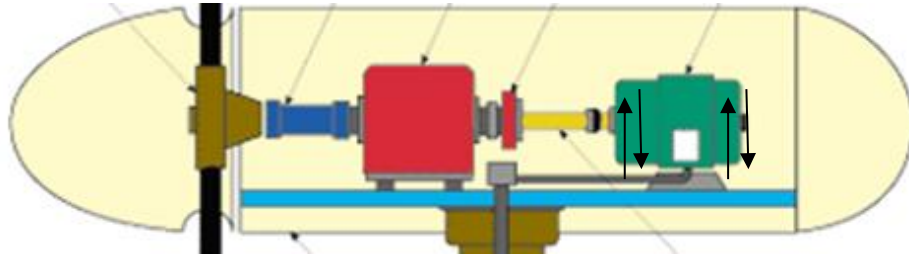


Figure 3.15 Up and down forces due to generator working [8]

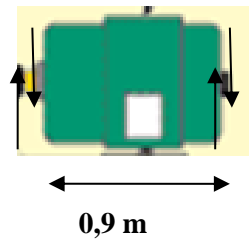


Figure 3.16 Schematic view of generator force couple

By dividing the generator torque to the length of the generator, force couples can be calculated.  $7,8 \text{ kN} / 0,9 = 9 \text{ kN}$ . Force couple can be divided into two parts due to four foot of the generator. By dividing two, every force magnitude can be determined.  $9 \text{ kN} / 2 = 4,5 \text{ kN}$ . Generator torque can be calculated by using the cross product. In order to determine the moment vector, force vector and position vector of these forces should be known.

$$\vec{M}_x = \vec{r} \times \vec{F}_z$$

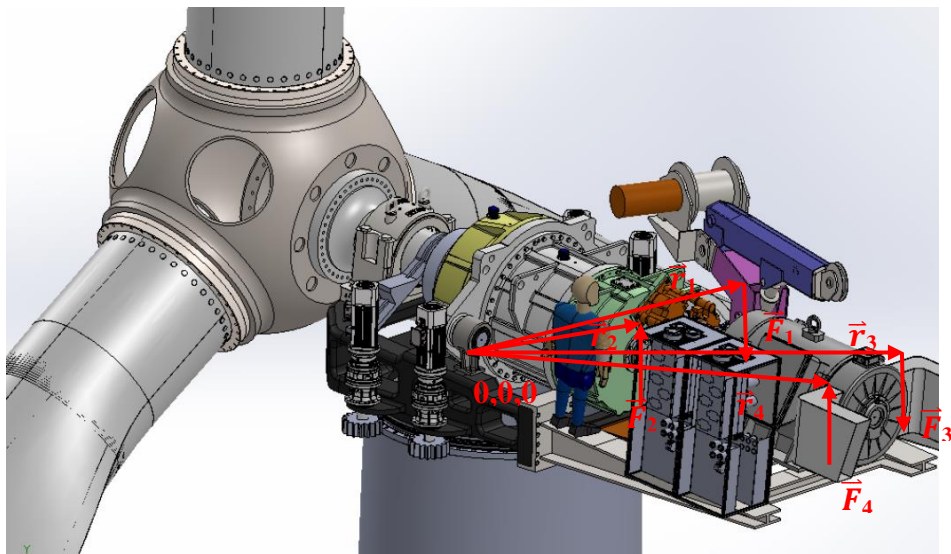


Figure 3.17 Position vectors and force couples on the wind turbine

In order to determine the position vectors, coordinate of the foot of the generator was firstly found out. Then, center of the mass of the yaw bearing was determined and from the differences of the coordinates, position vectors were calculated.

Magnitude of  $\vec{F}_1, \vec{F}_2, \vec{F}_3$  and  $\vec{F}_4$  is equal to 4,5 kN.

$$\vec{F}_1 = -4,5\mathbf{k} \text{ and } \vec{r}_1 = 1,97\mathbf{i} + 0,7\mathbf{j} + 0,23\mathbf{k}$$

$$\vec{F}_2 = 4,5\mathbf{k} \text{ and } \vec{r}_2 = 1,97\mathbf{i} - 0,1\mathbf{j} + 0,23\mathbf{k}$$

$$\vec{F}_3 = -4,5\mathbf{k} \text{ and } \vec{r}_3 = 2,7\mathbf{i} + 0,7\mathbf{j} + 0,23\mathbf{k}$$

$$\vec{F}_4 = 4,5\mathbf{k} \text{ and } \vec{r}_4 = 2,7\mathbf{i} - 0,1\mathbf{j} + 0,23\mathbf{k}$$

$$\begin{aligned} \vec{M}_x &= (1,97\mathbf{i} + 0,7\mathbf{j} + 0,23\mathbf{k}) \times (-4,5\mathbf{k}) + (1,97\mathbf{i} - 0,1\mathbf{j} + 0,23\mathbf{k}) \times (4,5\mathbf{k}) + (2,7\mathbf{i} + 0,7\mathbf{j} + \\ &0,23\mathbf{k}) \times (-4,5\mathbf{k}) + (2,7\mathbf{i} - 0,1\mathbf{j} + 0,23\mathbf{k}) \times (4,5\mathbf{k}) \\ &= -7,2\mathbf{i} \end{aligned}$$

### 3.5 Calculation of the Brake Torque on the Yaw Bearing for 500 kW HAWT

When emergency shutdown is applied, a braking torque on the yaw bearing is generated while rotational inertia of the system is countered. Mechanical brake is placed on the high speed shaft at the exit of the gearbox. It is composed of two brake calipers, a brake disc and brake pads. Mechanical brake is used for the purpose of an emergency stop or as a precaution during maintaining or servicing [3]. Mechanical brake on the high speed shaft of the gearbox of the designed horizontal axis wind turbine is shown in the Figure 3.18.

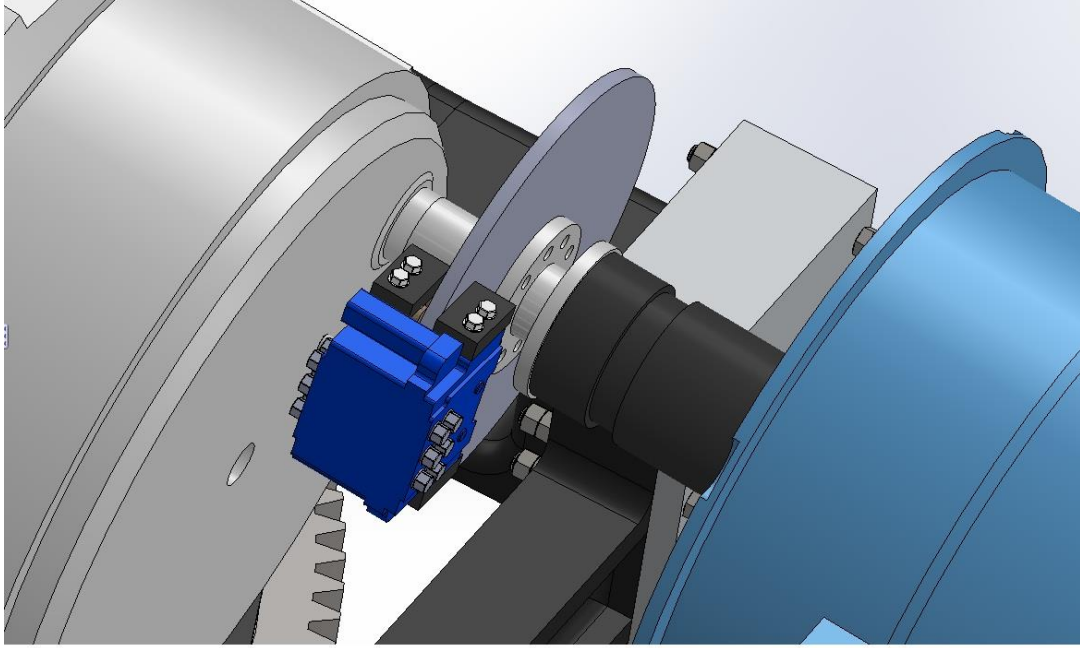


**Figure 3.18 Mechanical brake on the high speed shaft**

Torque on the high speed shaft during a brake can be calculated by using the formula;

$$T_r = I\alpha \text{ for the rotational systems} \quad (5)$$

In the formula, T represents the brake torque; I represents the inertia of the all rotating mass, r represents the radius of the rotor and  $\alpha$  represents the angular deceleration of the system. Rotational inertia is calculated by the help of system solid model with Solid Works. According to the code, rotary inertia of the designed wind turbine is 346.728,53  $\text{kgm}^2$  which was obtained from wind turbine project design team.

Angular deceleration was calculated by assuming the full speed of the wind turbine to go down to the zero in five seconds, where the rotational speed of the wind turbine is equal to 28 rpm. First, angular speed is calculated by using the formula given below. In the formula, ' $\omega$ ' represents the angular speed.

$$\omega \text{ (rad/sec)} = 2\pi * V_{\text{Rotational speed (rpm)}} / 60 \quad (6)$$

$$\omega = 2,93 \text{ rad/sec}$$

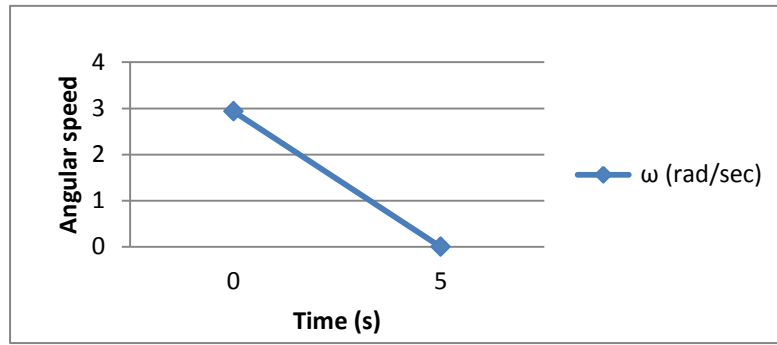


**Figure 3.19 Angular speed vs time**

Then, deceleration rate is found by dividing the difference between the initial and final angular speed with the time it takes during speed decrease. The angular deceleration was found as.

$$\alpha \text{ (rad/s}^2\text{)} = (2,93 - 0) / 5$$

**Table 3.8 Calculation of deceleration from rotational speed**

$V_{\text{rotational}}$ (rev/min)	$\omega$ (rad/sec)	$\alpha$ (rad/s <sup>2</sup> )
28	2,93	-0,58

In the light of this information, calculations are made and angular deceleration is found as 0,58 rad/s<sup>2</sup>. Radius of the rotor is known as 22,5 m. Then, torque which is generated because of the brake of the system is determined by using the formula given above:

$$T^* r = I \alpha \tag{7}$$

$$T^* 23 = 346728,53 \text{ kgm}^2 * 0,58 = 2033324 \text{ kgm/s}^2$$

**Table 3.9 Brake torque for a 500 kW horizontal axis wind turbine**

$I$ (total) (kgm <sup>2</sup> )	Brake torque (kNm)- ( $M_x$ )
346728,53	8,840

Brake torque is 8,840 kNm and is symbolized by  $M_x$ .

Due to braking, there is a force couple exists which try to rotate the bearing around x-axis. This force couple occurs on the points where the brake pads touch the surface of the brake disc in the up and down direction. By dividing the brake moment by the brake disc diameter this force couple can be determined.  $8,8 \text{ kNm} / 0,6 \text{ m} = 14,7 \text{ kN}$ .

An illustration shows the brake pad, brake disc and force vectors with position vector in Figure 3.20 below.

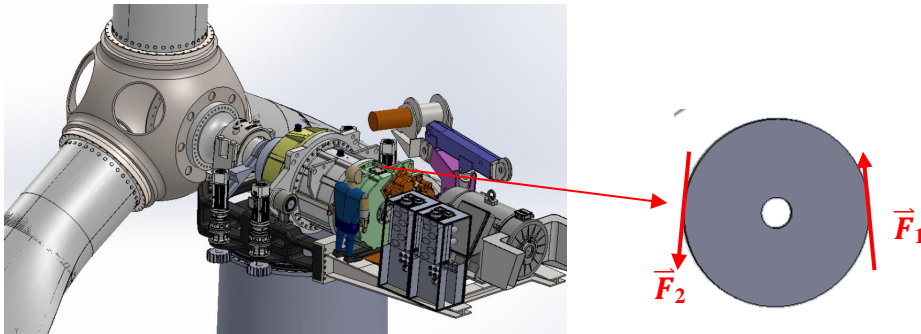


**Figure 3.20 Forces on the brake disc due to braking**

By using cross product, moment vector can be determined. Force and position vectors are given below.

$$\vec{F}_1 = 14,7\text{k} \text{ and } \vec{r}_1 = 1,2\text{i} + 0,6\text{j} + 0,8\text{k}$$

$$\vec{F}_2 = -14,7\text{k} \text{ and } \vec{r}_2 = 1,2\text{i} + 0,015\text{j} + 0,8\text{k}$$

$$\begin{aligned} \vec{M}_x &= (1,2\text{i} + 0,6\text{j} + 0,8\text{k}) \times 14,7\text{k} + (1,2\text{i} + 0,015\text{j} + 0,8\text{k}) \times -14,7\text{k} \\ &= 8,6\text{i} \end{aligned}$$

### 3.6 Resultant Forces and Moments on the Yaw Bearing of 500 kW HAWT

A table is given below which shows all the calculated forces and moments.

**Table 3.10 Forces and moments occurs on the yaw bearing**

Forces and Moments	
<b>Wind forces</b>	121,05 kN
<b>Gravitational forces</b>	-380,98 kN
<b>Torque due to wind forces</b>	169,5 kNm
<b>Torque due to gravitational forces</b>	-169,75 kNm
<b>Generator torque</b>	7,87 kNm
<b>Brake torque</b>	8,84 kNm

An illustration which shows the calculated forces and moments on the yaw bearing given below.

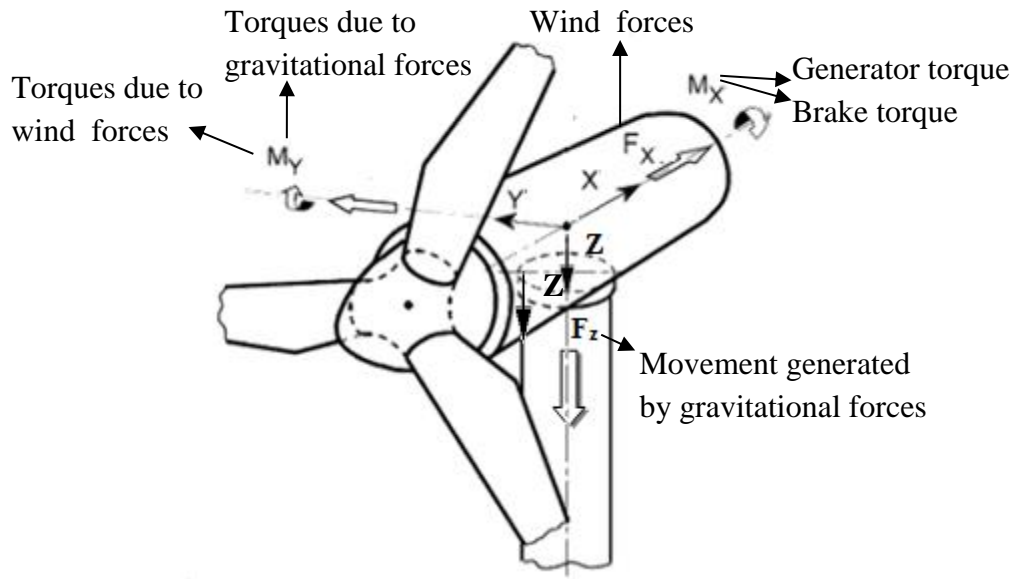


**Figure 3.21 Forces and moments effect the yaw bearing**

There are two loading cases that will be considered. One is the nominal working condition and second is the emergency stop condition.

During nominal working condition, aero braking is applied by misaligning blade position with respect to wind direction to facilitate normal turbine stop. Therefore, mechanical brakes are only used for emergency shutdown. As a result, during normal working condition mechanical brake torque does not happen where the other forces and moments in Figure 3.21 exist. Generator torque which is called  $\vec{M}_x$  occurs along the rotation of the main shaft axis, while torques due to wind forces and gravitational forces which are symbolized by  $\vec{M}_y$  occurs perpendicular to the axis of the shaft rotation. Additionally, moments because of the gravitational forces and moments due to wind forces are opposed to each other. Therefore, we can write the moment vector at the yaw bearing as follows.

$$\vec{M}_{\text{resultant}} = \sqrt{(\vec{M}_x^2 + \vec{M}_y^2)} \quad (8)$$

The resultant moment can be calculated as indicated below.

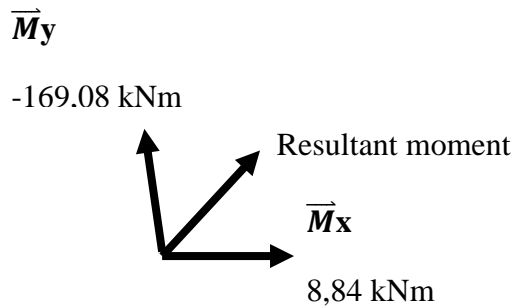
$$\begin{array}{c} \vec{M}_y \\ -169,08 + 169,5 = -0,42 \text{ kNm} \\ \vec{M}_{\text{resultant}} \\ \vec{M}_x \\ 30 \quad 7,87 \text{ kNm} \end{array}$$

Magnitude of the resultant net moment on the yaw bearing

$$= \sqrt{(7,87^2 + (-0,422)^2} = 7,88 \text{ kNm}$$

During emergency stop conditions, both generator torque and torque due to wind forces are canceled out because in order to stop the wind turbine, blades are firstly change their position and stop the wind effects then generator stops. Only braking torque and moments due to gravitational forces occur. Therefore, we can write the moment vector at the yaw bearing as follows.

$$\text{Resultant moment} = \sqrt{(\vec{M}_x^2 + \vec{M}_y^2)}$$



The resultant moment can be calculated as indicated below.

$$\text{Magnitude of the resultant moment} = \sqrt{(169,08^2 + 8,84^2)} = 247,22 \text{ kNm}$$

Resultant moments for two conditions are given in Table 3.11.

**Table 3.11 Resultant moments**

Resultant Moments	
<b>Nominal working condition</b>	7,88 kNm
<b>Emergency condition</b>	247,22 kNm

While designing yaw bearing for 500 kW horizontal axis wind turbine, emergency and nominal working conditions will be examined separately and design will be done according to the worst case.

## 4 Design & Analysis of the Yaw Bearing for a 500 kW HAWT

The literature survey and past applications indicate that slewing type bearing is suitable to use as a yaw bearing for the horizontal axis wind turbine in comparison to sliding bearing. Slewing bearing mechanism, selection and life calculations will be described in the following sections.

### 4.1 Slewing Bearing Mechanism and Slewing Bearing Types

Slewing bearings can bear radial and axial loads together with the moments occurred because of the rotation.

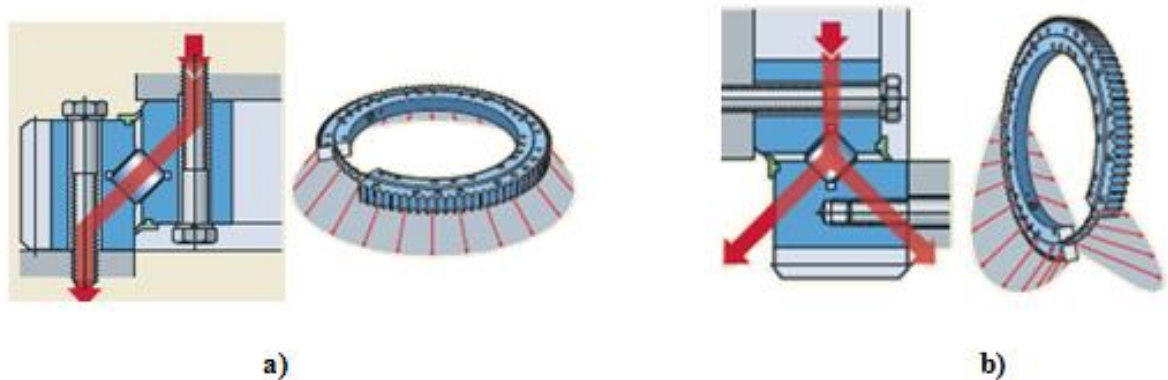


**Figure 4.1 a) Transmission of an axial loads in a slewing bearing b) Transmission of radial loads in a slewing bearing [20]**

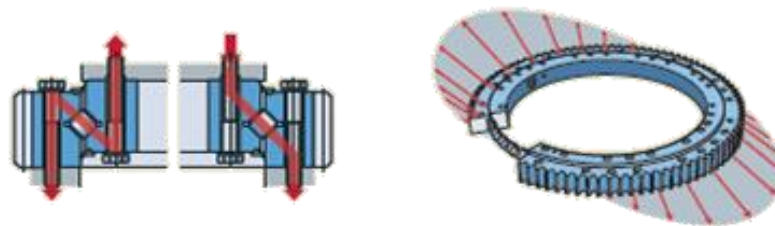


**Figure 4.2 Transmission of moments in a slewing bearing [20]**

Slewing bearings are large type of rolling element bearings. In general, a slewing bearing is composed of an inner ring, outer ring and rolling elements which can include balls or rollers [6]. A typical example of ball slewing bearing is shown in Figure 4.3.



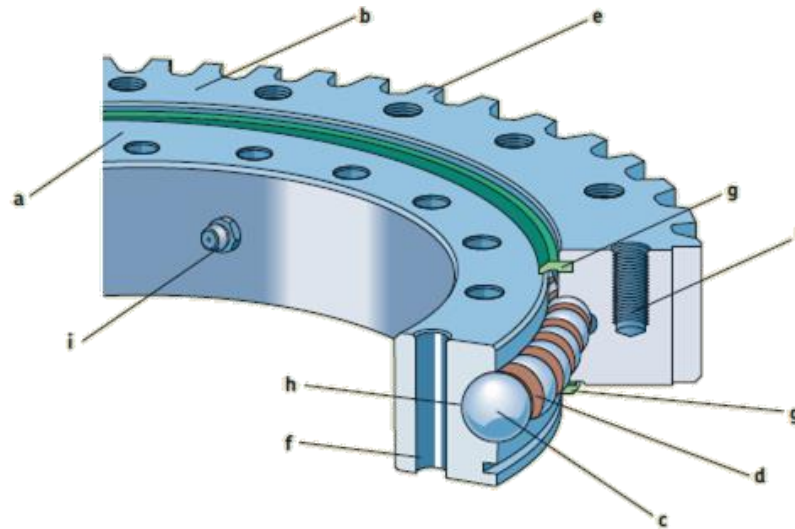


**Figure 4.3 An illustration of a slewing bearing [20]**

In the figure, (a) is the inner ring, (b) is the outer ring, (c) refers to rolling elements-balls or cylindrical rollers, (d) is polyamide spacer which divides rolling elements from each other. (e) is gear which can be either at inner or outer ring, (f) refers to bolt holes, (g) is seal made by acrylonitrile butadiene rubber (NBR) in order to prevent oil leakage from the bearing and to hold pollutants out of the bearing [6].

Slewing bearings can be designed with an external or internal gear according to the design need. Typical examples of cylindrical roller slewing bearings with external and internal gears are given in Figure 4.4.

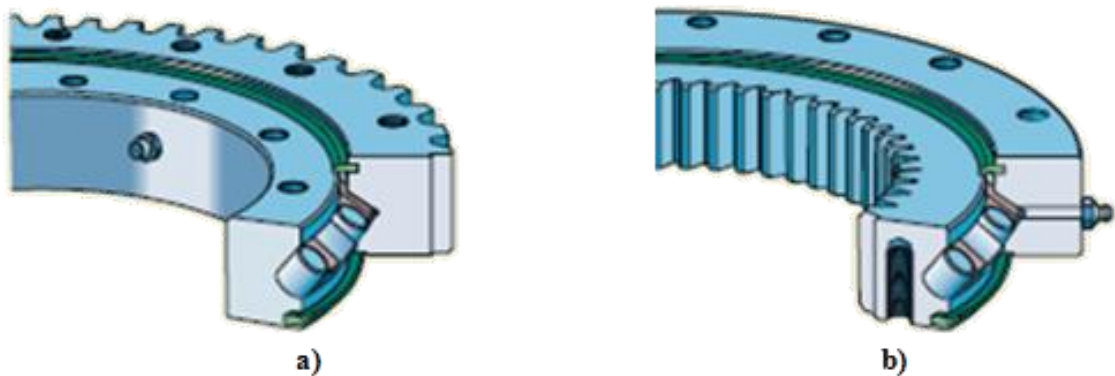


**Figure 4.4 a) Single row cylindrical roller slewing bearing with an external gear b) Single row cylindrical roller slewing bearing with an internal gear [6]**

Slewing bearings may vary. The proper type of slewing bearing should be selected with regard to the several factors such as type of loads and moments, accuracy, cost, working speed or sealing [6]. Slewing bearings can be categorized as ball slewing bearings and roller cylindrical bearings. A sample table of comparisons of different type of slewing bearings is given below;

**Table 4.1 Slewing bearing selection guide [6]**

Slewing Bearing Selection Guide					
Slewing Bearing Type	Suitability of bearings for				
	High running accuracy	High speeds	Heavy static loads	Vibration	Long service life
Single four point contact ball slewing bearing	-	+	+	o	o
Single row crossed cylindrical roller slewing bearings	+	-	o	+	+
'o' means suitable '-' means not recommended '+' means recommended					

It is clearly seen from Table 4.1 that cylindrical roller slewing bearings have superiorities in comparison with the ball slewing bearings in terms of service life, accuracy and vibration.

If general, it can be said that ball bearings are more appropriate for the applications which require high speed, low torque and having less contact points than rolling bearings and lower frictional resistance. Ball bearings get in touch with the inner and outer rings of the bearing like a point while roller bearings are contacting the raceways in a line. That's why the contact surface of the roller bearings are bigger than ball bearings and on the contrary to the ball bearings, roller bearings are suitable for applications which require heavier load carrying, long service life and durability under heavy or shock loads [9].

Shortly, it can be said that both cylindrical rollers and ball slewing bearings have advantages individually but due to accuracy, low vibration and service life requirements, it is decided to select one of the cylindrical roller slewing bearing types for the yaw bearing.

#### **4.2 Selection of Slewing Bearing for 500 kW HAWT**

There are different categories of cylindrical roller bearings: Four and eight point contact, one row roller, three row roller, bi-angular roller and taper designs. Gear drives are provided by inner or outer gear-drive, or driven directly by the inner or outer-ring. So as to decide which kind of cylindrical roller bearing is suitable for the designed horizontal axis wind turbine, first, the magnitude and direction of the loads should be known. Then, the size of the bearing is selected. Afterwards, suitable bearing type can be decided.

Based on the nacelle design, it is decided that the bearing will have an external gear where nacelle will be bolted on the inner ring. The outer ring of the bearing will be bolted to the tower. This means that outer ring will be stationary while nacelle is turning by the help of the inner ring. External gear has been preferred to create more space inside the tower. Additionally, dimension of the bearing has been determined according to the dimensions of tower and nacelle size.

First, design loads have been checked in order to select the appropriate slewing bearing type. Load ratio between the radial and axial loads should be in the permissible range. If  $F_r / F_a \leq 0,6$ ; it means that  $F_r$  may be neglected [6].

It is known from the calculations before that  $F_r = 121$  kN and  $F_a = 380,98$  kN. The ratio between  $F_r$  and  $F_a$  is equal to 0.31 which is in the allowable range. This means radial force can be neglected while selecting a bearing.

Secondly, a static limiting load diagram was used to determine the size and type of the rolling slewing bearing [6]. Figure 4.5 shows static limiting load diagram. X axis is maximum rated axial load and Y axis is maximum rated bending moment. Rated values can be obtained by multiplying with safety factor.

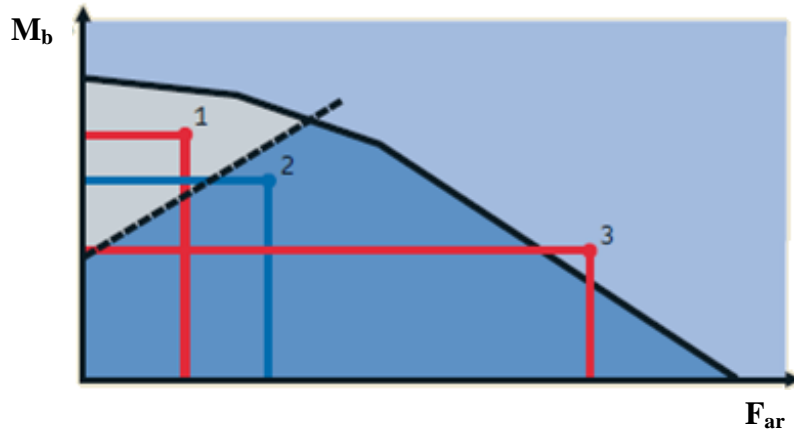


**Figure 4.5 Static force limiting diagram [6]**

In the figure solid line represents the limitation of raceway and dash line represents the limitation of bolts. There are numbers 1,2,3 on the diagram are given as design case examples. The point 1 is under the solid line and above dash line doesn't meet the requirements because of lacking in bolt force capacity. Point 2 which is under both dash and solid lines is adequate to satisfy all the requirements and suitable to use as a bearing. Last point 3 above the solid line is not adequate due to lack of raceway capacity [6].

Loads and moments on the yaw bearing of a horizontal axis wind turbine have already been calculated in the previous chapter. An illustration of the direction of the tilt moment, radial and axial forces on the yaw bearing are given in Figure 4.6 below.

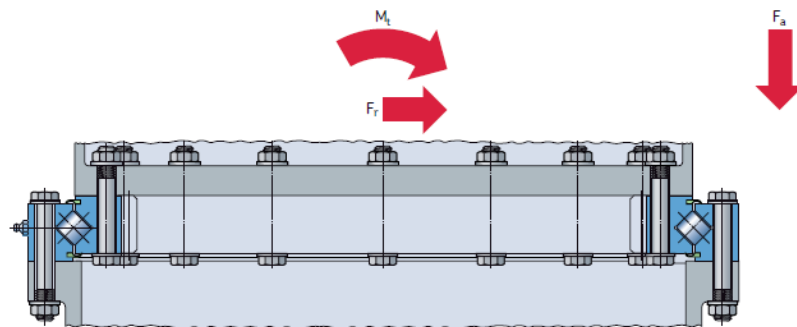


**Figure 4.6 Typical example of loads and moments on a slewing bearing [6]**

While selecting an appropriate bearing, emergency stop condition will be used as it generates more severe load combination on the bearings to be on the conservative side. It should be noted that during emergency shutdown, blades are oriented to generate zero torque. Therefore, generator torque and wind offset moments with respect to yaw bearing are neglected.

During operation of the wind turbine, yaw bearing is subjected to vibrations and disturbances. These vibrations increase the effects of static loads on the bearing higher than the typical values determined [10]. By using safety factor of 2, rated forces and moments are calculated. Based on this information, loads and moments are given in Table 4.2 below.

**Table 4.2 Rated forces and moments**

<b>Rated axial force and rated bending</b>	
<b>F<sub>a</sub></b>	761,96 kN
<b>M<sub>bending</sub></b>	494,44 kNm

Values with prime represent the moments and forces which were multiplied by 2 as safety factors. After calculating the rated values, a feasible bearing can be selected from the catalogue of slewing bearings. While selecting the bearing, domestic manufacturers are preferred. It's seen from one of the domestic manufacturer's catalogue that triple rowed roller bearing gives the best solution according to load ratings because three rollers arrangement provides two rollers to meet the axial and moment loads requirement while the third roller meets the requirement of radial loads. In the light of such information, one of the triple rowed roller bearing with external gear was selected as a suitable slewing bearing by checking the limit loading diagram from the catalogue.

## Bending Moment (kNm)

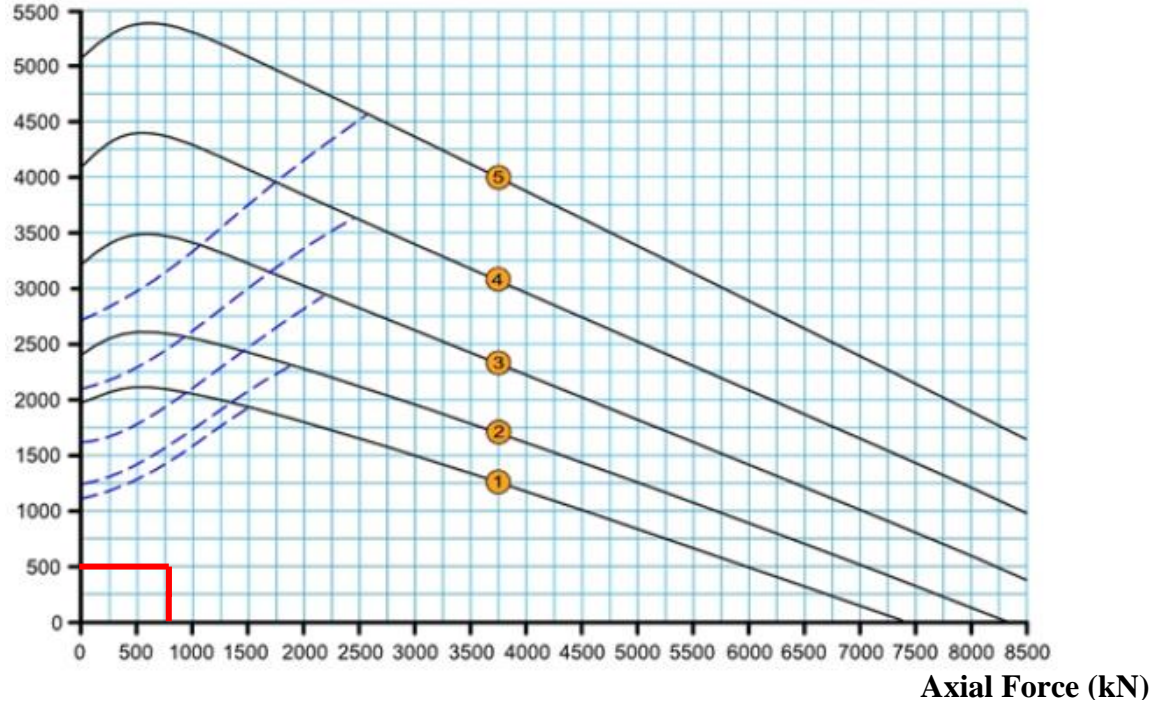


Figure 4.7 Static loading diagram of selected triple rowed slewing bearing [11]

It's indicated with red lines that all type of the bearings can be used as a yaw bearing because all of them meet the load requirements. However, number five has been selected due to large tower top flange size and bolt axis diameter. The selected ring dimensions given in Table 4.3.

Table 4.3 Bearing Dimensions [11]

		Ağırlık Weight	Diş Ring Dış Çap Outer Diameter	Diş Ring Fatura Çapı Diameter	Diş Ring İç Çap Diameter	İç Ring Dış Çap Diameter	İç Ring Fatura Çapı Diameter	İç Ring İç Çap Inner Diameter	Bilya Eksenli Ball Track Diameter	Diş Ring Delik Eksenli Ex. Bolt Circle Diameter	İç Ring Delik Eksenli In. Bolt Circle Diameter	Diş Ring Delik Çapı External Hole Diameter	İç Ring Delik Çapı Internal Hole Diameter	Klavuz Derinliği Thread Depth	Diş Ring Delik Adedi Number Of Bolt Holes	İç Ring Delik Adedi Number Of Bolt Holes	Diş Ring Kalınlık Ring Height	İç Ring Kalınlık Ring Height	Toplam Kalınlık Overall Height	Modül Module	Diş Sayısı Number Of Teeth
		kg	mm	mm	mm	mm	mm	mm	mm	mm	mm	mm	mm	mm			mm	mm	mm	m	z
1	I.1397.3R20.01.01	540	1397	-	1219	1218	-	1032	1250	1345	1145	26	26	-	36	36	123	106	132	12	87
2	I.1547.3R20.01.01	630	1547	-	1369	1368	-	1162	1400	1495	1295	26	26	-	36	36	123	106	132	14	84
3	I.1747.3R20.01.01	705	1747	-	1569	1568	-	1372	1600	1695	1495	26	26	-	40	40	123	106	132	14	99
4	I.1947.3R20.01.01	830	1947	-	1769	1768	-	1552	1800	1895	1695	26	26	-	46	46	123	106	132	16	98
5	I.2147.3R20.01.01	900	2147	-	1969	1968	-	1760	2000	2095	1895	26	26	-	54	54	123	106	132	16	111

Technical drawing of selected bearing is given below in Figure 4.8.

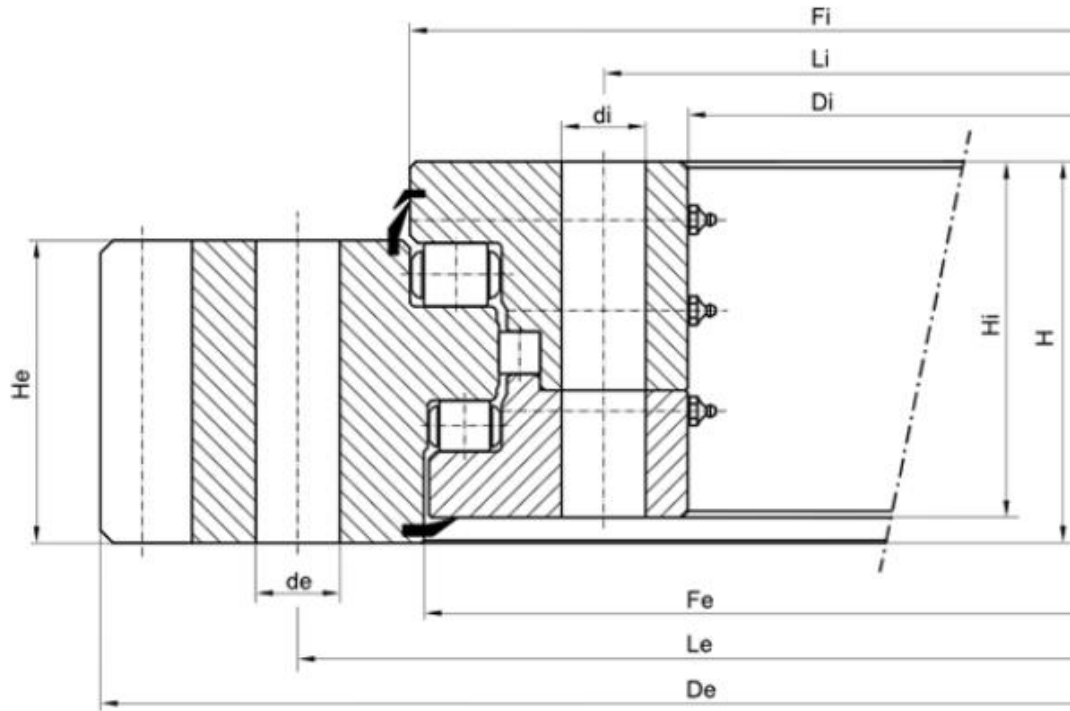


**Figure 4.8 Technical drawing of triple rowed roller bearing from the catalogue [11]**

In order to check if the selected bearing meets the load requirement or not, a diagonal red line is drawn and coincide with the intersection point of bending moment and axial force and then, the line is extended until the static load curve of the selected bearing in Figure 4.9. The moment and force values are obtained as 3400 kNm and 4800 kN, respectively. If these numbers are divided by 247 kNm and 381 kN, the factor of safety 13 is obtained.  $13 > 2$  which means our selected bearing is very safe. Therefore, the selected bearing meets the load requirements [12].

## (kNm)



Subsequent to bearing selection, life calculations and fatigue limits are verified. Fatigue life calculations given in detail in the following section.

The fatigue life shows how long or how many service hours a bearing can endure until the signs of fatigue can be seen. Material fatigue occurs because of cyclic stresses arise on the rolling elements and races during rotation. Life of the slewing bearings can be determined by using a statistical theory which is based on maximum contact stress as outlined by Lundberg and Palmgren. American Bearing Manufacturers' Association (ABMA) admitted as a standard ANSI/ABMA-9 in 1990 for ball bearings and ANSI/ABMA-11 in 1990 for roller bearings [10].

$$L_f = (f_0)^p \cdot 30000 \quad (9)$$



In the formula ' $L_f$ ' represents the life of the bearing and ' $f_n$ ' represents the dynamic load factor while  $p$  is equal to 3 for ball bearings and  $10/3$  for roller bearings [Lyc slewing bearing catalogue].

So as to determine the life of the bearing, a graph of the selected bearing which consists of both dynamic and static load curves is needed. There is a sample graph which includes both static and dynamic load curves of a slewing bearing given in Figure 4.10 below. This slewing bearing is similar with the selected slewing bearing from point of dimension, type and static loading curves.

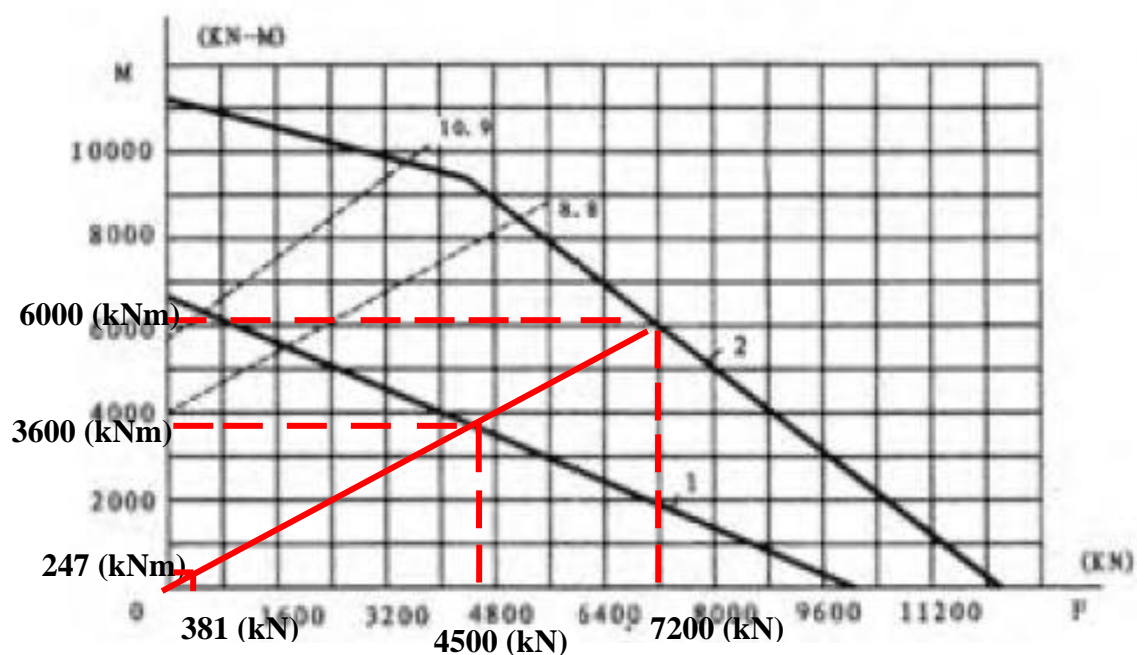


**Figure 4.10 Static and dynamic loading diagram of a similar triple rowed slewing bearing [13]**

In the graph, curve 1 represents the static loads, and curve 2 represents the dynamic loads. When the values of axial force and bending moment of real bearing are placed on the diagram, and intersect with the curve 1, it is clearly seen that nearly same values are obtained as static rated loads which mean dynamic loads can be checked by using this diagram. By extending the diagonal red line from the point of junction of the axial force and bending moment, dynamic load is obtained as 7200 kN and moment is obtained as 6000 kNm. Together with these values, dynamic load can be found as

$$7200 / 381 = 19 \text{ and } 6000 / 247 = 24$$

Small value which is equal to 19 is selected as dynamic load factor. Dynamic load factor is special for the bearing type [13].

$$L_f = 19^{(10/3)} * 30000 = 549077007 \text{ revolutions}$$

Mainly, the service life of a slewing bearing depends on the working conditions which are torque, speed of the bearing, ambient temperature and lubrication. Life which was calculated by using formula gives approximate life of the bearing and can be longer or shorter according to the outside factors [13]. Considering that there is no continuous rotation and speed is almost zero at the yaw bearings. The selected bearings satisfy life criteria.

#### 4.4 Material Selection of a Slewing Bearing and Production Method

Mostly, hardened steels are used for rings of the bearings and rolling elements applications. [10]

50 Mn which is carbon structural steel and 42CrMo which is alloy structural steel are mostly used in slewing bearing applications [13]. Chemical composition and mechanical properties are given in Table 4.4.

**Table 4.4 Chemical composition and mechanical properties of slewing bearing materials [13]**

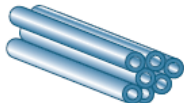


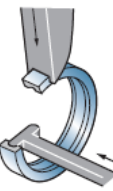
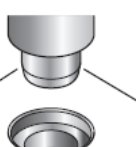
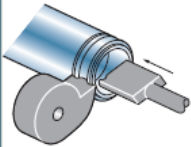
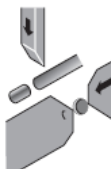
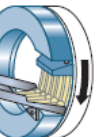
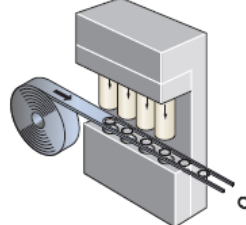
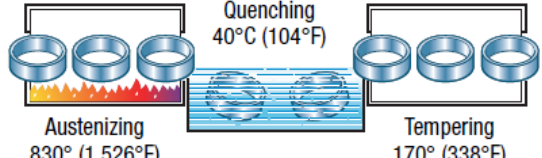
Material	Chemical component %					Mechanics Capability					
	C	Si	Mn	Cr	Mo	Tensile strength	Yield strength	Elongation	Reduction of area	Impact value	Standard
						MPA		%		J	
42CrMo	0,38-0,4	0,17-0,37	0,5-0,8	0,9-1,2	0,1-0,25	1080	930	12	45	63	GB/T3077
50Mn	0,48-0,56	0,17-0,37	0,7-1	-	-	645	390	13	40	31	GB/T699

Rolling elements are generally based on chrome steel GCr15 or GCr15SiMn. During material selection, operation circumstances, size of the bearing and load capacity should be considered. For large size rolling elements GCr15SiMn can be selected while for small size rolling elements GCr15 is selected. If the bearing operates slowly, steel 45 can be selected for low precision and load capability. However, for high precision and

load capability, 50Mn should be selected. 42CrMo is generally used for heavier loads, higher precision and large size of bearings [13].

Material of the slewing bearing has been selected as 42CrMo4 in ISO standards which corresponds to AISI 4140 steel due to its mechanical properties. Material of rollers has been selected as 100cr6 steel which is AISI 5210 according to ISO standards. Both of these are the materials accessible by domestic manufacturers and producible in Turkey.

Production methods and materials to manufacture rings, rolling elements and cage are given in Figure 4.11.

Operation	Rings	Rolling elements	Cage
Material	Tubes, bars 	Wire 	Coil strips 
Shaping	Turning  Forging  Rolling 	Cutting and cold heading  Ball blank 	Drawing steel cages  Molding of plastic cages Turning of solid metal cages
Heat treatment			

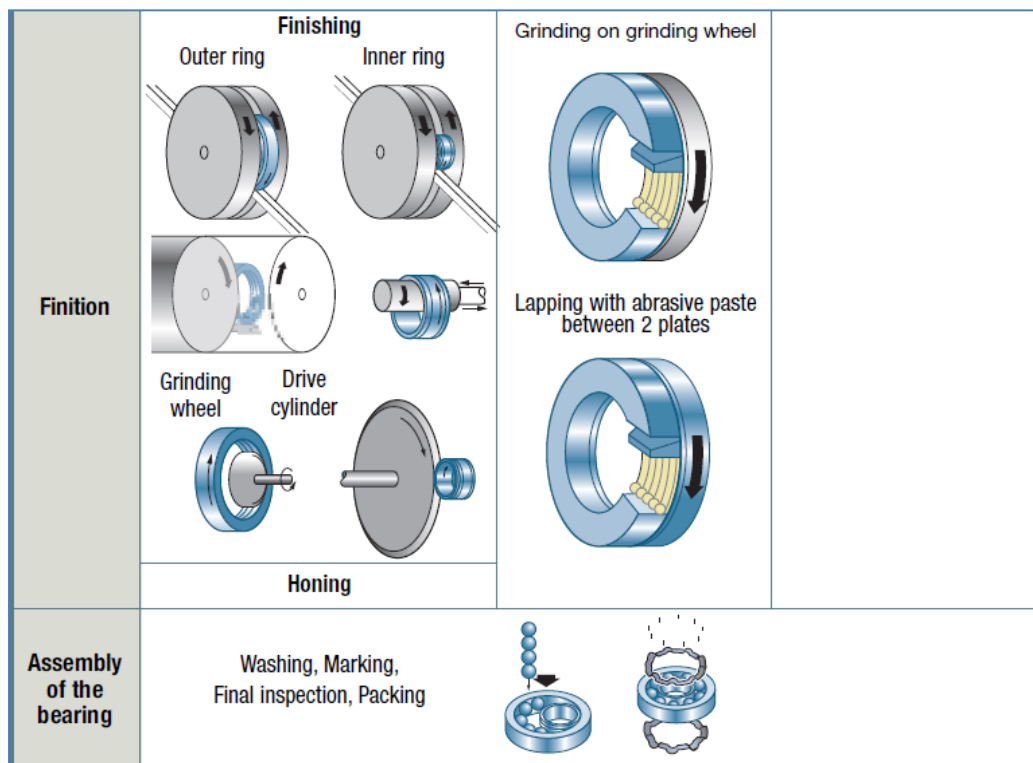


**Figure 4.11 Standard manufacturing process of slewing bearings [14]**

Although slewing bearings can bear loads in both radial and axial direction together with rotational moments, slewing bearings have some disadvantages because of being contact type of bearings. As the wind turbines are getting bigger and higher, slewing bearings used with these big size turbines have to be bigger and heavier in order to satisfy the heavily loads. Heavily loads cause damage on the bearing surfaces and inside the raceways, especially on the contact lines and points because of fretting, peeling or brinelling effects. Particularly, brinelling on the contact area is the biggest problem. At the beginning of the brinelling effect, marks are insignificant. Later, by the time, these scratches can cause deeper cuts, cavities, holes and can cause premature failure of the bearing [15]. In order to prevent these types of failures, an alternative bearing type as the yaw bearing of wind turbine is studied.

Hydrostatic bearing has been selected as alternative bearing type for yaw bearing of the selected horizontal axis wind turbine. Details about hydrostatic bearing design work are presented in the following chapter.

## 5 Design and Analysis of the Hydrostatic Yaw Bearing

As wind turbines get larger and heavier, yaw bearing gets larger depending on the size of the wind turbine. In order to bear these increasing loads, the yaw bearing needs to increase in size and weight, consequently increasing the cost in classical design [1]. In addition, together with larger wind turbine sizes, lives of contact type bearings get shorter. Because of the high costs and heavy loads, an alternative design is investigated. Table 5.1 compares three different bearing types.

**Table 5.1 Bearing selection for special performance requirements [16]**

Types of bearing	Accuracy of axial location	Low starting friction	Low running torque	Silent running	Simplicity of lubrication system
Rolling bearing	Good	Good	Good	Usually satisfactory	Good when grease lubricated
Hydrodynamic film bearing	Good	Fair	Good	Good	Usually requires circulation system
Hydrostatic film bearing	Excellent	Excellent	Good	Good	Special system necessary

As wind turbines get larger, non-contact type of bearings will be better to increase reliability and to extend the bearing life. From this point of view, hydrodynamic and hydrostatic bearings are preferred. When characteristics of hydrodynamic and hydrostatic type of bearings are compared, it is also evident in Table 5.1 that, starting friction is a major problem for hydrodynamic bearings. Hydrodynamic bearings rely on surface speed to generate operating lift force. Therefore, start up friction is high, which also causes wear. On the contrary, hydrostatic bearings do not have such a problem during start up and moreover, even at very low speeds they have very low sliding friction [10].

Considering various advantages and disadvantages of various bearing types as compared to classical rolling element bearings, hydrostatic bearings have been selected as the alternative design in this work. Working principles of hydrostatic bearings, major features and design aspects of a hydrostatic bearing will be explained in detail in the following section.

## 5.1 Hydrostatic Bearings

Hydrostatic bearing was first explored by L D. Girard who tried to operate a bearing which is fed by high pressure water for the railway propulsion system in 1851. Then, a hydrostatic annular thrust bearing was designed for a hydraulic turbine by Lord Rayleigh. He tried to determine load capacity, flow rate, and friction moment for a thrust bearing [17].

Hydrostatic bearings working principle is based on polar version of Reynolds equation. Reynolds was the first to formulate two sliding surfaces that are separated from each other by a viscous liquid by the help of hydrodynamic pressure in 1886 [18].

The first step to analyze a hydrostatic mechanism is to understand the Reynolds equation. Lubrication theory and Reynolds equation are briefed in the following sections.

### 5.1.1 Lubrication theory and Reynolds Equation

Generalized Reynolds equation is used as the basis for all of the hydrodynamic lubrication problems. Since most pressure pads are made in circular form in hydrostatic bearings a polar form of Reynolds equation has been used as it is easy to solve.

Polar form of Reynolds equation is given in the formula 10 below;

$$\frac{1}{r} \frac{\partial}{\partial r} \left( \frac{r}{\xi} h^3 \frac{\partial P}{\partial r} \right) + \frac{1}{r^2} \frac{\partial}{\partial \phi} \left( \frac{h^3}{\xi} \frac{\partial P}{\partial \phi} \right) = 6u (\cos \phi \frac{\partial h}{\partial r} - \sin \phi \frac{\partial h}{\partial \phi}) + 12 \Omega \frac{\partial h}{\partial \phi} + 12 \Omega \frac{\partial h}{\partial t} \quad (10)$$

In the formula,  $u$  represents the translational speed while  $\Omega$  represents the rotational speed.

According to the equation, in polar form of Reynolds equation, lower surface is sliding in  $x$ -direction at velocity  $u$  and  $\phi$  symbolizes the direction  $x$ .  $r$  symbolizes the geometry of the bearing,  $h$  is the film thickness and the change in  $h$  is in the direction of  $t$ .  $P$  represents the pressure and  $\xi$  symbolizes the viscosity in the equation.

There are some assumptions to simplify the equation [18]:

- ❖ Bearing is assumed as almost stationary,  $u \approx 0$  and  $\Omega \approx 0$  in the equation. This means bearing is sliding very slowly, and there is little or no rotation.
- ❖ Because of the symmetry,  
$$\frac{\partial}{\partial \phi} \approx 0 \rightarrow \frac{\partial h}{\partial \phi} \approx 0$$

- ❖ Bearing is assumed as steady which means that there is no change in  $h$  thickness in time, and there is no oscillation. Also, the thickness change in  $y$  direction is very small compared to the changes in other directions. That's why,  $\frac{\partial h}{\partial t} \approx 0$
- ❖ The lubricant is incompressible making density constant, which cancels  $\rho$ .
- ❖ The flow is laminar.
- ❖ Due to very slow motion, viscosity of the lubricant is assumed constant as in many other applications in the literature.

Then, Reynolds polar equation reduces to  $\frac{\partial}{\partial r}(rh^3 \frac{\partial P}{\partial r}) = 0$  for a hydrostatic bearing. This is the basic equation to find pressure distribution, load capacity, oil flow through integration.

### 5.1.2 Working Principles of Hydrostatic Bearings

Hydrostatic bearings are externally pressurized bearings, as lubrication oil is supplied by the help of an external source which is generally a pump. As hydrostatic bearing is being pressurized by an external pump changes in oil flow rate causes the change in the pressure. Oil pressure provides the lift force in the system to carry the work load. Hydrostatic bearings have some advantages in the area of load capacity and friction. Hydrostatic bearings do not need relative motion like hydrodynamic bearings which is another non-contact type bearing [18]. An illustration of a hydrostatic bearing with a circular pad is given in Figure 5.1.

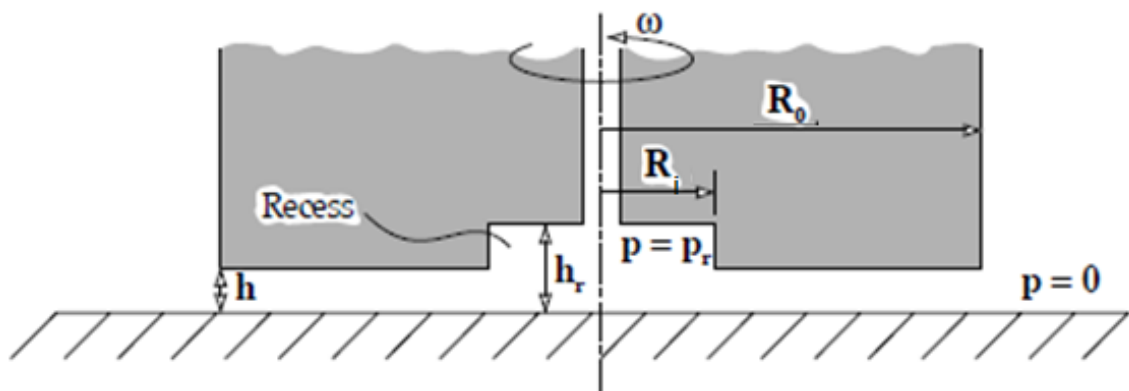


**Figure 5.1 Flat circular pad with a central recess [18]**

As can be seen in Figure 5.1 above that hydrostatic bearing has a circular pad with its recess and pressurized lubricant is fed into the recess. If the pressurized lubricant is supplied continuously, the lubricant separates bearing and the runner and forms an oil

film between two surfaces whose height is shown by 'h', also called as film thickness. Film thickness between the surfaces provides low friction coefficient or nearly zero friction coefficient during operation. This enables the bearing to carry the heavily loads while making rotary motion [19].

$R_o$  represents the outer radius of the bearing disk and  $R_i$  represents the radius of the inner recess. The ratio between  $R_o$  and  $R_i$  influences the area and flow factors which cause the change in the pressures. 'h<sub>r</sub>' symbolizes the depth of the pad. There is a relation between the film thickness and recess depth like  $h_r \gg h$ .  $h_r / h$  should be at least between 16 to 20 [18]. ' $\omega$ ' represents the rotary motion of the bearing.

Schematically, working principle of a hydrostatic bearing is given step by step below;

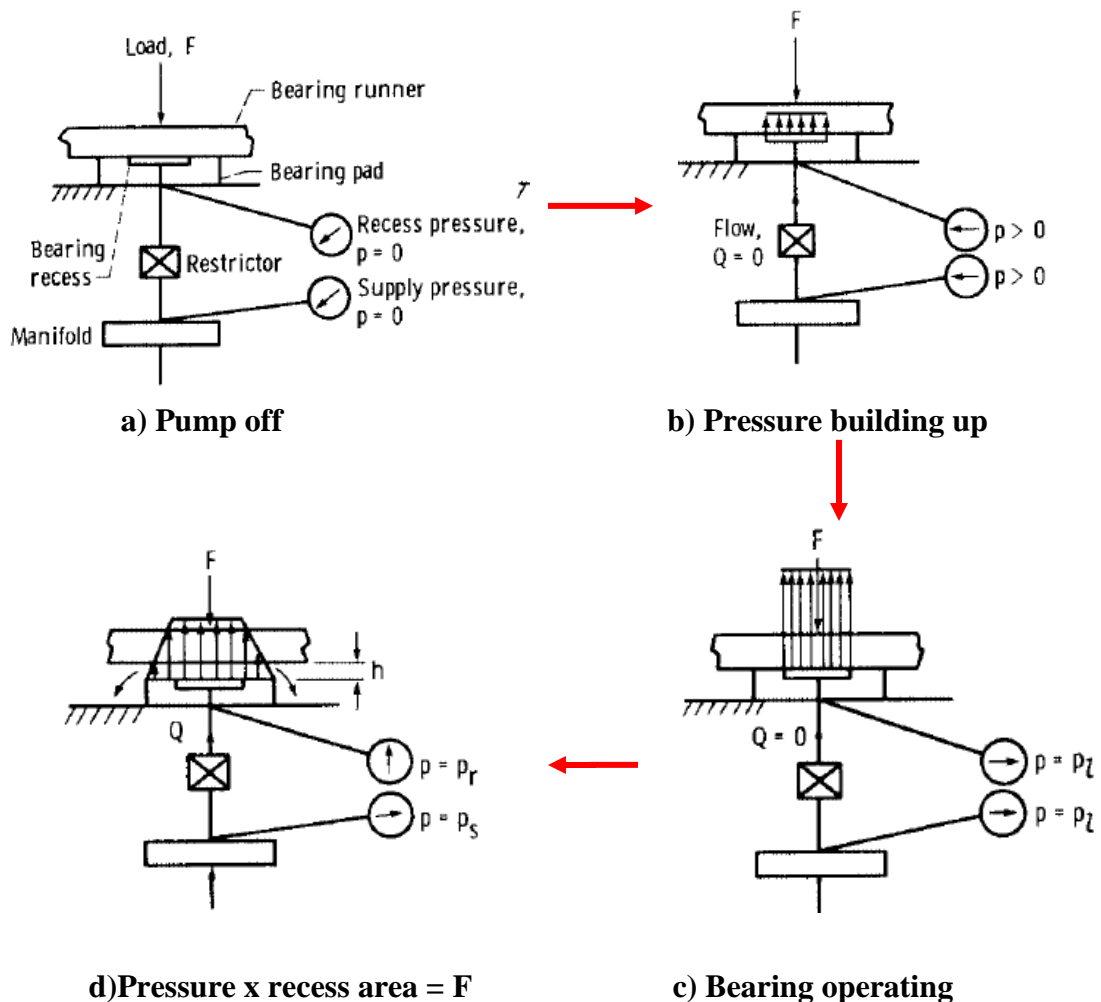
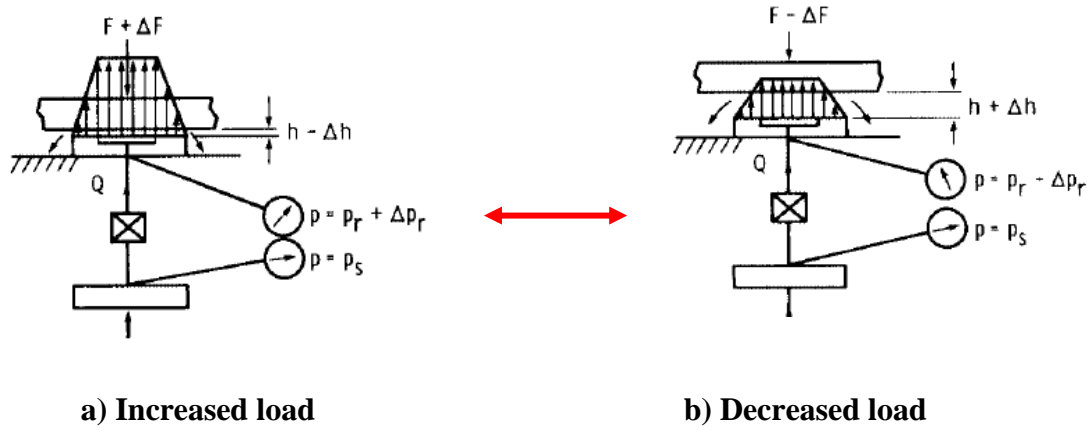


Figure 5.2 Schematic illustration of hydrostatic bearing operation [20]



During the pump off, pressure is zero and the runner is touching the bearing pad due to work load  $F$  that is applied on top of the bearing as shown in Figure 5.3. Along with pressure increase due to pump operation, pressure in the pad recess also increases. The pressure keeps increasing until the pressure reaches the level that it can lift the load. It is shown in that work load  $F$  can be lifted by the value of pressure multiplied by total recess area [20]. Together with lifting, oil will flow out of the bearing from sides of the recess and there would be decrease in pressure from recess towards the exit of the bearing [20].



**Figure 5.3 Schematic illustration of hydrostatic bearing under decreasing and increasing loads [20]**

Two conditions are represented in Figure 5.3. If the load is increased, the film thickness will be decreased until the total pressure in the recess and the pressure that film thickness creates will be equal to the applied force on the bearing. If the load is decreased, the film thickness will be increased until the total pressure in the recess and the pressure that the film thickness creates will be equal to the applied force on the bearing [20].

A general view of the hydrostatic bearing with the radial pressure distributions during operation and before operation is given below in Figure 5.4.

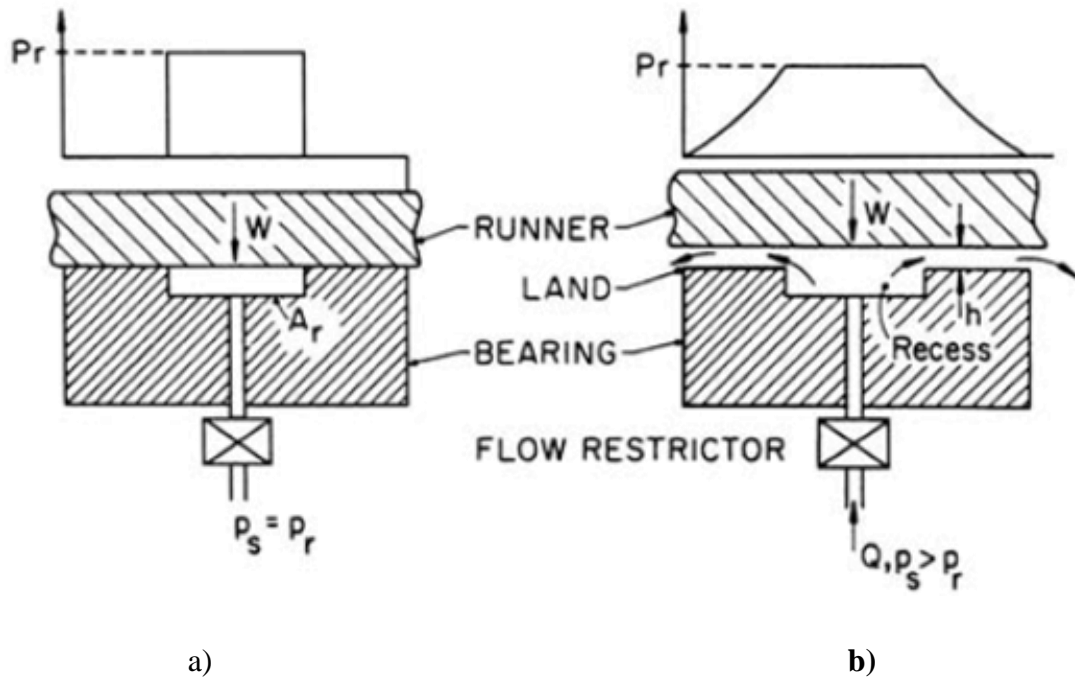


Figure 5.4 Hydrostatic bearing schematics a) before and b) after lift-off [21]

### 5.1.3 Type of Hydrostatic Bearings

According to the load directions, hydrostatic bearings can be classified into three main groups as radial, thrust and multidirectional bearings. As it is understood from the names that radial bearings support the load from radial directions, thrust bearings carry the loads from axial directions, and multidirectional bearings carry both radial and axial loads. Additionally, hydrostatic bearings can be classified into groups according to the pad types such as circular pad bearings, opposed circular pad bearings, rectangular pad bearings, opposed rectangular pad bearings, tapered pad bearings and screw nut assemblies [17]. A general classification of hydrostatic bearings is given in Figure 5.5.

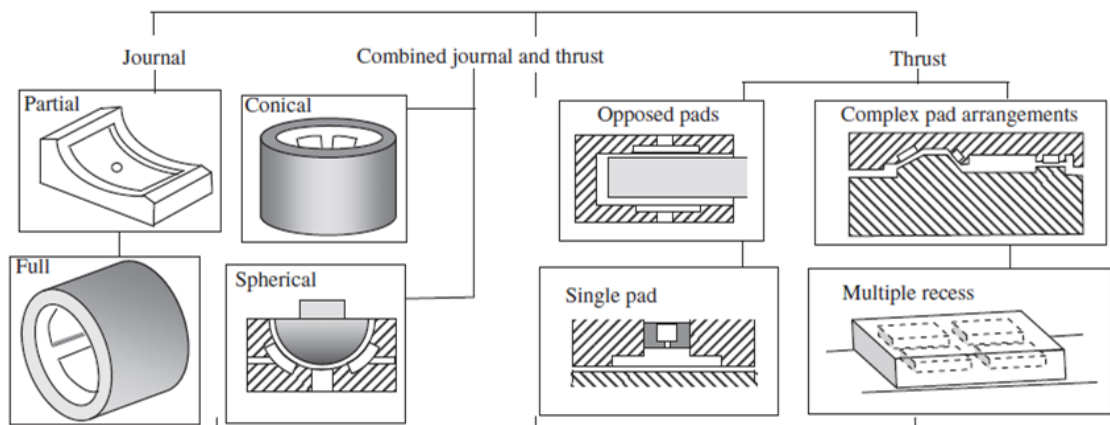


Figure 5.5 Hierarchy of Externally Pressurized Bearings. [22]

According to the function that the hydrostatic bearing will be used, one should select the hydrostatic bearing type and design by considering the functionality. There are some control parameters to design an appropriate hydrostatic bearing for proper operation. Details are given in the following section.

#### 5.1.4 Hydrostatic Bearing Design Considerations and Control Parameters

During designing a hydrostatic bearing, some design rules should be considered. First, bearing geometry should be designed in accordance with load, flow and stiffness. Then, second step is to select the restrictors for flow control [22]. There are some inputs needed while designing. Schematically, tribological system of a hydrostatic bearing with its required inputs and acquired outputs are given in Figure 5.6 below.

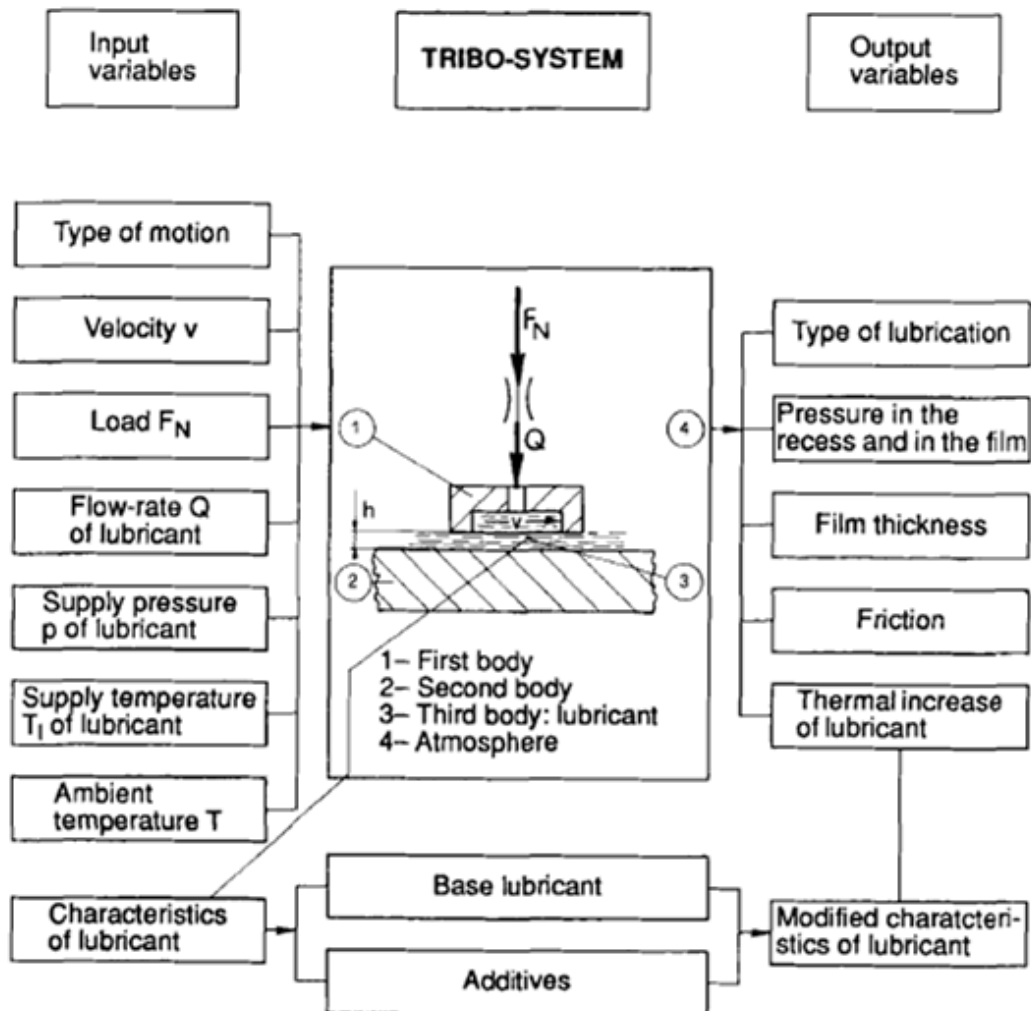


Figure 5.6 Design table of a hydrostatic bearing. [22]

In the figure, 1 represents the slider, 2 represents the runner, 3 represents the film thickness and 4 represents the surrounding atmosphere. It is indicated in the illustration,

at first type of motion and the velocity of the bearing should be determined as input. Flow rate, supply pressure and temperature are the other inputs to design. Then, a film thickness and created pressure in the recess can be calculated. According to the circumstances that the bearing operates, lubricant type can be changed.

Mainly, bearing geometry, flow control system, flow rate, fluid film force are considered as the critical parameters for the hydrostatic bearing design. Control parameters depend on each other. Because the control parameters are correlated with each other, the relationships between them should be concerned while designing a hydrostatic bearing.

General effects of changing some control parameters while designing a hydrostatic bearing is sequenced below [22]

- ❖ In order to provide adequate flow and cooling in hydrostatic bearing, flow rate must increase when there is an increase in the bearing area or sliding speed.
- ❖ There should be a larger film thickness of the large pads in case of a variation possibility in film thickness.
- ❖ If the pads are small, film thickness would be very small and flow rate would be little which requires an extra cooling for the system while large pads need large film thickness which provides enough flow for cooling.
- ❖ The relation between flow and fluid film depends on the pressure distribution along the bearing surfaces.
- ❖ Although the density of the lubricant is supposed to be stable, increase in the temperature may cause change the viscosity of the lubricant in the bearing and in the recess.
- ❖ The purpose of the usage of opposed pad bearings to increase the stiffness. Oppose pads do not affect the carrying load capacity.
- ❖ There are two important criteria which affect some of the critical parameters directly. One is area factor that which determine the load carrying capacity of a pad directly while the other is shape factor that which is affecting the flow rate.

While designing a hydrostatic bearing, the following questions should be considered: What type of loads should the bearing carry? What is the range of the film thickness? What is the pad geometry and what are the dimensions of the recesses? What type of

lubricant is selected? What is the supply pressure? What type of a flow restrictor is selected?

Step by step, in the light of the answers of these questions, a hydrostatic bearing for a yaw bearing of 500 kW HAWT design has been performed in the following section.

## 5.2 Designing a Hydrostatic Yaw Bearing for 500 kW HAWT

Design procedure of the hydrostatic yaw bearing is summarized as given in the Figure 5.7 below,

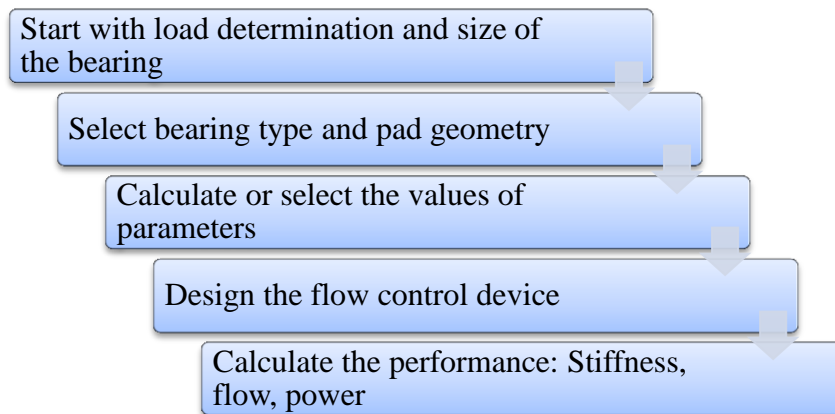


**Figure 5.7 Flow chart of design**

### 5.2.1 Load Determination

So as to design a hydrostatic yaw bearing, loads should be known. The forces and moments were already determined in the previous chapters during slewing bearing selection.

**Table 5.2 Determined forces and moments on the yaw bearing for a 500 kW HAWT**

Forces and Moments	
Wind forces	121,05 kN
Gravitational forces	-380,98 kN
Torque due to wind forces	169,5 kNm
Torque due to gravitational forces	-169,08 kNm
Generator torque	7,87 kNm
Brake torque	8,84 kNm
Resultant Moments	
Nominal working condition	7,88 kNm
Emergency condition	247,22 kNm

Wind forces build up radial forces while gravitational forces build up axial forces on the bearing. In previous chapters, resultant moments were calculated for both nominal working conditions and emergency conditions that resultant moments are acting on the bearing as bending moments. Bending moments cause force couple on the bearing and for both nominal and emergency conditions, schematic illustration of forces due to bending moments, gravitational forces and wind forces are given in below.

**First case:** Nominal working condition

Due to generator torque during operation, there is a force couple exist which try to rotate the bearing around x-axis.

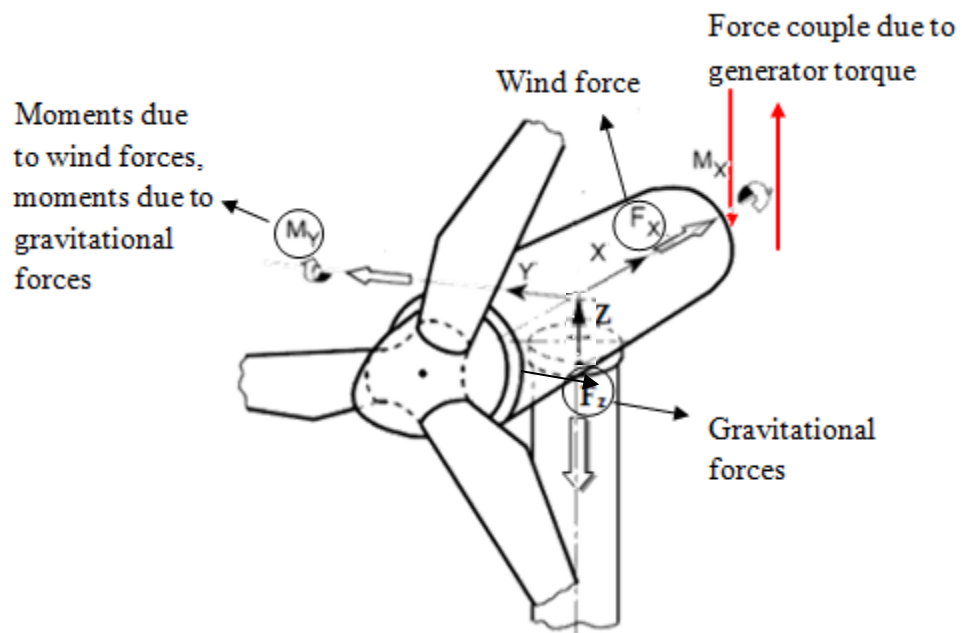


**Figure 5.8 Moments and forces @ nominal working condition**

Resultant moment is 7,88 kNm and this moment generate a couple force on the bearing. By dividing into the dimension of the bearing,

$$7,88 / 2,2 = 3,58 \text{ kN}$$

**Second case:** Emergency condition

Due to brake during emergency stop, there is a force couple exist which try to rotate the bearing around the x-axis.

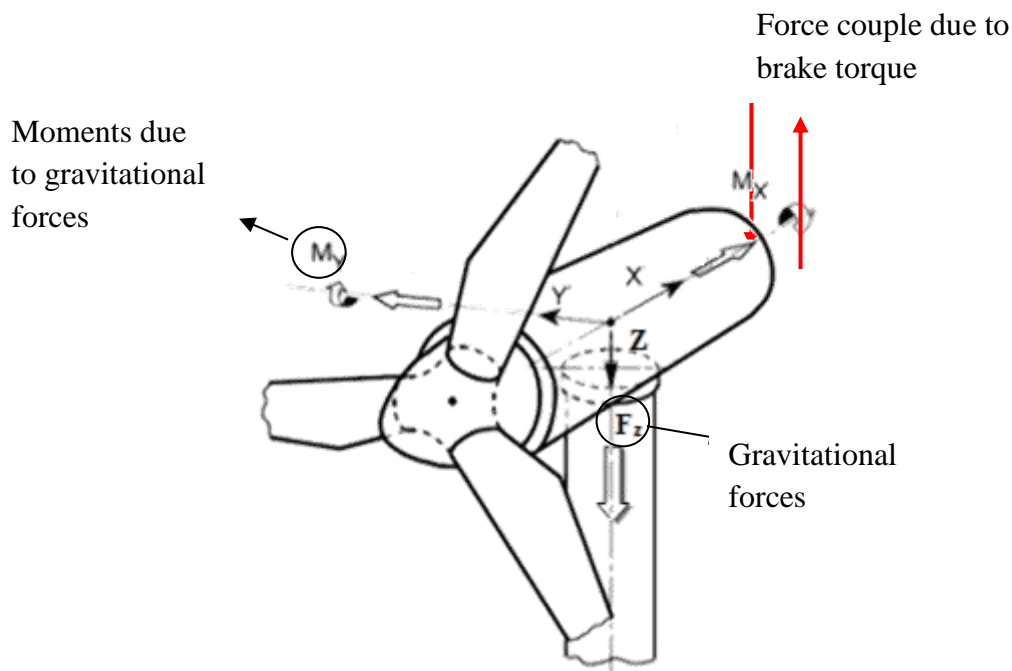


**Figure 5.9 Moments and forces @ emergency condition**

Resultant moment is 247,22 kNm and this moment generate a couple force on the bearing. By dividing into the dimension of the bearing,

$$247,22 / 2,2 = 112,37 \text{ kN}$$

During braking, turbine blades firstly stop and prevent the wind forces effects on the yaw bearing. That's why, wind forces and the moments due to wind forces are canceled out under the braking conditions.

In order to calculate the forces on the bearing easily, it's assumed that bearing is divided into two parts: Right and left part. This separation method is a useful way to determine up forces and down forces on the bearing. During calculations, worst case condition will be based on. For the braking period, force couple reaches the maximum value but wind effects neglect while wind forces are effective on the bearing during the nominal operation period. Therefore, calculations will be done according to the emergency condition together with wind force effects. Down and up forces are shown in Figure 5.10 below.

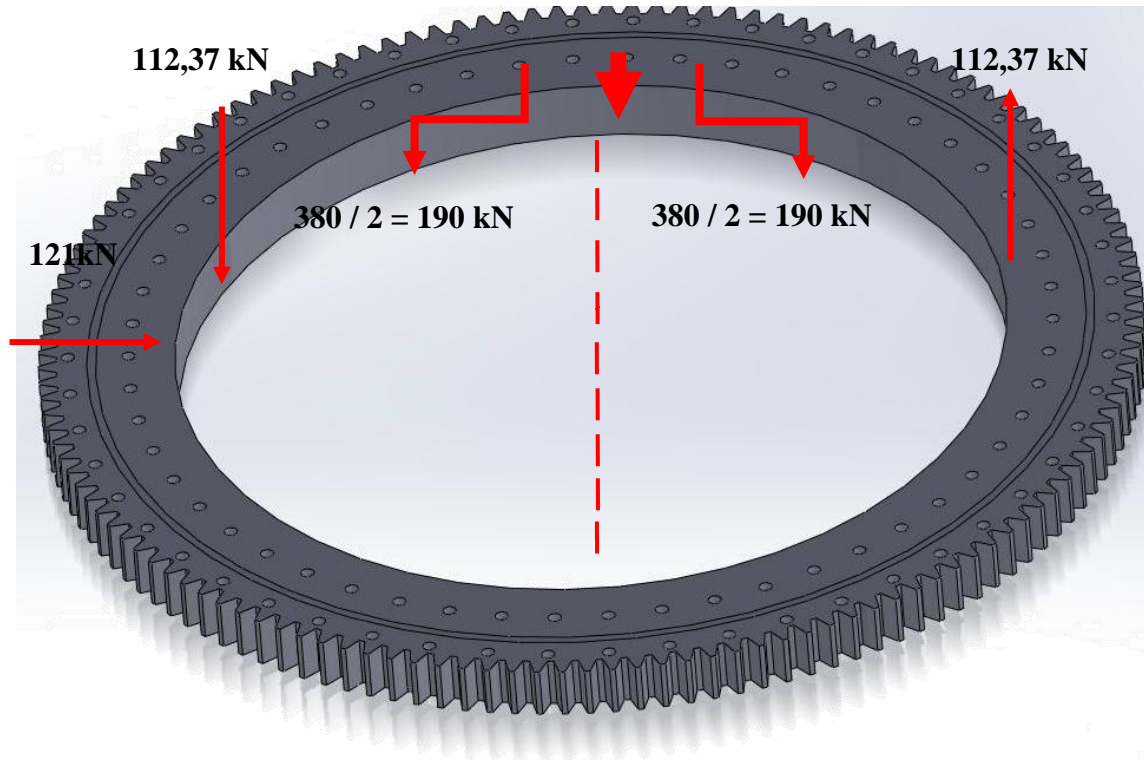


**Figure 5.10 Resultant forces on the yaw bearing for 500 kW HAWT**

It is seen from the figure that  $F_x$  is equal to 121 kN. Resultant moment converted into force and this force couple influences the system as a up vertical force from the right part of the bearing while influencing the system as a down vertical force from the left part of the bearing.

**Table 5.3 Loads on the yaw bearing for 500 kW HAWT**

Forces	(kN)
$F_x$ (radial forces)	121
$F_z$ (right side_total force)	77,63
$F_z$ (left side_total force)	-302

Bearing size has been determined based upon the wind turbine nacelle and flange dimensions as stated in the previous chapters.

### 5.2.2 Selection of Bearing Type and Pad Geometry

Bearing type selection should be made according to the load behavior. In the wind turbine yaw design problem the bearing is being exposed to radial and axial loads with bending moments. Therefore, the bearing has been designed as a combinational model. The pad configuration is selected as represented in Figure 5.11. This configuration can bear the thrust loads by the pads placed axially, and bear the radial forces by the pads placed radially like journal bearings.



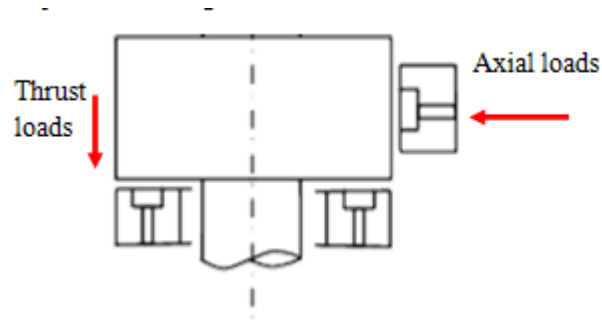


**Figure 5.11 Combination of journal and thrust bearings[23]**

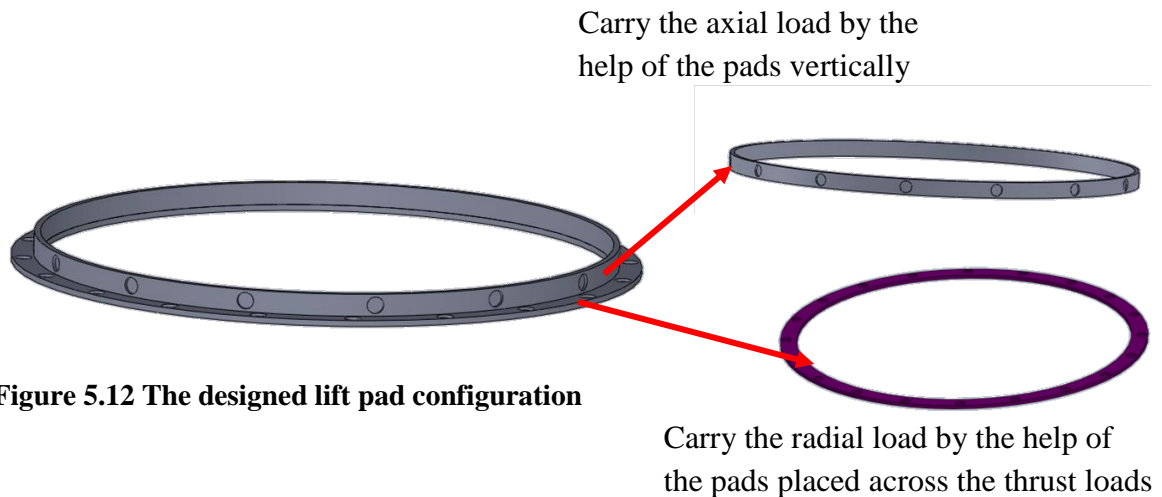
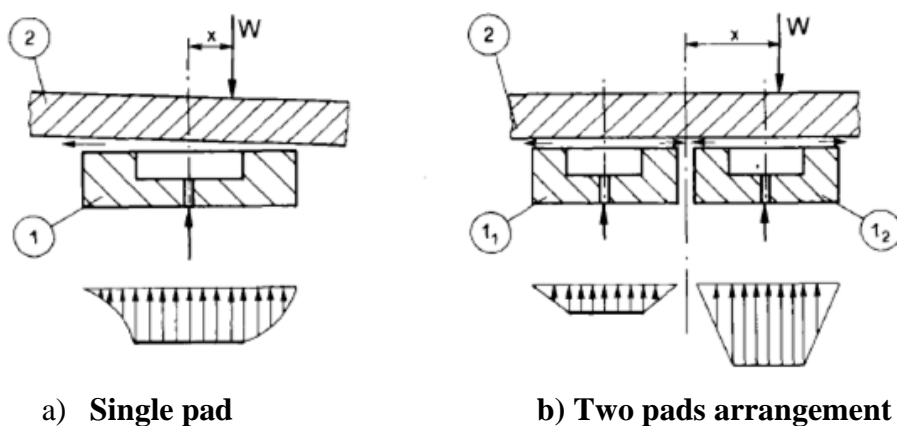


**Figure 5.12 The designed lift pad configuration**

It is seen in the Figure 5.12 that combinational type of bearing pads have been placed in multitudes. Each pad geometry is circular. The need to place more than one pad is obvious as seen from the Figure 5.12. The supported eccentric loads exert bending moments on the yaw mechanism in a way to tilt the bearing so that bearing runner may lean over the bearing pads due to unbalanced load and flow may leak from the opposite side of the load application [17]. In addition, the non-uniform pressure distribution inside the pad gives an indication of flow leakage from one side.



**a) Single pad**

**b) Two pads arrangement**

**Figure 5.13 Eccentric loads on hydrostatic bearings [17]**

In Figure 5.13, there is an eccentric load which is applied far away from the center of the bearing. As shown, with two pads bearing, the bearing can easily carry the load and it is clearly seen from the pressure distributions that right pad ( $l_2$ ) of the bearing pressure is higher to bear the load while left pad ( $l_1$ ) of the bearing pressure is lower. Inside the pads, both pads have uniform pressure distributions. Therefore, hydrostatic yaw bearing design has been designed as combinational load type with multiple pads.

Since both axial and radial loadings are present in the problem, a hydrostatic slideway design has been considered as illustrated in Figure 5.14. The hydrostatic slideway has one pad in radial direction and two opposed pads in axial direction. This configuration has been selected while designing the yaw bearing. However, rows of lift pads have been designed in both axial and radial load directions.

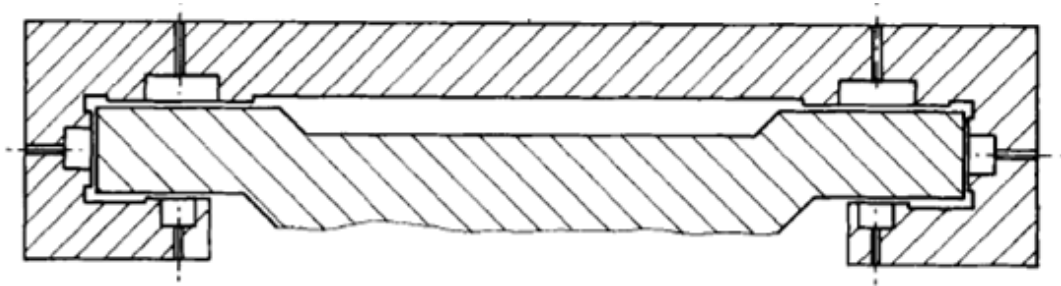


**Figure 5.14 Hydrostatic slideway [17]**

Additional pads in the axial direction opposed to the bottom pads of the hydrostatic slideway provide more stiffness without increasing the load carrying capacity of the bearing. Function of the opposed bearing is to make the bearing stiffer, while enabling the bearing to carry reversible axial load. An illustration of the hydrostatic yaw bearing which has been designed is given in the below in Figure 5.15.

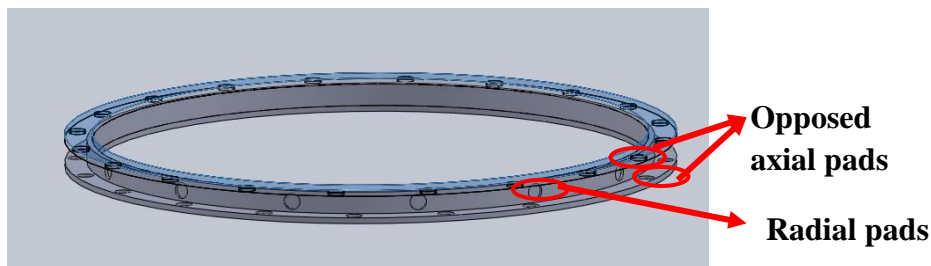


**Figure 5.15 Designed hydrostatic yaw bearing**

While designing opposed pads, there is no obligation to make the number of pads or pad sizes the same. However, in the current work all pads are made to same geometry in all

directions. This is to simplify the design as well as the fact that wind turbine can turn any direction and radial loads should be designed symmetrically.

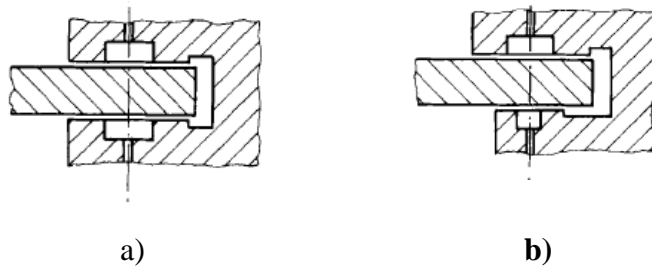


**Figure 5.16 Hydrostatic opposed pads: a) equal pads b) unequal pads [17]**

The pressure distribution between opposed pads can be different as it is given in Figure 5.17 below. The pressure distribution depends both the pad dimensions and film thickness values.

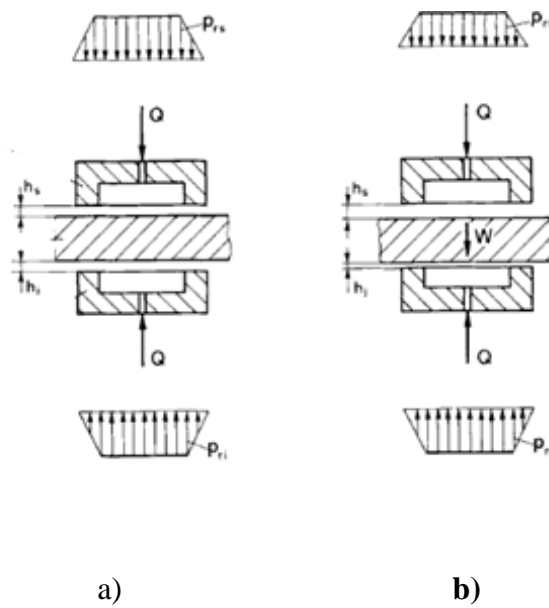


**Figure 5.17 Hydrostatic opposed axial bearing: pressure diagrams [17]**

Hydrostatic bearing pad geometry can be circular, rectangular, spherical or tapered. The geometry of the pads depends on the bearing geometry and dimension. Because the velocity of the bearing is taken null or very slow, power consumption is almost equal to the power consumption of the pump. Therefore, selecting the shape of the pad has not a crucial importance [17]. In the current problem circular pad geometry has been designed as it is the easiest type for manufacturing. General view of the circular pads on the deigned hydrostatic yaw bearing is shown in Figure 5.18 below.

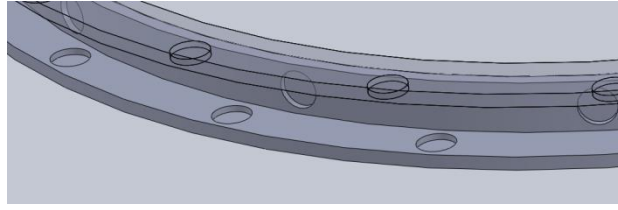


**Figure 5.18 Circular hydrostatic pads.[17]**

The position of the pads on the bearing and the number of lift pads the bearing have are determined by making some hydrostatic calculations according to pad and overall bearing geometry, loads and other hydrostatic parameters.

### **5.2.3 Determination of Hydrostatic Bearing Parameters**

Before selecting or designing any other bearing parameter, overall dimensions of the bearing should be known. The overall bearing dimensions have been determined according to the nacelle dimensions. Nacelle is placed on the inner ring of the bearing flanges where they are bolted together. Due to mounting of nacelle on the inner ring, outer ring of the yaw bearing is placed on the tower of the wind turbine, and it would be stationary while the nacelle will rotate with the inner ring. The overall bearing dimensions are given in Table 5.4.

**Table 5.4 Bearing dimensions**

Inner Ring Dimensions	mm
Inner diameter of the inner ring	2030
Outer diameter	2233
Inner diameter with bolt	1702

The inner ring of the yaw bearing is given in Figure 5.19 below. Bolting zone is colored with blue as shown on the inner ring in.

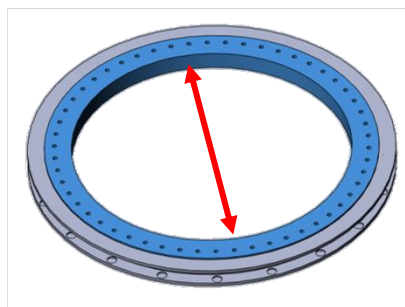


**Figure 5.19 Bolting places on the inner ring**

Selected pad dimensions,  $R_0$  and  $R_i$  are given in Figure 5.20 below. These dimensions have been selected according to the bearing dimensions and the inner ring surface area.

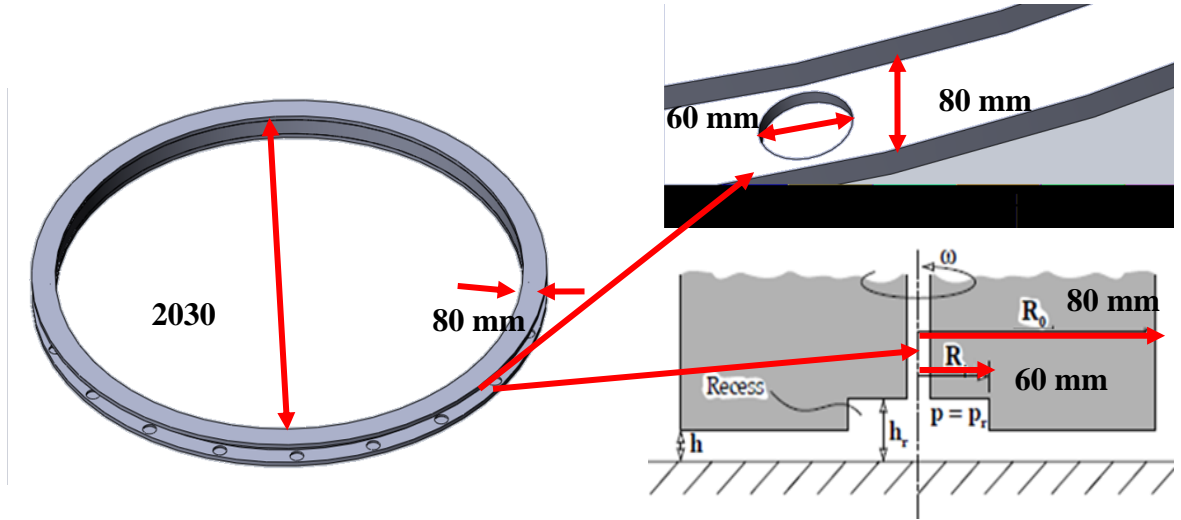


Figure 5.20 Inner ring of the hydrostatic yaw bearing

There is a ratio between the recess radius and outer radius that  $R_i/R_0$  is determining the load carrying capacity of a single pad and consequently the total load carrying capacity. Load carrying capacity of a single pad can be calculated by using the formula below.

$$W_{1\text{pad}} = A_o * a_f * (P_r - P_a) \quad (11)$$

In the equation,  $A_o$  represents the pad area,  $a_f$  represents the area factor,  $P_r$  represents the recess pressure while  $P_a$  represents the ambient (atmospheric) pressure. Area factor can be determined by the equation 11. The recess pressure can be calculated by the equation 12 below.

$$a_f = \frac{1 - (\frac{R_i}{R_0})^2}{2 \ln(\frac{R_0}{R_i})} \quad (12)$$

$$P_r - P_a = \frac{W}{A_o * a_f}$$

It is seen from the equations above that  $a_f$  is proportional to  $R_i/R_0$ . If the recess diameter increases, area factor increases and correspondingly load carrying capacity of each pad increases. However, this also affects flow and increases the flow rate because of the relation between flow factor and recess diameter [24]. Flow factor is symbolized with  $q_f$  in the equations. Flow rate, which is symbolized by  $Q$ , is regulated by the film thickness. By changing the working clearance, flow rate can be adjusted [10]. The

relation between flow factor, recess diameter, film thickness and flow rate is given in the equations 13 and 14 below.

$$q_f = \frac{\pi}{6 \ln\left(\frac{R_o}{R_i}\right)} \quad (13)$$

$$Q = q_f \frac{h^3}{\xi} (P_r - P_a) \quad (14)$$

In the previous section, it has been discussed that the hydrostatic yaw bearing has been designed as an opposed multipad configuration. If the design is opposed, the load equation is converted into the relation 15 given in below.

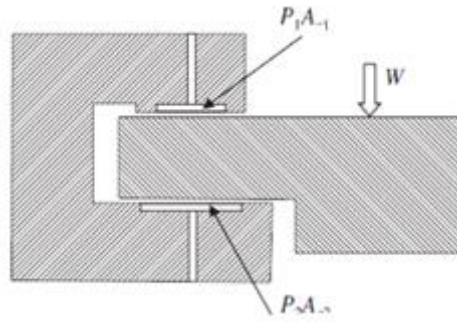


Figure 5.21 Opposed pad bearings, load determination of the pads[23]

$$W = (A_1 * P_1) - (A_2 * P_2) \quad (15)$$

$$W_{total_{upper}} = A_o * a_f * (P_r - P_a) * \# \text{ of pad} \quad W_{total_{lower}} = A_o * a_f * (P_r - P_a) * \# \text{ of pad}$$

Opposed pads are used to enhance the stiffness. The reverse pads on the upper side of the bearing supports the bearing against the loads due to upward forces occur due to bending moments induced by off center weights and torques occur due to emergency stop and generator counter moments.

The load capacity of each pad depends on the difference between upper and lower pad capacities. For multipad type of bearings, to be able to calculate the total load capacity of the bearing, the difference should be taken between the upper and lower pads load capacities [22]. It should be noted that as the surfaces move, the clearance at top and bottom side changes. With changing pad clearance, the lift force at either side also changes.

In Figure 5.21,  $h$  symbolizes the film thickness which is also called bearing clearance,  $h_r$  represents the recess depth and  $\omega$  represents the angular velocity which is assumed almost null for the designed hydrostatic yaw bearing. Clearance between parallel plates of the bearing separates two surfaces from each other and prevents contact of runner and slider. By the help of the clearance, the resistance against the flow coming from the recess is formed and this resistance provides to keep high pressure in the recess [10]. While deciding about the running film thickness, some factors should be considered [17]:

- ❖ Clearance height should be so thin as to satisfy the load requirement of the hydrostatic bearing.
- ❖ Film thickness should not be such thin as to cause contact between bearing runner and slider.
- ❖ Film thickness should be much bigger than surface roughness. In general film thickness should be higher than 3 times the surface roughness. Surface roughness is symbolized by  $\sigma$ . Typically  $\sigma$  is equal 16  $\mu$ inch for bearing surfaces. This means that clearance should be minimum 0,000001219 m (48  $\mu$ inch).
- ❖ Film thickness has direct effect on flow rate. That is why it should be sufficiently small to provide small flow rate.

In conjunction with clearance, recess depth should be minimum 16-20 times bigger than the selected clearance [3].

In the light of this information,  $h$  has been selected as 0,00005 m, and recess depth has been selected at approximately 10 mm proportional to pad dimensions.

.

Raising flow rate increases the required pump power which means more powerful pump is needed to provide more flow [24]. Pump power can be calculated using the equation given below.

$$P_{\text{pump}} = P_s * Q \quad (16)$$

On the other hand, if  $R_i / R_o$  decreases especially less than 0.4, load carrying capacity of a single pad will decrease together with reduction in area factor which causes pressure increase in recess. In order to increase the recess pressure, a more powerful pump is required. The optimum radius ratio range is between 0,4 to 0,6. Minimum pumping power can be obtained with this ratio [24].

As a last input which has to be decided before load calculations is the viscosity of the selected lubricant. To separate two plates of the bearing from each other, a fluid lubricant placed in the gap between them. Fluid lubricant can be divided into two groups as liquid and gaseous lubricants. In hydrostatic applications, generally liquid type lubricants are being used. Liquid lubricants can be synthetic or mineral based. In the usual course of the hydrostatic bearings, mineral based lubricants are being used [17].

The principal of selecting the lubricant type is selecting the viscosity of the liquid. Viscosity can be described as the resistance against to flow. Viscosities of the lubricants are decreased with temperature but for the hydrostatic design, it was assumed as stable. Viscosity selection should be done by taking into consideration two parameters: Minimum ambient temperature and maximum hydrostatic yaw bearing operation temperature. Normally, for high speed machines, lower viscosity required but designed hydrostatic yaw bearing has nearly null speed, that's why one of the values can select from the range.

**Table 5.5 Typical minimum viscosity values for hydraulic components [25]**

Component Type	Minimum Permissible Viscosity(cSt)	Minimum Optimum Viscosity(cSt)
Vane	25	25
External gear	10	25
Internal gear	20	25
Radial piston	18	30
Axial piston	10	16

From Table 5.5 the range for viscosity is indicated between 10 to 25 cSt which means viscosity can be between 0,01 to 0,025 Pa-s. Therefore, viscosity has been selected as 0,02 Pa-s to do the calculations for this designed hydrostatic yaw bearing which has and external gear.

Finally, a flow control or restriction is needed to complete the hydrostatic bearing design. Flow control device selection and its design are given in the following section in detail.



#### 5.2.4 Design of Flow Control Device

Although it is assumed that the bearing geometry and the lubricant viscosity are steady, according to the loads on the bearing, bearing clearance and flow rate may change. There can be unexpected load decrease or increase. Instant increase in load may cause contact between the runner and slider of the bearing due to lack of film thickness. Similarly, an instant decrease in load may cause instability of the bearing. For such situations, bearing needs a flow control mechanism to inhibit the possible failure and instabilities of bearing [21]. If the film thickness decreases due to increasing loads, pressure inside the recess increases to be able to carry the load by the help of these restrictors, and this increase goes on until the system balances [22]. A single restrictor combined with a single pad hydrostatic bearing is given in Figure 5.22 below.

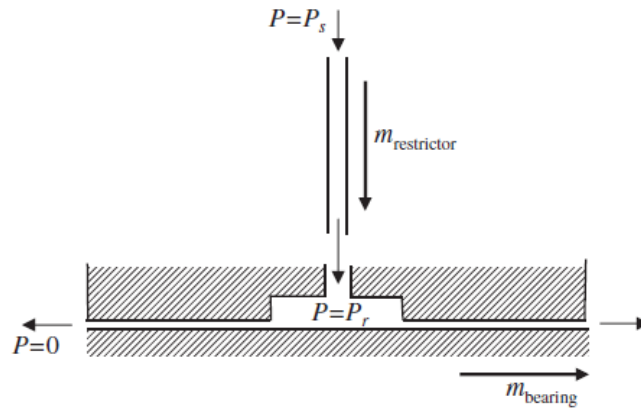


**Figure 5.22 Circular pad bearing with restrictor [22]**

When there is more than one pad on the hydrostatic bearing, every pad should have a flow restrictor that total flow passing from the restrictors is equal to the flow that goes out of the bearing [22]. Another illustration which shows both the stiffness, pressure and film thickness change along with the restrictor under given load  $W$  is given in Figure 5.23.

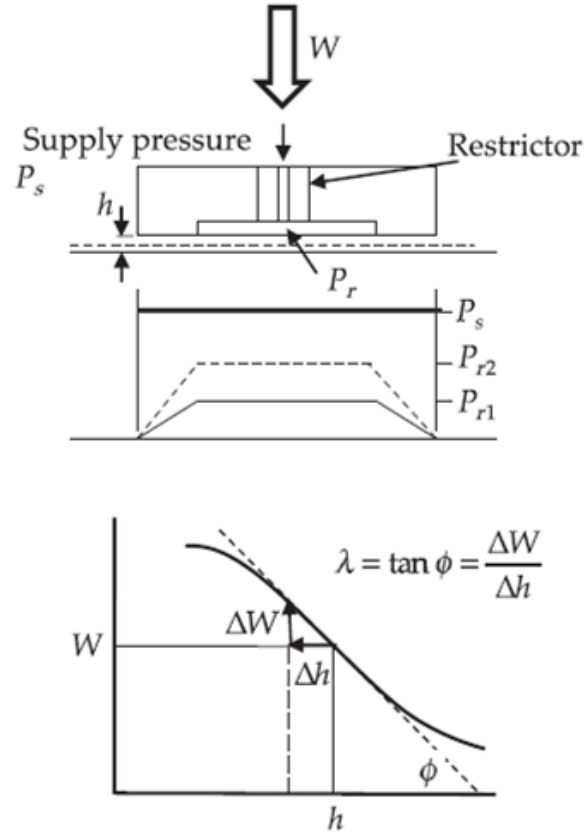


**Figure 5.23 Effect of a restrictor on pad pressures [22]**

In Figure 5.23,  $P_s$  represents the supply pressure which is the flow pressure up to the restrictor,  $P_{r1}$  represents the outflow pressure from the restrictor under low load while  $P_{r2}$  represents the outflow pressure from restrictor under high load. Under load  $W$ , lubricant is coming from the reservoir with pressure  $P_s$  and after passing from the restrictor, flow goes into the bearing recess with pressure  $P_r$ . According to the load change, flow and film thickness will be changed and film stiffness will be provided by the help of restrictor [22].  $\lambda$  represents the stiffness of the film in Figure 5.23 above. Bearing stiffness can be calculated by using the formula (17) which is equal to the load change rate regarding the film thickness [24].

$$\lambda = - \frac{dW}{dh} = -3 \frac{W}{h} * \frac{\epsilon}{1+\epsilon} \quad (17)$$

In the formula 17,  $\epsilon$  means the resistance ratio which is equal to  $R_i / R_o$ . The negative sign means that load is changing contrary to the film thickness [24].

#### 5.2.4.1 Flow Control Types

There are three types of flow control restrictors which both control flow and provide stiffness for the hydrostatic bearings are [26];

- ❖ Constant flow valve-pump compensation
- ❖ Orifice
- ❖ Capillary

These three types of restrictors also known as fixed-flow restrictors. There is another type of restrictor called variable flow restrictor. As opposed to the fixed-flow restrictors, variable restrictors can change the flow by the help of a valve with respect to pressure variation. Hydrostatic bearings with variable type of restrictors have higher stiffness than fixed-flow restrictors at the expense of higher costs. Fixed-flow restrictors are commonly used in common hydrostatic bearing applications [24].

From the point of using the hydrostatic bearing efficiently, the most important thing is selecting the correct flow control mechanism for the designed hydrostatic yaw bearing. Even though fixed flow restrictor types cause more power consumption than the variable types, initial cost is much less than variable restrictor systems. In this work a fixed flow restriction system has been designed. In the following section all types of fixed-flow restrictors will be examined in detail [27]

##### 5.2.4.1.1 Constant -Flow Compensation

Constant flow compensated hydrostatic bearings are working under constant flow as indicated in the name. The flow coming from the restrictors never change even there is a pressure decrease or increase in recess [26]. Constant flow is provided by a valve or a pump. There is an illustration of types of the constant flow compensation below [22].

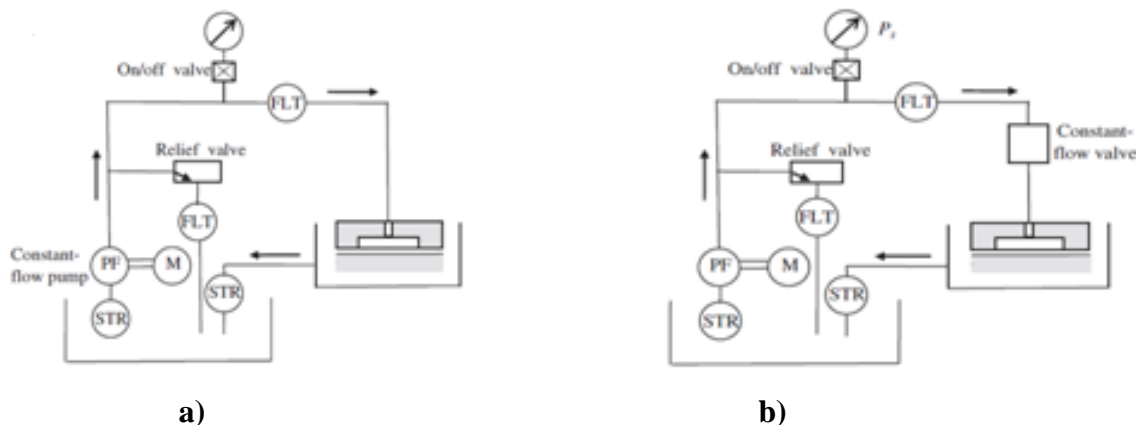


**Figure 5.24 Constant flow control system a) A constant flow pump b) A constant flow valve for each recess [22]**

Constant flow can be obtained by the help of a constant-flow valve or a constant-flow pump for a single pad hydrostatic bearing. For the bearings which have more than one pad, there should be valves or pumps as the number of pads [22]. An illustration for a multipad design of hydrostatic yaw bearing is given in Figure 5.25 below.

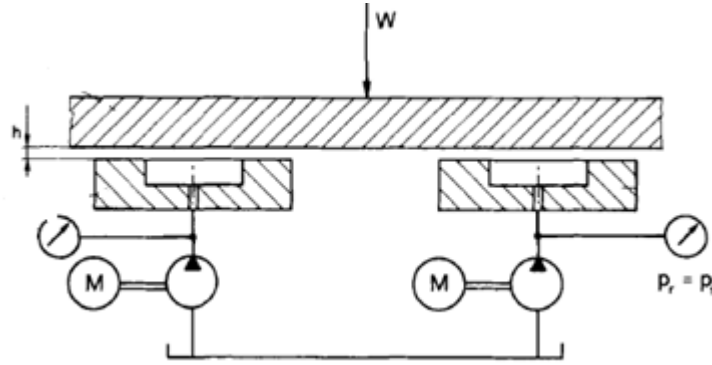


**Figure 5.25 Constant flow control system: one pump for each bearing [22]**

Therefore, for the purpose of designing the hydrostatic yaw bearing in this work, constant flow type of restrictors are not suitable because of multiple pads and the need for many valves or pumps which cause high initial and maintenance cost.

#### **5.2.4.1.2 Orifice**

Orifices are known as turbulent flow type of control restrictors due to having large Reynolds numbers [22]. Typical orifice type compensation is given in Figure 5.26 below.

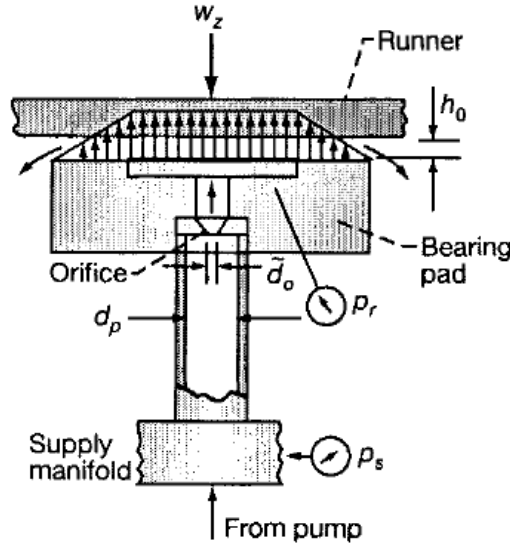


**Figure 5.26 Orifice-compensated hydrostatic bearing [26]**

In Figure 5.26,  $d_p$  represents the pipe diameter and orifice diameter is shown with  $d_o$ . Pipe diameter should be minimum 10 times greater than the orifice diameter. Due to choking risk, orifice diameter  $d_o$  should not be less than  $5 \times 10^{-4}$  m. The length of the orifice should be short in the direction of the flow compared to the length of the capillary [26].

By assuming the lubricant as incompressible, flow rate inside the orifice can be calculated with the equation (18) given below;

$$Q_o = k_o (P_s - P_r)^{\frac{1}{2}} \quad (18)$$

In the equation 18,  $k_o$  is a constant and its unit is  $m^4 (sN)^{1/2}$ . The equation to calculate  $k_o$  is given below.

$$k_o = \frac{\pi c_d (d_o)^2}{\sqrt{8\rho}} \quad (19)$$

In the formula,  $c_d$  represents the orifice discharge coefficient that it is approximately equal to 0,6 for orifices whose Reynolds number is higher than 15. For the orifices which Reynolds number lower than 15, the following equation 20 can be used.

$$c_d = 0,2\sqrt{Re} \quad (20)$$

For an orifice Reynolds number can calculate by using the equation 21 below,

$$Re = \frac{d_o}{\xi} [2\rho(P_s - P_r)]^{\frac{1}{2}} \quad (21)$$

Finally, the flow rate equation for a hydrostatic bearing with orifice type restrictor is obtained by substituting the values in the flow rate equation (22);

$$Q = \pi \frac{d^2}{2} \left( \frac{P_s - P_r}{2\rho} \right)^{\frac{1}{2}} C_d \quad (22)$$

It is clearly seen from the equation that flow in the orifice is proportionate to the square root of the pressure drop.

#### 5.2.4.1.3 Capillary

Capillary is known as laminar flow type of control restrictors [22]. General assumption for laminar flow that Reynolds number should be less than 1000. Reynolds number can be determined by using the equation 23 given below [26].

$$Re = \frac{4\rho q_c}{\pi \xi d_c} < 1000 \quad (23)$$

In the equation 23,  $q_c$  represents the flow rate in the capillary,  $\xi$  represents the lubricant viscosity,  $\rho$  represents the density of the lubricant and  $d_c$  represents the diameter of the capillary tube. Capillary tubes are long, narrow tubes which have very small diameter. Diameter of the capillary should be large enough to let the lubricant flow, and not less than  $6 \times 10^{-4}$  m for the purpose of preventing clog [26]. An example of capillary type compensator is given in Figure 5.27 below.

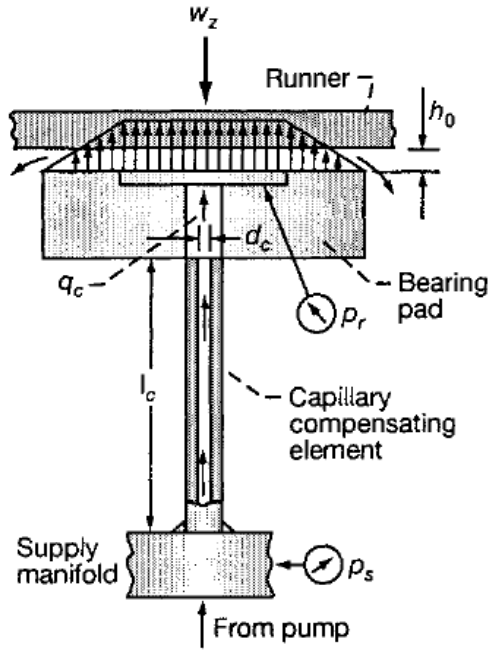


**Figure 5.27 Capillary compensated hydrostatic bearing [26]**

It is clearly seen from Figure 5.27 that capillary has very small diameter and relatively long tube. The length of the tube is typically at least 20 times greater than the diameter of the tube [26]. For accuracy, it is better to select the ratio between the length and diameter of capillary tube almost 100 [16]. The laminar flow inside the capillary can be determined by using the equation 24 given below.

$$Q_c = \frac{R_c(P_s - P_r)}{\xi} \quad (24)$$

It is understood from the equation 24 that laminar flow inside the tube is only dependent on the viscosity because the flow inside the tube occurs due to shear forces while the turbulent flow in orifices occurs due to inertia. The flow is also dependent on the density of the lubricant [24]. Besides, the flow through the capillary tube is directly proportional to the pressure difference, which means increasing load will cause increases in the pressure inside the recess and decreases the flow inside the capillary tube [16] [26]. In the equation 25,  $R_c$  represent the hydraulic resistance of the capillary tube which is proportional to the length of the tube. The equation for the resistance of capillary is given below.

$$R_c = \frac{\pi d_c^4}{128 l_c \xi} \quad (25)$$

Due their low cost and robust operation, capillary type flow restriction has been designed for the wind turbine yaw bearing.

#### 5.2.4.2 Stiffness Changes According to the Flow Control Mechanism

Stiffness can be described as the resistance which causes variations in film thickness. Every flow control device provides the bearing with different stiffness because of different reaction under loads [18].

##### 5.2.4.2.1 Stiffness with Constant Flow Method

In constant flow method lubricant always comes from the restrictor with a constant flow rate.

Stiffness is the rate of change in film thickness according to the changing loads;

$$\lambda = - \frac{dW}{dh} \quad (26)$$

Recess pressure can be obtained by reorganizing the equation of flow rate to provide required film thickness as;

$$Q = q_f \frac{h^3}{\xi} (P_r - P_a) \quad \longleftrightarrow \quad (P_r - P_a) = \frac{Q \xi}{h^3 q_f} \quad (27)$$

By replacing recess pressure with its open form found out above in the load equation;

$$W = (P_r - P_a) a_f A_o \quad \longleftrightarrow \quad W = \frac{Q \xi}{h^3 q_f} a_f A_o \quad (28)$$

By taking differential of the load formulation with respect to film thickness;

$$\lambda = - \frac{dW}{dh} \quad \longleftrightarrow \quad \lambda = - \frac{d \left( \frac{Q \xi}{h^3 q_f} a_f A_o \right)}{dh} \quad \longrightarrow \quad \lambda = \frac{3W}{h} \quad (29)$$

It is seen from the formulation that due to viscosity term in the equations, stiffness depends on the temperature of the bearing. Along with this method, lubricant flow can not change during operation which is a significant benefit for large multipad hydrostatic bearings. From a different point of view, this constant flow rate is a drawback because also stiffness can not change and can not be arranged with respect to the hydrostatic bearing type [18].

##### 5.2.4.2.2 Bearing Stiffness with Orifice

Figure 5.28 shows a simple orifice type control mechanism.



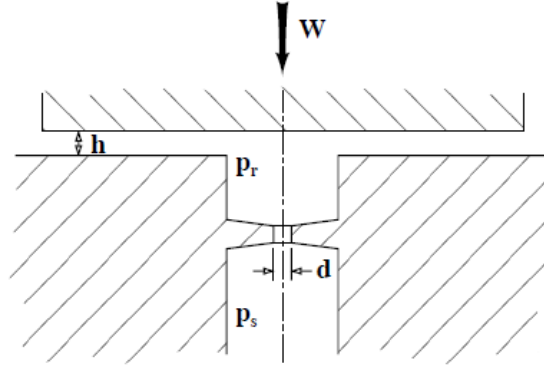


**Figure 5.28 Flat circular pad bearing with orifice flow control [18]**

In the figure,  $d$  represents the diameter of the orifice. Flow rate which is passing through the orifice can be calculated by using the equation;

$$Q = \pi \frac{d^2}{2} \left( \frac{P_s - P_r}{2\rho} \right)^{\frac{1}{2}} C_d \quad (30)$$

In the equation 30  $\rho$  represents the density of the lubricant and  $C_d$  represents the discharge coefficient.

By using the general expression for the flow rate, recess pressure with orifice type flow restrictors can be obtained;

$$Q = \pi \frac{d^2}{2} \left( \frac{P_s - P_r}{2\rho} \right)^{\frac{1}{2}} C_d \quad \longleftrightarrow \quad Q = q_f \frac{h^3}{\xi} (P_r - P_a) \quad (31)$$

$$(P_r - P_a) = \frac{\pi d^2 \xi}{2h^3 q_f} \left( \frac{P_s - P_r}{2\rho} \right)^{\frac{1}{2}} C_d \quad (32)$$

And substituting recess pressure into the stiffness equation;

$$\lambda = - \frac{dW}{dh} \quad \longleftrightarrow \quad \lambda = - \frac{3\pi d^2 \xi a_f}{2h^4 q_f} \left( \frac{P_s - P_r}{2\rho} \right)^{\frac{1}{2}} C_d \quad \longrightarrow \quad \lambda = \frac{3W}{h} \quad (33)$$

It is seen from the equation (33) that stiffness equation of the orifice type restrictor is the same with the stiffness equation of the constant flow compensation type restrictor. Therefore, same considerations are valid for both constant flow compensation and orifice.

Orifice type restrictors can be easily affected by the impurities that may occur due to corrosion in the lubricant. Therefore, pollutants in the lubricant can cause change in the stiffness by the time. Providing greater stiffness in percentage as compared to the capillary is the advantage of the orifice systems [18].

#### 5.2.4.2.3 Bearing Stiffness with Capillary

Figure 5.29 shows a simple capillary type control mechanism.

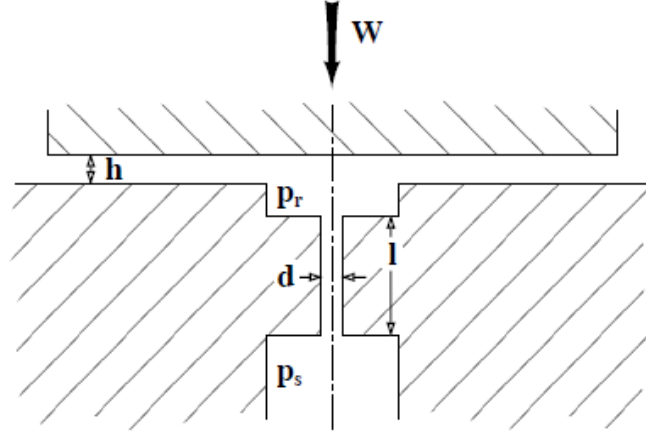


**Figure 5.29 Flat circular pad bearing with capillary controlled flow [18]**

By making the flow through the capillary equal to the total flow through the system recess pressure can be obtained, and be substituted into the load equation to find stiffness in terms of film thickness;

$$Q_c = \frac{R_c(P_s - P_r)}{\xi} \longleftrightarrow Q = q_f \frac{h^3}{\xi} (P_r - P_a) \longrightarrow (P_r - P_a) = \frac{P_s}{1 + h^3 q_f R_c}$$

$$W = (P_r - P_a) a_f A_o \longleftrightarrow W = \frac{P_s a_f A_o}{1 + h^3 q_f R_c}$$

$$\lambda = - \frac{dW}{dh} \longleftrightarrow \lambda = \frac{3W}{h} \frac{1}{1 + 1/(h^3 q_f R_c)} \quad (34)$$

It can be easily understood from the stiffness equation 34 that capillary provides less stiffness than orifice and constant flow control mechanism. Even so, capillary controlled hydrostatic bearings can provide even higher stiffness values than typical rolling element bearings by adjusting design parameters and working pressures. Due to removal of the viscosity term during the equalization of the two flow equations, bearing stiffness is also free from the temperature change because of balancing viscosity effect on the capillary flow equation [18].

#### 5.2.4.3 Selection of Flow Control Mechanism for the Hydrostatic Yaw Bearing

If the restrictors are put in an order with respect to increasing stiffness, it can be said that the least one is the capillary, then the orifice and constant-flow control systems have the highest stiffness [22]. Although constant flow control has better stiffness performance than the other two, due to its high cost and maintenance requirement, orifice or capillary systems are preferred in general bearing applications. Figure 5.30 shows the relation between stiffness and restrictor types below.

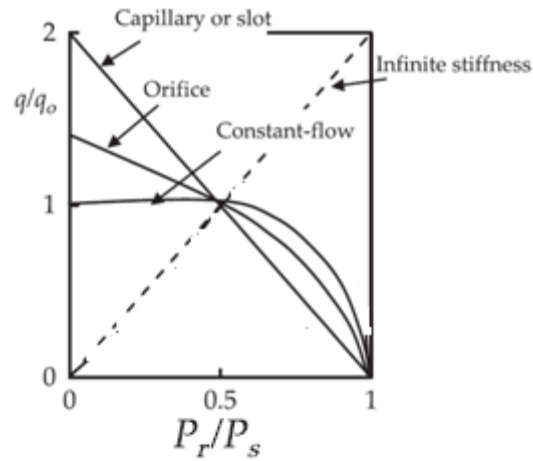


**Figure 5.30 Flow and pressure characteristics of various flow control devices [22]**

It is shown in Figure 5.30 that pressure flow relation effects the stiffness directly. A Table 5.6 given below which compares the characteristics of the fixed flow restrictors

**Table 5.6 Ranking of compensating elements [26]**

Consideration	Compensating element		
	Capillary	Orifice	Constant-flow valve
Initial cost	2	1	3
Cost to fabricate and install	2	3	1
Space required	2	1	3
Reliability	1	2	3
Useful life	1	2	3
Commercial availability	2	3	1
Tendency to clog	1	2	3
Serviceability	2	1	3
Adjustability	3	2	1

\* Ranking 1 denotes best or most desirable element for that particular consideration

Generally, for the hydrostatic bearing applications capillary tubes, which are called laminar-flow restrictors, are preferred due to the fact that they are easily obtainable and cheap. Sometimes, small diameter-long length tubing or hypodermic needles can be also used as a capillary type compensator. Designing a capillary system is also very straightforward and easy to adjust [17]. By cutting a small diameter tube at the required length, a capillary can be easily produced [22]. Besides, the most important feature of a capillary is that it is independent of the viscosity which makes it independent of temperature [28]. On the contrary, orifice type restrictors are dependent on the temperature because in flow equation of the orifice, there is no viscosity term which can cancel the viscosity impact on flow through the bearing gap. Although orifices are more compact than capillary tubes and make the system stiffer relatively to the capillary tubes, orifices are not suitable for the heavy load applications and the applications where the temperature is always changing. Another disadvantage of the orifice systems is that the stiffness is not constant during flow; while the stiffness is almost constant in the capillary tube even the clearance of the bearing changes [22].

Considering the large variations in temperature where wind turbines may operate, temperature independent stiffness and operation is very important for wind turbine yaw bearing systems. With all of the above mentioned superiorities, capillary type system is selected as restrictor for the designed hydrostatic yaw bearing. A typical capillary glass tube is given in Figure 5.31 below.

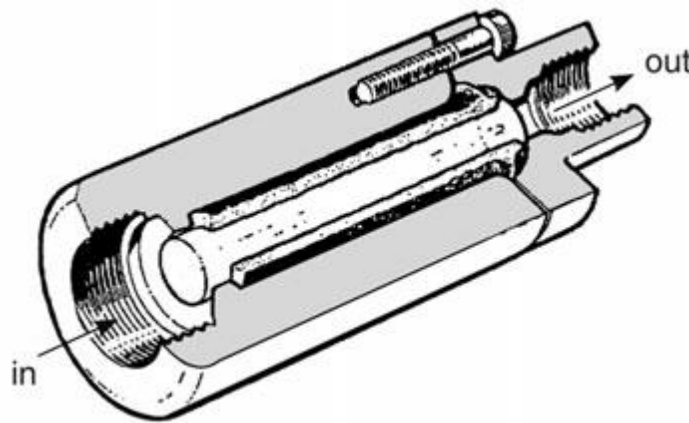


**Figure 5.31 A glass capillary tubing restrictor [24]**

After determining the restrictor type, the most important issue is determining the dimension and the material type of the capillary tube restrictor to benefit from the compensator efficiently.

#### 5.2.4.3.1 Capillary Tube Selection

During sizing the capillary tube two main rules should be considered: capillary diameter should be larger than 0.0006 m to avoid tube clogging, and the ratio between the diameter and length should be minimum 20. In the light of this information, a capillary tube selection can be made by using the chart below after making some calculations as discussed in the latter sections.

O.D.(mm)	W.T. (mm)												
	0.05-0.07	>0.07-0.10	>0.10-0.14	>0.14-0.19	>0.19-0.24	>0.24-0.30	>0.30-0.39	>0.39-0.49	>0.49-0.59	>0.59-0.99	>0.99-1.4	>1.4-2.0	
0.20-0.30													
>0.30-0.40													
>0.40-0.50													
>0.50-0.80													
>0.80-1													
>1-1.5													
>1.5-2													
>2-2.5													
>2.5-3													
>3-3.5													
>3.5-4													
>4-5													
>5-6													
>6-8													
Stainless Material: 304, 321, 316L, 310S						Copper Material: T2, H62, H65, H68							
Titanium Material: TA1, TA2						Aluminium Material: L2Y2, LF21							
Special sizes and materials are available upon request													

**Figure 5.32 Capillary tubing size chart [29]**

During operation, capillary tubes may be exposed to high or fluctuating temperatures and pressures. The tubing material should bear these conditions. Wear is also a big problem for a capillary, if many particles go through inside the lubricant. The pollutants and particles may clog the tube because of its small diameter. By considering both cost and endurance, stainless steel type capillary has been selected for the hydrostatic yaw bearing compensator.

#### 5.2.4.3.2 Pump Selection and Supply Pressure

Wind turbines have braking system which is being controlled by a hydraulic system. Pressurized hydraulic oil is being used in the hydraulic system. This pressurized oil is maintained by a pump in a wind turbine. According to the required pressure and type of the application, pump is selected by the designer of the wind turbine [30].

In the designed wind turbine with slewing bearing, hydraulic pump has been selected in order to handle the brake system. The other purpose of this pump is to supply oil to the hydrostatic bearing. This pump's characteristics are taken as the basis for the designed

hydrostatic yaw bearing. Additionally, for the designed hydrostatic yaw bearing system, another pump is considered as backup for the safety of the system. In any case, if the main pump fails to provide oil, the second pump should operate.

From the literature survey, it is seen from the investigations that for a 600 kW horizontal axis wind turbine, a pump with an operating pressure  $10^7$  Pa can be used [22]. As of this work the hydraulic system and the pump had not been determined by the turbine design team. Therefore, pump pressure values in the order of  $10^7$  Pa have been used for the design calculations as the supply pressure of the designed 500 kW horizontal axis wind turbine. As a starting point, a hydraulic pump has been selected with operating pressure at 250 bar ( $2,5 \times 10^7$  Pa) and the flow rate of 70 lt/min ( $0,001166667 \text{ m}^3/\text{s}$ ).

### 5.2.5 Design and Performance Determination of the Hydrostatic Yaw Bearing of 500 kW HAWT

Figure 5.33 shows work flow for a hydrostatic bearing system. This figure is an example with a single pad, compensated hydrostatic bearing operation.

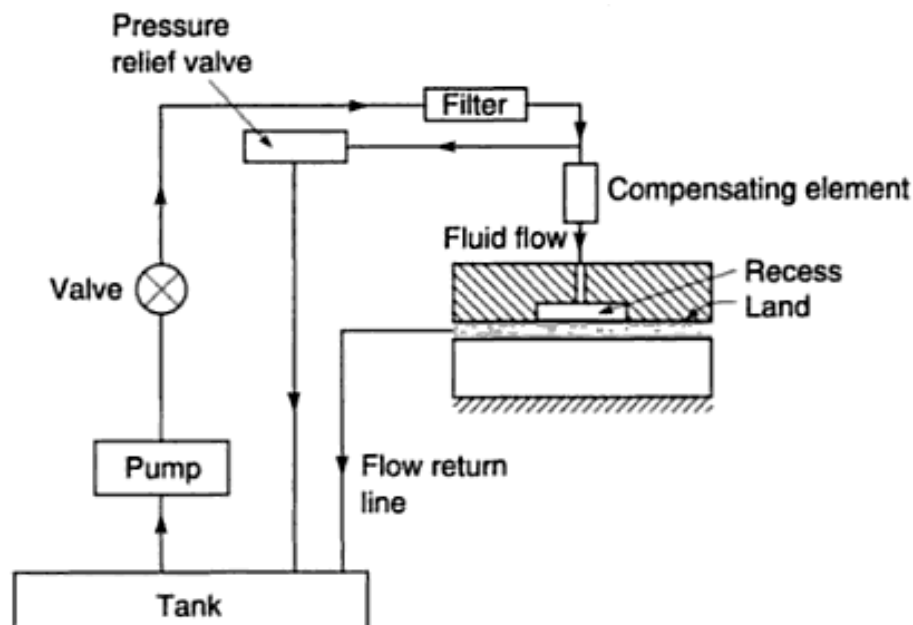
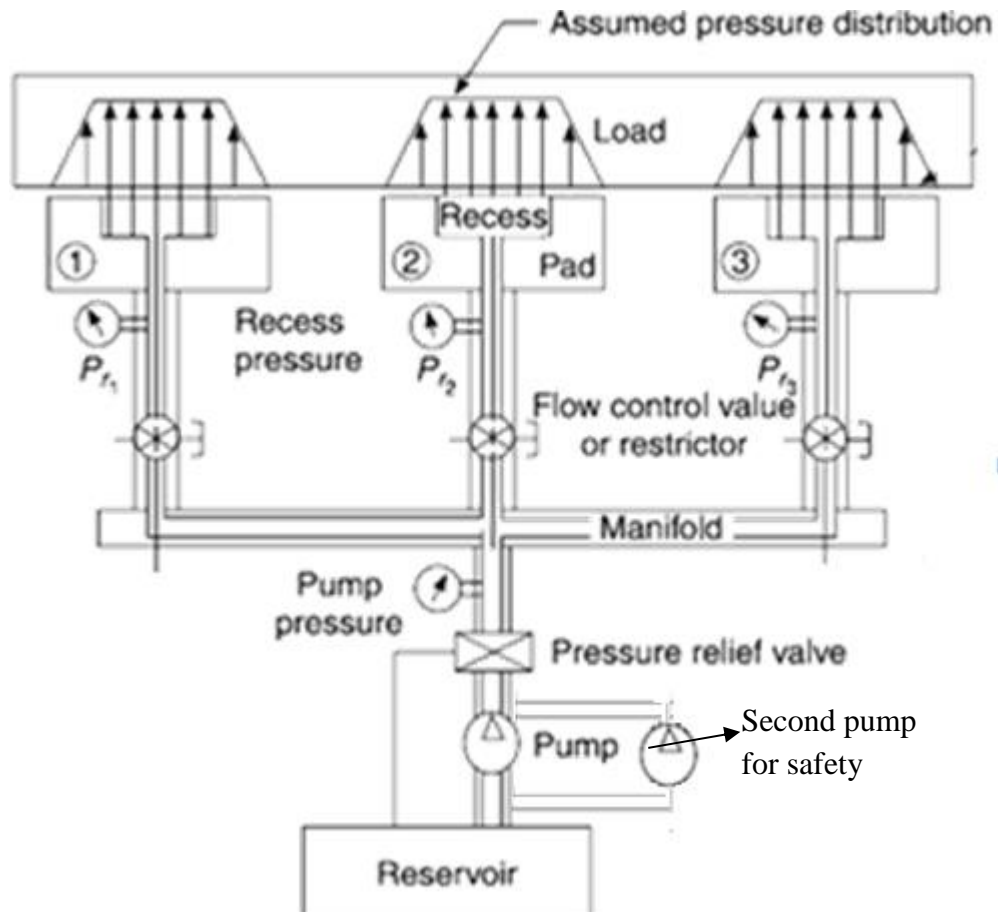


Figure 5.33 Working principle of hydrostatic bearing [24]

Before the main calculations, the selected multipad configuration of the intended hydrostatic yaw bearing with the restrictors and operation system is given in Figure 5.34 below.



**Figure 5.34 Mechanism of designed hydrostatic yaw bearing [24]**

As illustrated in Figure 5.34, lubricant is pumped from the reservoir, and distributed from the main pump through a pipe manifold to the thinner tubing which are called restrictors. In the designed hydrostatic yaw bearing, capillary tube is used as a restrictor. Then, oil reach pads and recesses with decreasing pressure, and from the recesses oil flows through to the bearing lands. After leaking through the bearing lands, the lubricant turns back to the reservoir. This illustration also indicates the second backup pump for the safety of the designed multipad hydrostatic yaw bearing mechanism. All of the inputs selected and determined by making some calculations from the previous sections are listed in the

**Table 5.7** table below.



**Table 5.7 Inputs for a 500 kW hydrostatic yaw bearing calculations**

INPUTS	
$F_x$ (radial forces)	121 kN
$F_z$ (axial forces)	-380 kN
$F_z$ (left side_total force)	-302,370 kN
$R_i$	60 mm
$R_o$	80 mm
$h_{min}$	0,05 mm
Viscosity ( $\xi$ )	0,02 Pas
$P_s$	10.000.000 Pa
$P_a$	101.325 Pa
$D_{cap}$	1 mm

It is seen from the table that some of the inputs such as total loads which the bearing is exposed have been determined by making some load calculations as discussed in the previous chapters. All of the other parameters have been selected according to some default values from the literature. For initial calculations, supply pressure has been selected as the hydraulic pump supply pressure of a sample 600 kW commercial wind turbine from the literature. For later iterations, the calculated/selected pump value has been used.

### 5.2.5.1 Design Calculations of the Hydrostatic Yaw Bearing

Mathematical equations and formulas that are used in the design are given below in step-by-step format with the sequence they are used.

1- Calculation of  $A_o$ ,  $A_i$ ,  $a_f$  and  $q_f$  by using the equations 36, 37, 38, 39

$$A_o = \pi R_o^2 \longrightarrow A_o = \pi * 0,04^2 = 0,005026548 \text{ m}^2 \quad (36)$$

$$A_i = \pi R_i^2 \longrightarrow A_i = \pi * 0,03^2 = 0,002827433 \text{ m}^2 \quad (37)$$

$$a_f = \frac{1 - (\frac{R_i}{R_o})^2}{2 \ln(\frac{R_o}{R_i})} \longrightarrow a_f = \frac{1 - (\frac{0,3}{0,4})^2}{2 \ln(\frac{0,4}{0,3})} = 0,760388015 \quad (38)$$

$$q_f = \frac{\pi}{6 \ln(\frac{R_o}{R_i})} \longrightarrow q_f = \frac{\pi}{6 \ln(\frac{0,4}{0,3})} = 1,820060497 \quad (39)$$

**Table 5.8 Calculated area, area factor and flow factor for upper and lower pads**

Outputs	
$A_o$	0,005026548 m <sup>2</sup>
$A_i$	0,002827433 m <sup>2</sup>
$a_f$	0,760388015
$q_f$	1,820060497

2- Checking if the supply pressure is sufficient to carry the load.

$$P_s * A_i * \# \text{ of pad} > 302,4 \text{ kN} \quad (40)$$



**Figure 5.35 a) Upward forces on upper pads. b) Downward forces on the lower pads**

To be able to see the supply pressure is enough to bear this load firstly, # of pad should be calculated.

$$W = A_o * a_f * P_s * \# \text{ of pad} > 302,4 \text{ kN} \quad (41)$$

Due to being opposed pad type of bearing equation will be solved in two parts:

$$\begin{array}{c}
 W_{\text{total lower}} \\
 \downarrow \\
 W_{\text{lower}} = A_o * a_f * (P_s) * \# \text{ of pad} - W_{\text{upper}} = A_o * a_f * (P_s) * \# \text{ of pad}
 \end{array}$$

Due to being opposed pad bearing, difference between the lower pads load carrying capacity and upper pads load carrying capacity is equal to the load carrying capacity of bearing.

First, the minimum number of pads to carry the upward vertical forces is calculated according to the loads to check how many pads at the supply pressure will be sufficient.

$$W_{upper} = A_o * a_f * P_s * \# \text{ of pad}$$

Plug in design values calculate the number

$$112.372 = 0,005 * 0,76 * 10^7 * \# \text{ of pad}$$

**# of pad** is calculated as minimum 3. Then, with 3 pads load check can be done;

$$P_s * A_i * \# \text{ of pad} > 112.372 \text{ N,}$$

$$10.000.000 * 0,002827433 * 3 = 84823 \text{ N} < 112.372 \text{ N}$$

It's seen from the calculation that with this supply pressure, there should be more pad than 3 to bear the loads.

**Table 5.9 Load check for upper pads by trial and error**

# of pads	$A_i \text{ (mm}^2\text{)}$	$P_s \text{ (Pa)}$	$W_{\text{(load check)}} \text{ (N)}$	$W \text{ (N)}$
3	0,002827	10.000.000	84.823	112.372
4	0,002827	10.000.000	113.097	112.372

Then, **# of pads** should be minimum 4. Considering the symmetric nature of the system and the two halves of the bearing, this means 4 pads for the right half of the bearing, and 4 pads for the left half. In total, 8 pads are needed for the upper side of the bearing. With 4 pads, load carrying capacity of the upper bearing is 113.097 N which is higher than the needed 112.372 N.

Second, the minimum number of pads to carry the downward vertical forces is calculated according to the loads to check how many pads at the supply pressure will be sufficient.

$$W_{total_{lower}} = A_o * a_f * P_s * \# \text{ of pad} > 112.372 + 302.370 \text{ N}$$

$$= 0,005 * 0,76 * 10000000 * \# \text{ of pad} > 414.742 \text{ N}$$

**# of pad** is calculated as minimum 11. Then, with 11 pads load check can be done;

$$P_s * A_i * \# \text{ of pad} > 414742 \text{ N,}$$

$$10000000 * 0,002827433 * 11 = 311017 \text{ N} < 414742 \text{ N}$$

It's seen from the calculation that the supply pressure is not enough to carry the load. There are two options: Increasing the supply pressure or increasing the number of pad.

Because the supply pressure was assumed as constant, by increasing the number of pads, this problem can be solved.

Number of pads is found out by increasing the number of pad one by one with a method trial and error.

**Table 5.10 Load check for lower pads by trial and error**

# of pads	$A_i$ (mm <sup>2</sup> )	$P_s$ (Pa)	$W_{(load\ check)}$ (N)	$W$ (N)
11	0,002827	10.000.000	311.017,6727	414.742
12	0,002827	10.000.000	339.292,0066	414.742
13	0,002827	10.000.000	367.566,3405	414.742
14	0,002827	10.000.000	395.840,6744	414.742
15	0,002827	10.000.000	424.115,0083	414.742

$10.000.000 * 0,002827433 * 15 = 424.115 > 414.742$  That's why 15 pads are enough to carry the load with this supply pressure  $10^7$  Pa.

Therefore, number pads should be minimum 15. This means 15 pads for the right half of the bearing, and 15 pads for the left half. In total, 30 pads are needed for the lower side of the bearing.

- 3- Calculations for recess pressure, flow rate, capillary resistance and finally the length of the capillary tube according to the selected diameter for upper and lower sides of the bearing.

$$(P_r - P_a) = \frac{W}{A_o * a_f * \# \text{ of pads}} \quad (42)$$

$$(P_r - P_a)_{upper} = \frac{112372}{0,005 * 0,76 * 4} = 7.350.095,819 \text{ Pa}$$

$$(P_r - P_a)_{lower} = \frac{414742}{0,005 * 0,76 * 15} = 7.234.052,232 \text{ Pa}$$

$$Q = q_f \frac{h^3}{\xi} (P_r - P_a) \quad (43)$$

$$Q_{upper} = 1,82 * \frac{0,00005^3}{0,02} * 7.350.095,819 = 0,0000836 \text{ m}^3/\text{s}$$

$$Q_{lower} = 1,82 * \frac{0,00005^3}{0,02} * 7.234.052,232 = 8,22901 \text{E-}05 \text{ m}^3/\text{s}$$

$$R_c = \frac{(P_s - P_r)}{Q} \rightarrow \begin{cases} R_{c\_upper} = \frac{2.548.579,181}{0,0000836} = 30.481.707.353 \text{ Ns/m}^5 \\ R_{c\_lower} = \frac{2664622,768}{8,22901E-05} = 32380850626 \text{ Ns/m}^5 \end{cases} \quad (44)$$

$$R_c = \frac{\pi d_c^4}{128 l_c \xi} \rightarrow l_c = \frac{R_c * \pi * d_c^4}{128 \xi} \rightarrow \begin{cases} l_{c\_upper} = \frac{30.481.707.353 * \pi * 0,001^4}{128 * 0,02} = 0,037 \text{ m} \\ l_{c\_lower} = \frac{32380850626 * \pi * 0,001^4}{128 * 0,02} = 0,039 \text{ m} \end{cases} \quad (45)$$

- 4-  $D_{cap}$  was selected 0,01 m as a preliminary selection.  $l_{cap} / D_{cap}$  should be minimum 20. This ratio is higher than 20 for both the upper pads and lower pads. That's why, 0,01 m capillary diameter is suitable the capillary tubes of upper and lower pads.

**Table 5.11 Calculated capillary diameter and capillary lengths for upper and lower pads**

Outputs	
<b>Dcap_lower</b>	0,001m
<b>Dcap_upper</b>	0,001 m
<b>lcap_lower</b>	0,039 m
<b>lcap_upper</b>	0,037 m
<b># of padslower</b>	15 + 15
<b># of padsupper</b>	4+4

Then, the same procedure is applied to the pads on the lateral side of the bearing for radial forces, and all the parameters have been calculated. The bearing has been

- 5- Designed with the same dimensions with the lower and upper side of the bearing. So,  $R_i$  and  $R_o$  are same together with  $A_i$ ,  $A_o$ ,  $a_f$ ,  $q_f$ .
- 6- Checking if the supply pressure is sufficient to carry the load or not.

$$P_s * A_i * \# \text{ of pad} > 121.000 \text{ N}$$

To be able to check the load, number of pads should be determined.

$$W = A_o * a_f * P_s * \# \text{ of pad} > 121.000 \text{ N}$$

$$W = 0,005 * 0,76 * 10^7 * 4 = 152.885 \text{ N} > 121.000 \text{ N}$$

4 pads seem to bear the loads. Let's check the supply pressure is enough or not.

$10^7 * 0,002827433 * 4 = 113.097 \text{ N} < 121.000 \text{ N}$  therefore number of pads should be increased until carry the load.

**Table 5.12 Load check for lateral pads by trial and error**

# of pads	$A_i (\text{mm}^2)$	$P_s (\text{Pa})$	$W_{(\text{load check})} (\text{N})$	$W (\text{N})$
4	0,002827	10.000.000	113.097	121.000
5	0,002827	10.000.000	141.371	121.000

Calculations made with 5 pads and  $10^7 * 0,002827433 * 5 = 141.371 \text{ N}$  was found. Therefore, 5 pads can bear the loads with this supply pressure. Considering symmetric nature of the bearing, 5 + 5 pads will be used to bear the radial loads.

7- Calculations of recess pressure, flow rate, capillary resistance and finally the length of the capillary tube according to the selected diameter for upper and lower sides of the bearing.

$$(P_r - P_a) = \frac{W}{A_o * a_f * \# \text{ of pads}} = \frac{121000}{0,005 * 0,76 * 5} = 6.331.553,014 \text{ Pa}$$

$$Q = q_f \frac{h^3}{\xi} (P_r - P_a) = 1,82 * \frac{0,00005^3}{0,02} * 6.331.553,014 = 7,20238\text{E-}05 \text{ m}^3/\text{s}$$

$$R_c = \frac{(P_s - P_r)}{Q} = \frac{1984233,732}{7,20238\text{E-}05} = 49.526.982.942 \text{ Ns/m}^5$$

$$R_c = \frac{\pi d_c^4}{128 l_c \xi} \longrightarrow l_c = \frac{49.526.982.942 * \pi * 0,001^4}{128 * 0,02} = 0,061 \text{ m}$$

$\frac{l_c}{d_c}$  should be minimum 20  $\longrightarrow \frac{0,061}{0,001} = 61$  which means this diameter is suitable for the capillary. 0,27 m will be the capillary length for the radial loads.

**Table 5.13 Calculated capillary diameter and capillary lengths for lateral pads**

Outputs	
$D_{\text{cap\_lateral}}$	0,001 m
$l_{\text{cap\_lateral}}$	0,061m
$\# \text{ of pads}_{\text{lateral}}$	5+5

After determining all of the design parameters, the last step is to develop a hydraulic circuit design for the 500 kW hydrostatic yaw bearing.

### 5.2.5.2 Hydraulic Circuit Design

Electrical analogy of the 1 pad of a hydrostatic bearing together with its oil circulation system is given in figure 5.38 and 5.39 below.

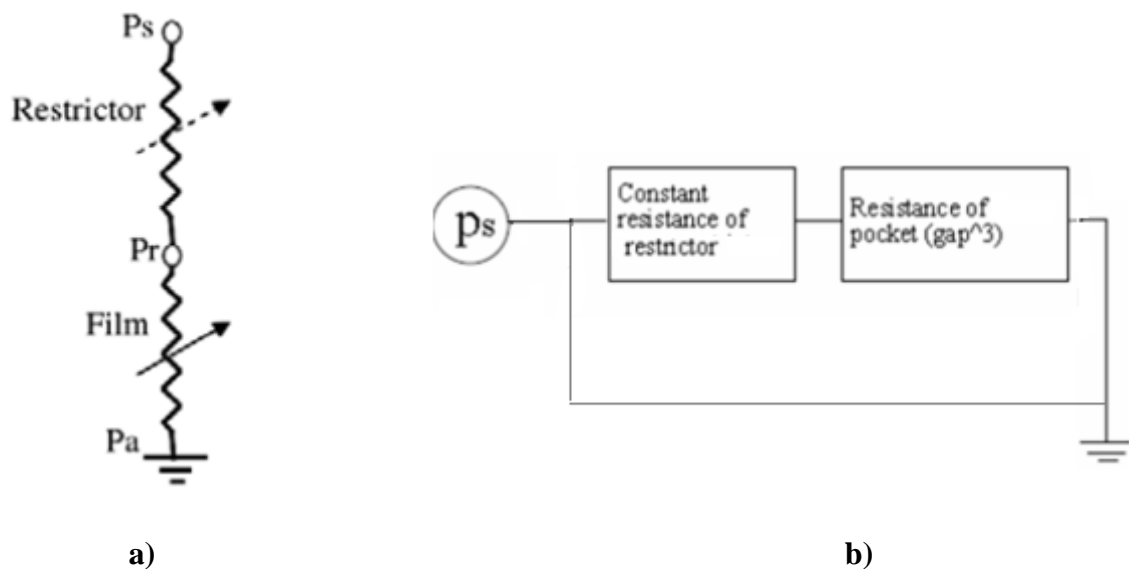


**Figure 5.36 a) Electrical analogy of 1 pad of hydrostatic bearing b) Schematic view of oil circulation of 1 pad of hydrostatic bearing [31]**

It's seen from the figures that lubricant is going out the reservoir with supply pressure and come to the restrictor which cause pressure drop due to the resistance of the flow control mechanism. Then, the lubricant reaches to the bearing gap and goes on radials out to the reservoir again to be pumped to the system.

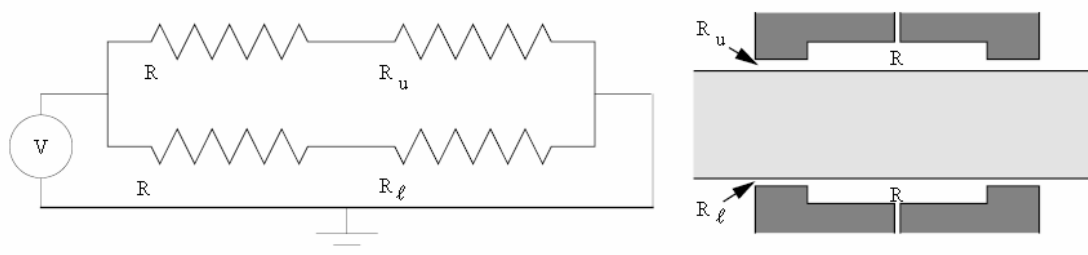
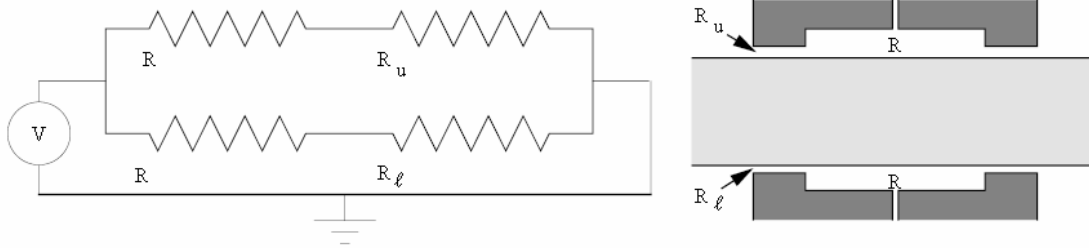
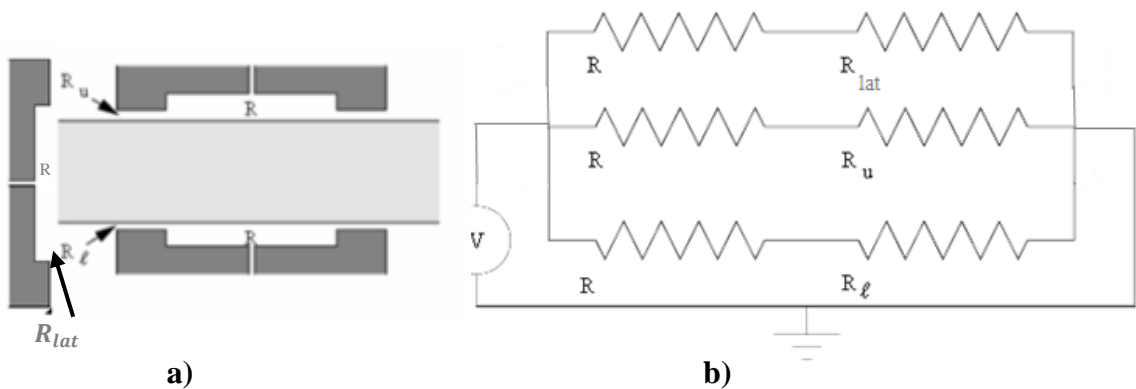


Figure 5.37 presents an illustration of the opposed pad hydrostatic bearing circuit design.



**Figure 5.37 Fluid flow into the bearing by regulating by resistance [32]**

By considering this design, opposed pads are combined with the lateral pads and the intended hydrostatic yaw bearing design schematic demonstration with the circuit are given below.



**Figure 5.38 Hydrostatic yaw bearing: a) Schematic view b) Circuit design**

Flow diagram of the designed combinational hydrostatic yaw bearing is given below. This diagram shows the logic of the flow inside the hydrostatic system.

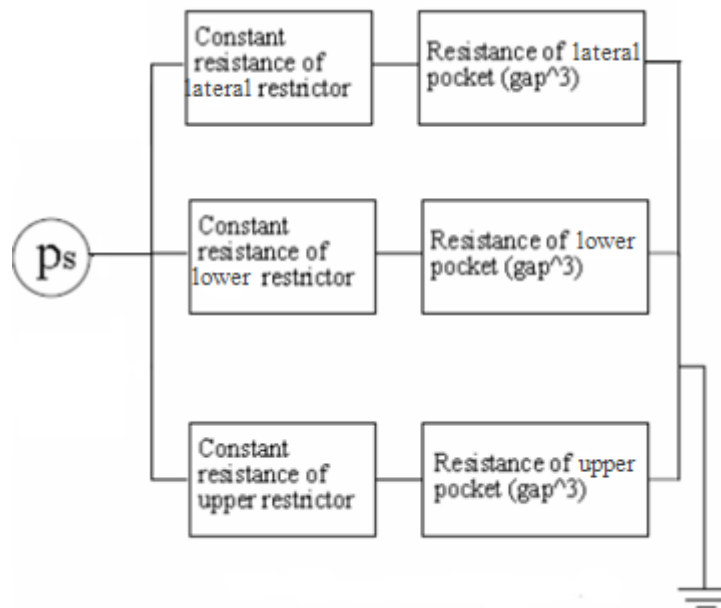


**Figure 5.39 Schematic view of oil circulation of combinational hydrostatic pad.**



There would be three main circulation pipes that one is for the upper pads, one is for the lower pads and one is for the lateral pads. From the pump, lubricant will distributed to these three main pipes and every pump has its own flow rate by the help of the valves. Valves will separate main pipes each other. From the main pipes, lubricant will flow towards to the restrictors. Figure 5.40 shows that how the flow will be distributed in the hydrostatic circuit. Upper bearing has 8 pads that 4 of them will be used and rest of them will stay as safety. Lower bearing has 30 pads that 15 of them work and the rest of them stay in case of one pad has stopped. Lateral bearing has 10 pads that the same rule goes for also this bearing.

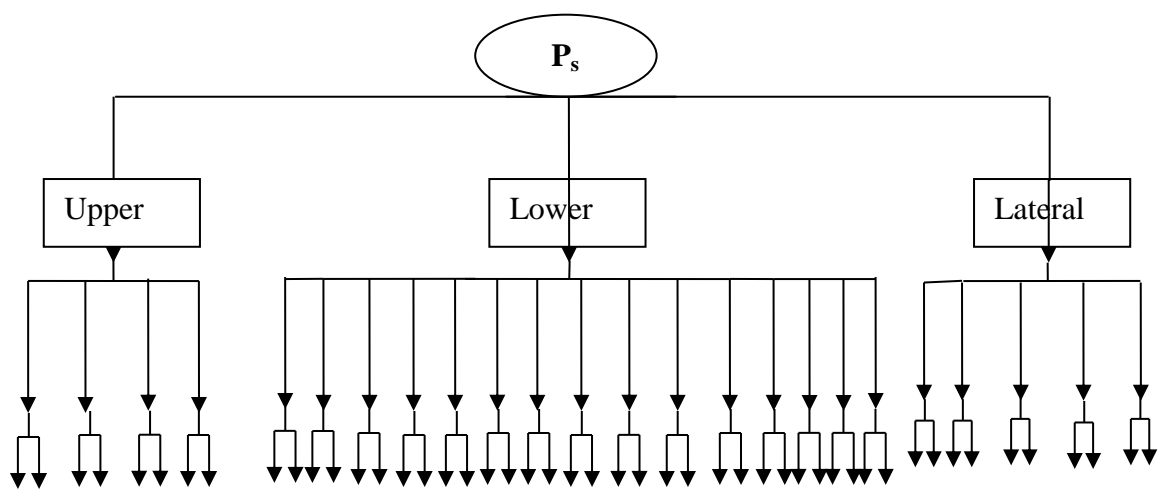


**Figure 5.40 Schematic view of oil circulation and pipe design**

Every circuit line has its own restrictor. That's why,  $4 + 15 + 5 = 24$  capillary tubes are needed. In order to keep in safe  $24 \times 2 = 48$  capillary tubes are needed.

### 5.2.5.3 Solid Design of the Designed Hydrostatic Yaw Bearing

By the help of Solid Works, inner ring of the hydrostatic bearing was drawn with the number of pads determined from the calculations and outer ring was drawn to support inner ring.



**a)**



**b)**

**Figure 5.41 a) Inner ring with pads b) Outer ring**

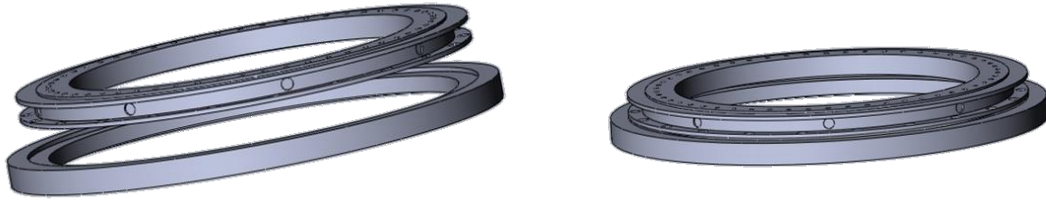


**Figure 5.42 Inner and outer rings before mounting**

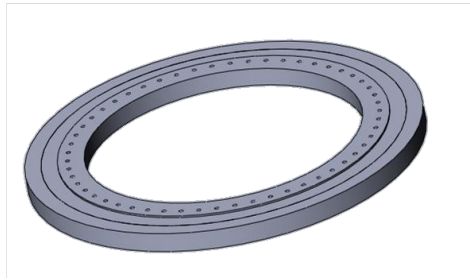


**Figure 5.43 Hydrostatic yaw bearing after inner and outer rings assembled**

#### **5.2.5.4 Production Method and Material Selection**

Due to being a non-contact type of bearing, material selection while designing a hydrostatic bearing has not crucial importance like the other type of bearings. During operation the bearing surfaces do not touch each other by the help of liquid film between them. The important parameters should be taken into account while selecting the material are the situations that can originate during operation. The conditions and effects on the materials are listed below [22];

- ❖ During operation, bearing may be exposed to high working pressures. Soft materials can easily wear. In order to prevent undesirable damage, soft materials should be excluded.
- ❖ During operation, bearing may be exposed to high fluctuating temperatures. Materials which have high thermal expansion coefficient will easily change bearing critical dimensions.
- ❖ Some lubricants may cause corrosion on the bearing surfaces by reacting with the bearing material. Bearing materials should be inert to lubricant and should be selected to prevent any reaction between the material and the lubricant.
- ❖ Bearing material should have overall resistance to corrosion

Machining is the basic method to produce recesses. Generally, milling or grinding is used to produce recesses for journal bearings. Electrical discharge machining, electroplating or etching can be also used to manufacture bearings [22].

## **6 Design Iterations**

The most important case while studying and designing hydrostatic yaw bearing is to select the parameters to design a bearing with the optimum performance. These parameters can be related to the geometry of the bearing, type of the bearing or supply system.

A yaw bearing design for a 500 kW horizontal axis wind turbine by using the hydrostatic bearing and its features has been performed in the previous chapters. In order to develop an optimum design, some of the parameters have been examined and as necessary, some design parameters have been changed.

### **6.1 General Procedure**

This investigation is carried out a hydrostatic bearing in order to use as a yaw bearing for 500 kW HAWT. Designing a hydrostatic bearing is very complex because lots of design parameters should be considered. While designing the yaw bearing, some assumptions were done in the area of pad geometry, supply pressure. By changing the parameters assumed in the calculations before, the effects of the parameters on the design will be shown and optimum design is tried to be selected.

#### **6.1.1 Design Iteration-1**

Stiffness is one of the most important parameters of hydrostatic bearings. A multidirectional hydrostatic bearing with capillary restrictors was designed during this work. It was already mentioned in the pump selection chapter that supply pressure is assumed  $10^7$  Pa but according to the designer of the hydraulic pump, supply pressure would be  $2,5 \times 10^7$  Pa. There is a graph which shows the relation between W-h with respect to supply pressure.

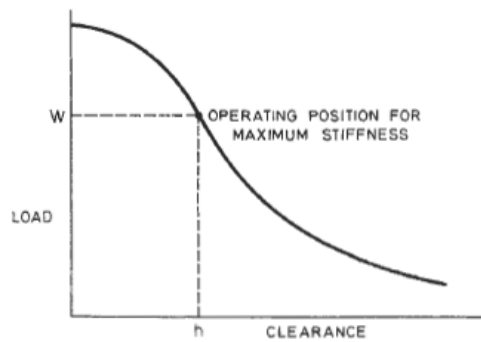


**Figure 6.1 General load characteristics [16]**

In figure, optimum operating conditions are shown. The graph shows the optimum point for the stiffness of the bearing according to the film thickness and applied load.

In this stage, firstly designed hydrostatic yaw bearing will be checked according to this graph. Then, by changing the supply pressure, film thickness will be determined.

The graph of load versus film thickness for the designed hydrostatic yaw bearing is given below.

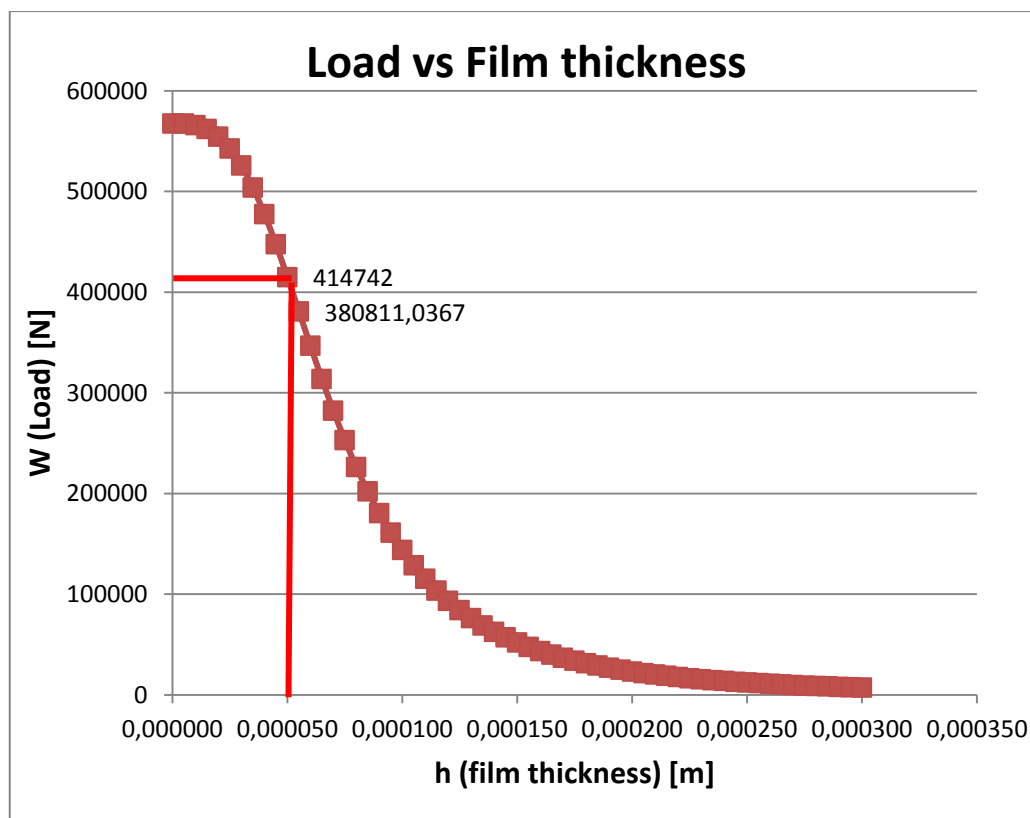


**Figure 6.2 Loads vs film thickness @  $10^7$  Pa**

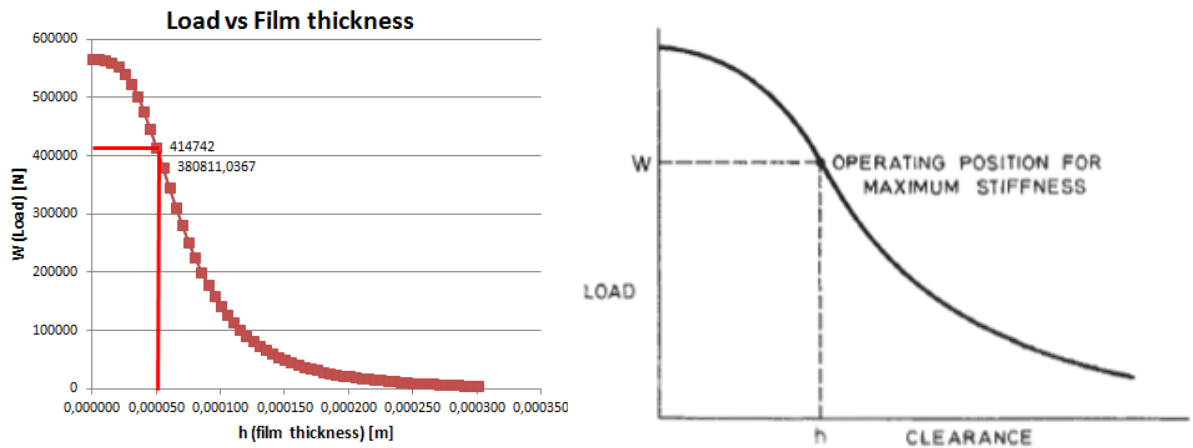


**Figure 6.3 Comparison to load vs film thickness graphs**

When two graphs are compared, film thickness seems to be selected great with regard to the load. Together with 0,00005 m film thickness and with 15 pads, this optimum graph can be realized under  $10^7$  Pa supply pressure.

There are 4 cases to compare with the initial case which is given in the graph as supply pressure  $10^7$  Pa.

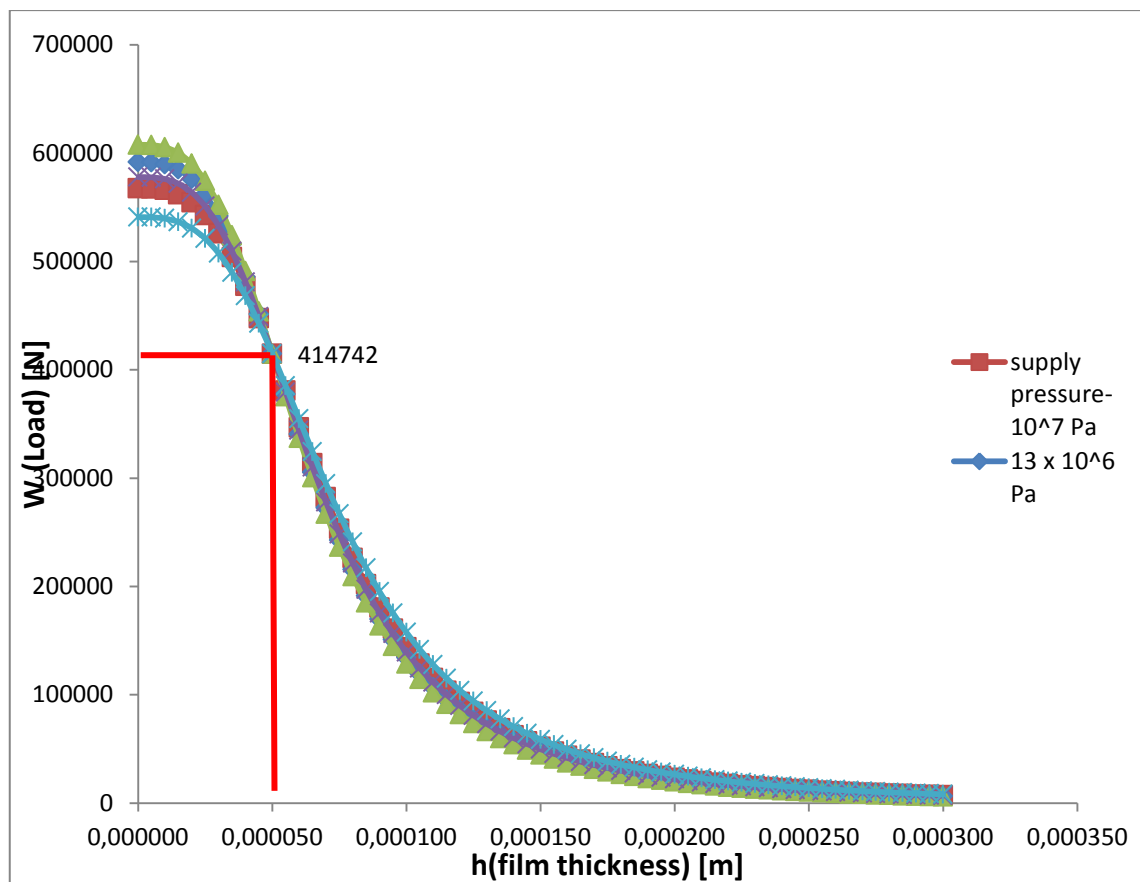


**Figure 6.4 Loads vs film thickness for 5 cases**

In order to obtain the optimum stiffness, parameters change with regard to changes in supply pressure is given in Table 6.1 below.

**Table 6.1 Differences in parameters with regard to changing supply pressures**

<b>h</b>	<b>Ps (Pa)</b>	<b>Pr-Pa (Pa)</b>	<b># of pads</b>	<b>Q (m<sup>3</sup>/s)</b>
<b>0,00005</b>	2500000	1839166	59	0,000020921
<b>0,00005</b>	10000000	7234052	15	0,000082290
<b>0,00005</b>	13000000	9042565	12	0,000102863
<b>0,00005</b>	16000000	10851078	10	0,000123435
<b>0,00005</b>	19000000	13563848	8	0,000154294

If the supply pressure increase while the film thickness and pad area keep same, recess pressure will increase together with the flow rate and a few numbers of pad can bear the lift. Therefore, if the pump is selected  $25 \times 10^6$  Pa supply pressure, due to decrease in recess pressure 59 pads can bear the load with 0,00005 m film thickness. 59 pads are too much to design with capillary because of its cost, maintenance and assembly. Therefore, along with this supply pressure, another pad configuration should be made.

### 6.1.2 Design Iteration-2

In order to decrease the numbers of pads to make the bearing more economic, pad dimensions are changed. If only the size of the inner radius is changed and outer radius keeps same, it would affect the ratio. Moreover, changing the ratio would influence the stiffness of the bearing. It's already mentioned in the prior sections that, too big ratios and too small ratios cause trouble in pump power. Too big ratios increase the flow rate and together with increase in flow rate, pump power will increase which makes the pump expensive. Too small ratios cause decrease in load carrying capacity of one pad that a pump which works at higher pressures is needed. This also makes the pump expensive. That's why; the ratio should be selected carefully.

At the beginning of the design phase, pad geometry was determined as circular and inner radius was selected as 30 mm while outer radius was selected 40 mm.  $\frac{R_i}{R_o} = 0,75$  which is a big ratio that it's not preferred to increase the inner radius more.

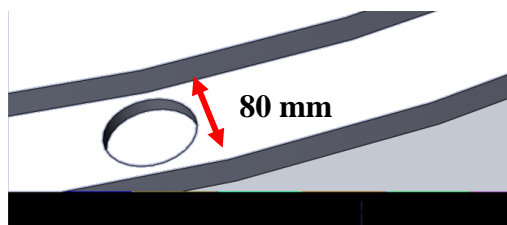


**Figure 6.5 Pad geometry of first design**

In addition, the bearing width is 80 mm and there is no space to increase radius of the pad. Therefore, by changing the pad shape, number of pads is trying to be decreased.

Circular pads will be designed as if putting circular pads side by side and the shape of one pad would seem like rectangular as given in Figure 6.6 below.

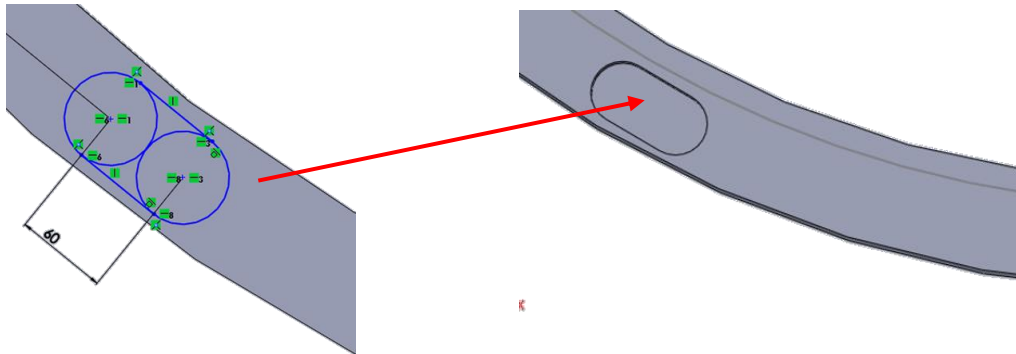


**Figure 6.6 New pad geometry**

In hydrostatic bearing applications, rectangular pads can be used with the rounded corner like given in the figure below.

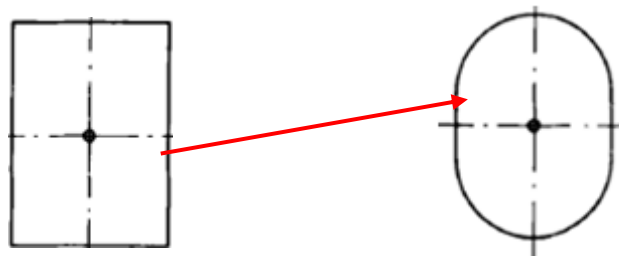


**Figure 6.7 Rectangular pad with rounded corner rectangular pad [18]**

Therefore, in iterations, rectangular shape of pad formulas will be based on while the shape of the pad is rounded corner rectangular pad.

Firstly, the geometry parameters are defined according to the rectangular pad.

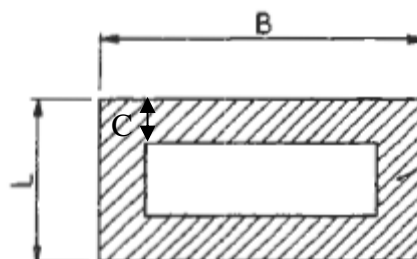




**Figure 6.8 Rectangular pad parameters [17]**

According to the pad geometry, 3 dimensions should be defined. L represents the pad height, B represents the width of the pad and C represents the gap between the pad and bearing. It's known that total height of the bearing is 80 mm.

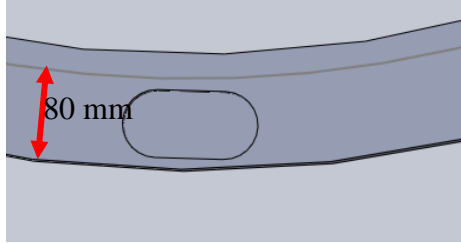


**Figure 6.9 Height of the bearing**

Rectangular pad geometries were selected in harmony with the circular pads geometry. According to the space to put the pads, it's decided to use six different pad geometry which are given in the table below.

**Table 6.2 Pad geometries**

Inputs				
Trials	LxB	L	B	C
1	60x120	60	120	10
2	60X180	60	180	10
3	50X100	50	100	15
4	50X150	50	150	15
5	50x120	50	120	15
6	50X180	50	180	15
7	600X100	60	100	10
8	60X150	60	150	10

There are two cases to be considered. First case is being done with the parameters used in the first design. Thus, supply pressure is  $10^7$  Pa. Second case, the supply pressure will be changed as 2.500.000 Pa. Both of the cases are performed to see the effects of the bearing geometry on the bearing performance.

**First case: @ 10.000.000 Pa supply pressure.**

1- Calculation of  $A_o$ ,  $A_i$ ,  $a_f$  and  $q_f$  by using the equations and tables given below.

$$A_o = L \cdot (B + 2 \cdot C) \quad (46)$$

$$A_i = L * B \quad (47)$$

The area and flow factor can be determined by using the figure given below shows the ratio between B/L and C/L.

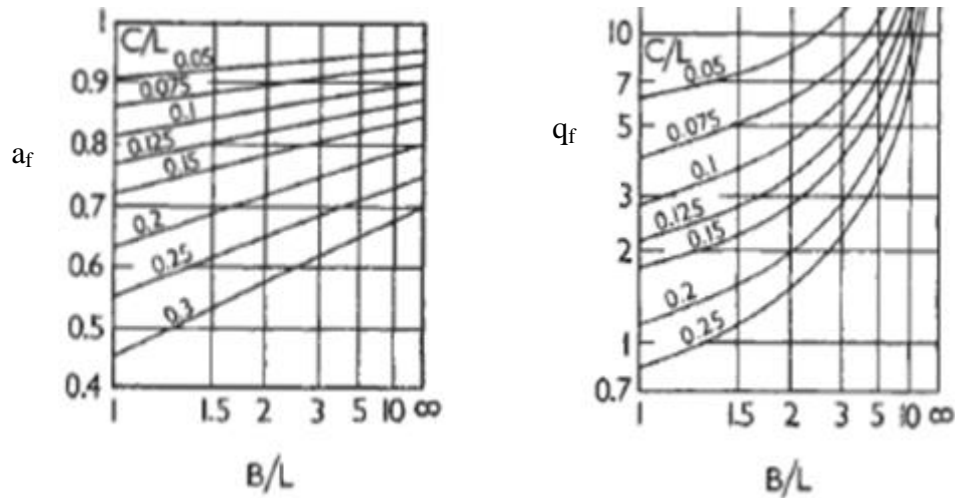


Figure 6.10 Pad coefficients [17]

Table 6.3 Calculated area, area factor and flow factor for lower pads

Outputs						
Trial number	C/L	B/L	$a_f$	$q_f$	$A_i$	$A_o$
1	0,166667	2	0,75	2,5	0,0072	0,0084
2	0,166667	3	0,78	3	0,0108	0,012
3	0,3	2	0,58	1,5	0,005	0,0065
4	0,3	3	0,63	2	0,0075	0,009
5	0,3	2,4	0,58	1,5	0,006	0,0075
6	0,3	3,6	0,63	2	0,009	0,0105
7	0,166667	1,666667	0,75	2,2	0,06	0,0072
8	0,166667	2,5	0,8	3,1	0,09	0,0102

It is known from the literature that C/L is recommended to be designed less than 2,5 [?17]

2- Checking if the supply pressure is sufficient to carry the load.

$$P_s * A_i * \# \text{ of pad} > 414.742 \text{ N}$$

To be able to check the load condition, number of pads should be considered. Total pad number for each pad geometries is given in Table 6.4.

**Table 6.4 Calculated number of pads for each geometry**

Outputs	
Trial number	# of pads
1	7
2	5
3	12
4	8
5	10
6	7
7	8
8	6

$$W_{\text{total lower}} = A_o * a_f * P_s * \text{\#of pad} > 112.372 + 302.370 \text{ N}$$

It's seen after checking the load conditions that determined number of the pads are sufficient to bear the loads.

3- Calculations for recess pressure, flow rate, capillary resistance and finally the length of the capillary tube according to the selected diameter for upper and lower sides of the bearing by using with the formulas below. Diameter was selected 0,001 m like before.

$$(P_r - P_a) = \frac{W}{A_o * a_f * \text{\# of pads}}, \quad Q = q_f \frac{h^3}{\xi} (P_r - P_a), \quad R_c = \frac{(P_s - P_r)}{Q}, \quad l_c = \frac{R_c * \pi * d_c^4}{128 \xi}$$

**Table 6.5 Calculated parameters for rectangular pads bearing with  $10^7$  Pa supply pressure**

Outputs				
Trial number	$P_r - P_a$ (Pa)	Q	$R_c$	$l_c$
1	9.396.145,125	0,000146815	342.2883.703	0,0042
2	8.854.059,829	0,000166014	6292.346.132	0,0077
3	9.159.372,237	0,000085869	8.609.646.966	0,0105
4	9.135.141,093	0,000114189	66.865.647.60,96	0,00078
5	9.525.747,126	0,00008930	4.175.942.596	0,005
6	8.948.709,643	0,000111859	8.492.534.860	0,0104
7	9.591.898,148	0,000131889	2.326.030.096	0,0028
8	8.463.439,542	0,000163979	8.752.548.937,49	0,00068

4-  $D_{cap}$  was selected 0,001 m as a preliminary study.  $l_c / D_c$  should be minimum 20 for a capillary compensated design. That's why the ratios for all trails are given in table below.

**Table 6.6 Capillary length to diameter ratios**

Outputs	
Trial number	$l_c / D_c$
1	4,2
2	7,7
3	10
4	0,7
5	5
6	10,5
7	3
8	0,7

It's seen from the table that all of the ratios are below the minimum value. That's why, some iteration should be done to find the optimum diameter and length. From the iterations selected capillary diameters and calculated lengths are given in the table.

**Table 6.7 Capillary lengths and diameters**

Trial number	$D_c$ (m)	$l_c$ (m)	$l_c / D_c$
1	0,002	0,067	33,6
2	0,0015	0,039	26
3	0,0015	0,053	35
4	0,003	0,063	21
5	0,002	0,082	40
6	0,0015	0,052	35
7	0,002	0,045	23
8	0,003	0,063	21

**Second case: @ 2.500.000 Pa supply pressure.**

The same procedure will be applied to calculate the parameters again.

1- Calculation of  $A_o$ ,  $A_i$ ,  $a_f$  and  $q_f$  by using the equations and tables given below.

$$A_o = L*(B + 2*C)$$

$$A_i = L* B$$

The area and flow factor can be determined by using the figure given below shows the ratio between B/L and C/L.

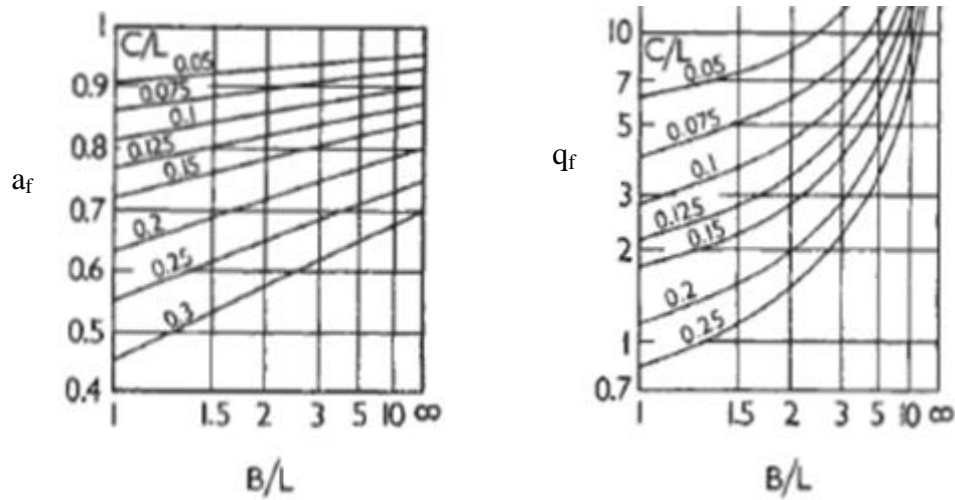


Figure 6.11 Pad coefficients [17]

Geometric parameters will be same with the previous case.

Table 6.8 Calculated area, area factor and flow factor for lower pads

Outputs						
Trial number	C/L	B/L	$a_f$	$q_f$	$A_i$	$A_o$
1	0,166667	2	0,75	2,5	0,0072	0,0084
2	0,166667	3	0,78	3	0,0108	0,012
3	0,3	2	0,58	1,5	0,005	0,0065
4	0,3	3	0,63	2	0,0075	0,009
5	0,3	2,4	0,58	1,5	0,006	0,0075
6	0,3	3,6	0,63	2	0,009	0,0105
7	0,166667	1,666667	0,75	2,2	0,06	0,0072
8	0,166667	2,5	0,8	3,1	0,09	0,0102

2- Checking if the supply pressure is sufficient to carry the load.

$$P_s * A_i * \# \text{ of pad} > 414.742 \text{ N}$$

To be able to check the load condition, number of pads should be considered. Total pad number for each pad geometries are given in Table 6.9.

**Table 6.9 Calculated number of pads for each geometry**

Outputs	
Trial number	# of pads
1	28
2	19
3	36
4	31
5	40
6	27
7	32
8	22

$$W_{\text{total lower}} = A_o * a_f * P_s * \text{\#of pad} > 112.372 + 302.370 \text{ N}$$

It's seen after checking the load conditions that determined number of the pads is sufficient to bear the loads.

3- Calculations for recess pressure, flow rate, capillary resistance and finally the length of the capillary tube according to the selected diameter for upper and lower sides of the bearing by using with the formulas below. Diameter was selected 0,001 m like before.

$$(P_r - P_a) = \frac{W}{A_o * a_f * \text{\# of pads}}, \quad Q = q_f \frac{h^3}{\xi} (P_r - P_a), \quad R_c = \frac{(P_s - P_r)}{Q}, \quad l_c = \frac{R_c * \pi * d_c^4}{128 \xi}$$

**Table 6.10 Calculated parameters for rectangular pads bearing with  $2,5 \times 10^7$  Pa supply pressure**

Outputs				
Trial number	$P_r - P_a$ (Pa)	Q	$R_c$	$l_c$
1	2.349.036,281	0,00003670	1352417598	0,00165
2	2.330.015	0,00004369	1571588934	0,0019
3	2.389.401	0,00002240	413985825	0,0005
4	2.357.455	0,0001639	1398770132	0,00016
5	2.381.436	0,000022	772115098	0,00094
6	2.320.035	0,000029	2711653522	0,0033
7	2.397.974	0,000033	21244079	0,000026
8	2.308.210	0,00045	2022831208	0,00016

4-  $D_{cap}$  was selected 0,001 m as a preliminary study.  $l_c / D_c$  should be minimum 20 for a capillary compensated design. That's why the ratios for all trails are given in table below.

**Table 6.11 Capillary length to diameter ratios**

Outputs	
Trial number	$l_c / D_c$
1	1,7
2	1,9
3	0,5
4	0,16
5	0,94
6	3
7	0,02
8	0,15

It's seen from the table that all of the ratios are below the minimum value. That's why, some iteration should be done to find the optimum diameter and length. From the iterations selected capillary diameters and calculated lengths are given in the table.

**Table 6.12 Capillary length and diameter**

Trial number	$D_c$ (m)	$l_c$ (m)	$l_c / D_c$
1	0,0025	0,064	26
2	0,0025	0,053	23
3	0,0035	0,076	22
4	0,005	0,102	21
5	0,003	0,07	25
6	0,002	0,05	26
7	0,0095	0,212	22
8	0,005	0,098	20

## 6.2 Comparison

Firstly, cases will be examined in themselves then, results of the two cases will be compared to each other and last design will be selected.

### 6.2.1 First case

If we compare the results according to the number of pads and stiffness;

**Table 6.13 Stiffness comparison of the trials**

Trial number	# of pads	Stiffness	Dc (m)	lc (m)
1	7	3797832	0,002	0,067
2	5	11714028	0,0015	0,039
3	12	3341649	0,0015	0,053
4	8	5190195	0,003	0,063
5	10	1946578	0,002	0,082
6	7	7530333	0,0015	0,052
7	8	1988091	0,002	0,045
8	6	14016530	0,003	0,063
9	15	12129609	0,001	0,0039

Number 9 is the circular pad hydrostatic bearing.

Number 2,8 and 9 seem great durable according to the stiffness results but number 9 needs  $15 + 15 = 30$  pads that it costs too much. That's why, number 2 or 8 can be selected as the most suitable bearing geometries @  $10^7$  Pa supply pressure.

### 6.2.2 Second case

If we compare the results according to the number of pads and stiffness;

**Table 6.14 Stiffness comparison of the trials**

Trial number	# of pads	Stiffness	Dc (m)	lc (m)
1	28	375383,6	0,0025	0,064
2	19	771288,3	0,0025	0,053
3	36	53642,19	0,0035	0,076
4	31	280562	0,005	0,102
5	40	90036,05	0,003	0,07
6	27	624269,5	0,002	0,05
7	32	4542,282	0,0095	0,212
8	22	885776,9	0,005	0,098
9	59	2550184	0,001	0,0032



Number 9 is the circular pad hydrostatic bearing. With a lower supply pressure number of pads incredibly increases especially with circular pads. According to the stiffness, number 2,6,8,9 can be selected but due to extreme number of pads it's eliminated.

Between three of trials, best one looks number 2 because of its less pad numbers. The design looks like this with  $19+19 = 38$  pads.

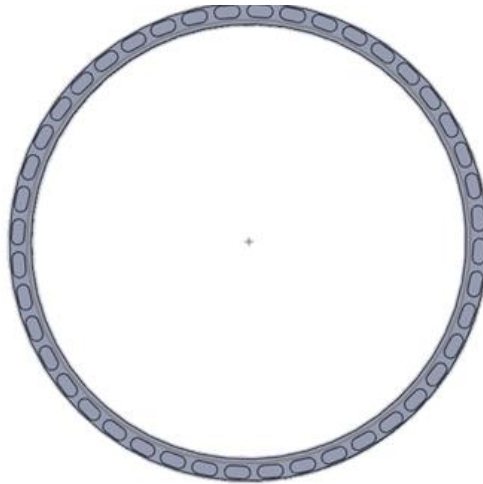


**Figure 6.12 Pad design according to the case two**

It looks like annular type of hydrostatic bearing. That's why, maybe it would be better to design hydrostatic yaw bearing as annular type given in figure below.

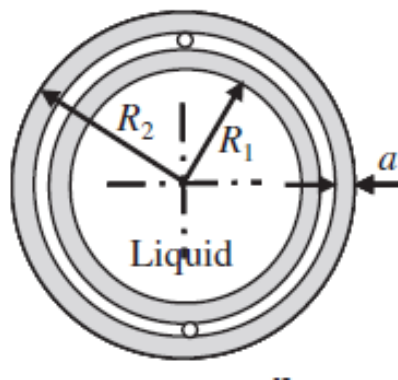


**Figure 6.13 Annular pad hydrostatic bearing [23]**

## 7. Conclusion & Future Work

- ❖ Typically hydrostatic bearings are high cost systems as compared rolling element bearings. However, the main disadvantage of high initial costs for hydrostatic bearings does not exist for wind turbine systems. This cost is mainly associated with necessity of a high pressure pump and hydraulic system. However, in wind turbines, there is already a hydraulic circuit including pumps for brake system. Therefore, the only additional cost is the machining of the lit pads or pressure pockets. Compared to the cost of very large diameter slew roller bearings, the machining cost is much less. In short, in large wind turbines hydrostatic bearings have cost advantage over classical slew bearings.
- ❖ As added advantage over classical rolling element systems operating life of a hydrostatic bearing is almost infinite or incomparably long. Besides, losses due to friction are lower than slewing bearings.

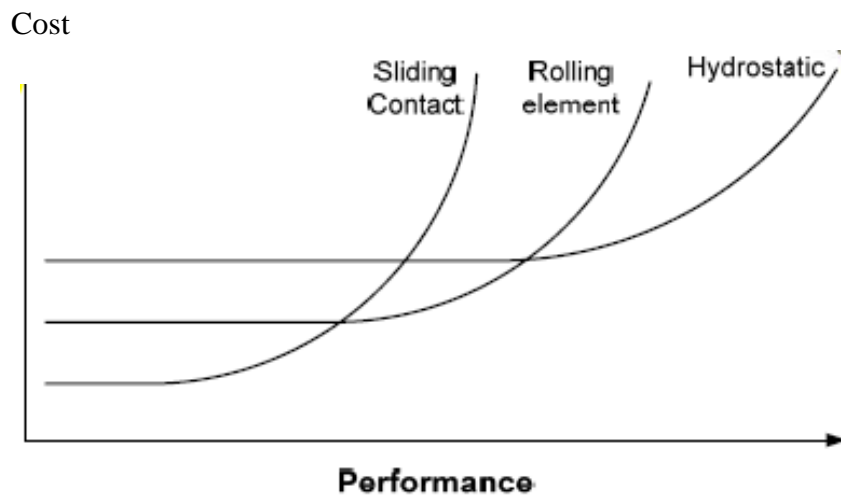


**Figure 6.14 Annular pad hydrostatic bearing [33]**

Because the hydrostatic bearing is a non-contact type bearing, there is nearly zero friction which reduces the power consumption to a minimum, and gives better performance. It is also seen from the figure that performance of hydrostatic bearings is better in a long period.

- ❖ In this study, a hydrostatic yaw bearing has been successfully designed for a 500 kW horizontal axis wind turbine. An optimization study has also been conducted for the pad geometry to select the optimum size of the capillary and reduce the cost. The optimum design has been developed according to the supply pressure of  $10^7$  Pa and  $2,5 \times 10^7$  Pa. The design and optimization work indicates that hydrostatic bearing systems constitute robust, low cost and high performance alternative to current rolling element yaw bearing systems.
- ❖ As future work, more detailed analysis can be made as actual turbine hydraulic system pressure and viscosity values are determined. In this work, some of the load values have been taken as large lumps for conservative analysis. More detailed load distribution can be used for a refined design.

## REFERENCES

- [1] Madge, H., J., Minadeo, D., A.;  
'<http://www.faqs.org/patents/app/20120134841#ixzz28KilUdoO>
- [2] Hoffmann R., ‘ ‘ A comparison of control concepts for wind turbines in terms of energy capture’ ’, MSc Thesis, 2002, Technical University of Darmstadt
- [3] Det Norske and Riso National Laboratory, ‘ ‘Veritas Guidelines for Design of Wind Turbines’ ’, 2002
- [4] Manwell, J., F., McGowan, J.G., Rogers, A.,L., ‘ ‘ Wind Energy Explained: Theory, Design and Application’ ’, 2009
- [5] [http://en.wikipedia.org/wiki/Yaw\\_bearing](http://en.wikipedia.org/wiki/Yaw_bearing)
- [6] SKF, Slewing Bearing selection manual, <http://www.skf.com/files/884465.pdf>
- [7] [http://www.ewec2010proceedings.info/posters/PO.221\\_EWEC2010presentation.pdf](http://www.ewec2010proceedings.info/posters/PO.221_EWEC2010presentation.pdf)
- [8] <http://www.iowaenergycenter.org/wind-energy-manual/wind-energy-systems/>
- [9] Temiz V., İTU, class notes
- [10] Dekker, M., ‘ ‘ Bearing Design in Machinery. Engineering Tribology and Lubrication’ ’, 2003
- [11] Reel Makina,  
[http://reelmakina.com/?title=uc\\_sira\\_masurali\\_yataklar&m=Urunler&id=30&ek=3&m\\_id=25&ust=30](http://reelmakina.com/?title=uc_sira_masurali_yataklar&m=Urunler&id=30&ek=3&m_id=25&ust=30)
- [12] LYC Slewing ring catalogue,  
<http://www.lycbearings.com/LYC%20Slewing%20Bearing%20Catalog.pdf>
- [13] LYC Slewing bearing catalog- load calculation, [www.lycbearing.com](http://www.lycbearing.com)
- [14] SNR Bearing technology,  
<http://www.google.com.tr/url?sa=t&rct=j&q=&esrc=s&frm=1&source=web&cd=2&ve>

d=0CDcQFjAB&url=http%3A%2F%2Fwww.ntn-snr.com%2Findustry%2Ffr%2Fen-en%2Ffile.cfm%2F02-Bearing\_technology.pdf%3FcontentID%3D4674&ei=2lgJUsP1LMnpPJm3gPgK&usg=AFQjCNFMk0qact\_IUbfh3BliUW-17yL1hA&sig2=89SmbpccqnsJxLM9QB3R5A

- [15] SKF Brinelling and other problems on bearing,  
[http://www.vsm.skf.com/~media/Files/enUS/Automotive/457640\\_58\\_64.ashx](http://www.vsm.skf.com/~media/Files/enUS/Automotive/457640_58_64.ashx)
- [16] Neale M., J., ‘‘ Tribology Handbook second edition’’, 1995
- [17] Bassani R., Piccigallo B., ‘‘ Hydrostatic Lubrication’’, 1992, Elsevier
- [18] Stachowiak G., W., Batchelor A., W., ‘‘Engineering Tribology’’
- [19] Khonsari M., M., Booser E., R., ‘‘ Applied Tribology-Bearing Design and Lubrication’’
- [20] Hamrock B., J., ‘‘Lubrication of Machine Elements’’, 2006, John Wiley & Sons
- [21] Bhushan B., ‘‘ Modern Tribology Handbook’’, 2000
- [22] Rowe W., B., ‘‘Hydrostatic, Aerostatic and Hybrid Bearing Design’’
- [23] Anders A., ‘‘ Aeroelastic Simulation of Wind Turbine Dynamics’’, 2005
- [24] Venkatesh V., C., Izman Z., ‘‘ Precision Engineering’’, 2007, McGraw-Hill, New Delhi
- [25] [http://www.vp-scientific.com/Viscosity\\_Tables.htm](http://www.vp-scientific.com/Viscosity_Tables.htm)
- [26] Hamrock B., J., Schmid R., S., Jacobson B., O., ‘‘Fundamentals of Fluid Film Lubricants’’, 2004
- [27] Hirani H., ‘‘ Hydrostatic Bearings: An Introduction’’, class notes
- [28] Yagi, S., ‘‘ Bearings for Wind Turbine’’, NTN Technical Review No.71, 2004
- [29] <http://www.procapillarytube.com/upload/attachment/201104/1303113172.pdf>
- [30] Stolarski T., A., ‘‘ Tribology in Machine Design’’, 1990

[31] Huang H., Lin C., Al-Bender F., ‘’ Design Analysis of Recess-Type Hydrostatic Slide System’’

[32] <http://www.mech.utah.edu/~me7960/lectures/Topic11-NonContactBearings.pdf>